INFORMATION TO USERS

This manuscript has been reproduced from the microfilm master. UMI films the text directly from the original or copy submitted. Thus, some thesis and dissertation copies are in typewriter face, while others may be from any type of computer printer.

The quality of this reproduction is dependent upon the quality of the copy submitted. Broken or indistinct print, colored or poor quality illustrations and photographs, print bleedthrough, substandard margins, and improper alignment can adversely affect reproduction.

In the unlikely event that the author did not send UMI a complete manuscript and there are missing pages, these will be noted. Also, if unauthorized copyright material had to be removed, a note will indicate the deletion.

Oversize materials (e.g., maps, drawings, charts) are reproduced by sectioning the original, beginning at the upper left-hand corner and continuing from left to right in equal sections with small overlaps.

Photographs included in the original manuscript have been reproduced xerographically in this copy. Higher quality 6" x 9" black and white photographic prints are available for any photographs or illustrations appearing in this copy for an additional charge. Contact UMI directly to order.

ProQuest Information and Learning
300 North Zeeb Road, Ann Arbor, MI 48106-1346 USA
800-521-0600

UMI®

Theoretical study of the propagation of non-ideal detonations

by

Jean-Philippe Dionne

Department of Mechanical Engineering
McGill University
Montréal, Québec, Canada

March 2000

A thesis submitted to the
Faculty of Graduate Studies and Research
in partial fulfillment of the requirements for the degree of
Doctor of Philosophy
in
Mechanical Engineering

0-612-64549-5

Abstract

The propagation of non-ideal detonations arising from friction, heat transfer and reactions steps involving a competition between exothermic and endothermic reactions (pathological detonations) has been studied theoretically by including source terms in the 1-D conservation equations of momentum and energy. To predict the steady-state non-ideal detonation velocity, the detailed structure of the detonation has been considered. The Generalized C-J criterion has been used to seek a singularity-free solution from the whole spectrum of possible solutions to the differential equations for the structure.

For pathological detonations, the steady-state analysis predicts a detonation velocity in excess of the ideal C-J value in the $H_2 - Cl_2$ mixture, in agreement with experimental observations. Unsteady pathological detonation calculations with a simplified two-rate law model have also been carried out. The resulting asymptotically stable detonations are found to be in agreement with the steady-state predictions.

For non-ideal detonations due to friction, the Generalized C-J criterion is found to break down for very low detonation velocities. An alternative criterion based on matching the detonation wave with the back boundary condition is used instead. A continuous spectrum of steady-state solutions has been found for detonation velocities ranging from the ideal C-J value down to that of a sonic wave. For activation energies above some critical value, multiple steady-state solutions have been found for a given friction factor, and various detonation regimes have been defined.

An unsteady analysis of the transient development of non-ideal detonations due to friction has been carried out to determine whether the solutions from the steady-state analysis can be approached asymptotically. Friction and heat transfer are found to increase the instability of the detonation wave. Oscillatory and even chaotic detonations were observed for values of the activation energies corresponding to stable detonations in absence of source terms (ideal detonation). Moreover, the transient analysis has revealed that in the case of multiple steady-state solutions, only that with the highest detonation velocity could be approached asymptotically. The transient results of detonation with friction and heat transfer have been found to be in qualitative agreement with the experimental gaseous detonations propagating in porous media and in obstacle fields.

Résumé

La propagation de détonations non-idéales résultant de la présence de friction, de transfert de chaleur et d'une compétition entre des réactions exothermiques et endothermiques (détonations pathologiques) a été étudiée théoriquement en incluant des termes-source dans les équations de conservation de la quantité de mouvement et de l'énergie. Afin de prédire les célérités de détonations stationnaires, la structure détaillée de la détonation a été considérée. Le critère généralisé de Chapman-Jouguet (C-J) a été utilisé pour trouver une solution non-singulière parmi les solutions possibles aux équations de conservation pour la structure.

Dans le cas des détonations pathologiques, l'analyse stationnaire prévoit une célérité de détonation excédant la valeur idéale C-J dans le mélange $H_2 - Cl_2$, en accord avec les observations expérimentales. Des calculs de détonations instationnaires avec un modèle de réaction simplifié à deux étapes ont aussi été réalisés. Les détonations asymptotiquement stables résultant de ces calculs sont en accord avec les prédictions de la théorie des détonations stationnaires.

Le critère généralisé de C-J n'est pas valide pour les célérités de détonation très basses résultant d'un niveau élevé de friction. Un autre critère, basé sur le raccordement entre la zone de réaction stationnaire et l'écoulement instationnaire en aval, doit être utilisé. Des solutions stationnaires sont obtenues pour les célérités de détonation allant de la valeur C-J idéale jusqu'à celle d'une onde sonore. Pour les énergies d'activation au-dessus d'une valeur critique, il existe des solutions stationnaires multiples pour une valeur donnée du coefficient de friction, et plusieurs régimes de propagation ont été définis.

Une analyse instationnaire du développement des détonations non-idéales à été menée afin de déterminer si les solutions stationnaires peuvent être approchées asymptotiquement. La friction et le transfert de chaleur rendent les détonations plus instables. Des détonations oscillatoires et même chaotiques ont été observées pour des valeurs de l'énergie d'activation correspondant à des détonations stables en l'absence de termes-source (détonation idéale). De plus, l'analyse instationnaire révèle que dans le cas de solutions stationnaires multiples, seule celle correspondant à la plus grande célérité de détonation peut être approchée asymptotiquement. Ces résultats instationnaires sont en accord avec les observations expérimentales de détonations gaseuses se propageant dans des milieux poreux et dans des champs d'obstacles.

Acknowledgements

First of all, I wish to acknowledge my supervisor Prof. John Lee, for his constant support and guidance throughout the course of my graduate studies. He instilled in me his passion for scientific research and provided the motivation to always go further. Although I will miss his invaluable advice and the countless discussions I have had with him on detonation science, I will not forget them.

A special thanks to Prof. Martin Brouillette from Université de Sherbrooke with whom I have had very fruitful exchanges on non-ideal detonation theory in the early phases of my Ph.D. I wish to express my gratitude to Randy Chue, who was always willing to offer a helping hand and who graciously permitted me to modify his Lagrangian detonation code for my purposes. Many thanks are also due to Kiumars Mazaheri who allowed me to include source terms in his Eulerian detonation code.

I am very grateful to some of my "colleagues" who contributed significantly to the completion of my thesis. A very special thanks to Eddie Ng, who patiently and devotedly helped me in the final weeks with my numerical simulations. I hope he also benefited from this experience. I would also like to express my gratitude to Rémi Duquette and Akio Yoshinaka for their dedicated assistance in the pathological detonation experiments, and to Teresa Mihalik for revising the manuscript.

I acknowledge all the members of the Shock Wave Physics Group (SWPG) with whom I have had the chance to interact with over the 7 years I spent in this dynamic and active research group. The friendly and supportive environment provided by the SWPG has made the years very enjoyable. A very special thanks to Julian Lee who introduced me to the field of detonation physics, and made me realize the rewards of scientific research.

Finally, I must also acknowledge my family and friends who have always supported me and encouraged me to achieve my goals. I am especially indebted to my wife Louise, who always believed in me, even in the most difficult times. Her love, patience, understanding and ever-lasting support allowed me to confidently pursue my academic goals.

Table of Contents

List of Figures

List of Tables

Nomenclature

A	Normalized tube area
c	Sound speed
c_b	Sound speed in the burned products
c_e	Equilibrium sound speed
c_f	Frozen sound speed
C_{p_f}	Frozen heat capacity at constant pressure
C_{v_f}	Frozen heat capacity at constant volume
C_h^{sm}	Coefficient of heat transfer for a smooth tube
D	Detonation velocity
D_h	Hydraulic tube diameter
DEN	Denominator of the du/dx equation
e	Sum of the internal and kinetic energies
E_a	Activation energy of the chemical reactions
E_{a_1}	Activation energy of the exothermic chemical reactions
E_{a_2}	Activation energy of the endothermic chemical reactions
f	Source term in the momentum conservation equation
h	Enthalpy per unit mass
H	Total enthalpy
h_c	Heat transfer coefficient
k	Pre-exponential factor in the chemical rate law
k_f	Friction factor
k_s	Equivalent sand roughness
m	Source term in the mass conservation equation
M	Mach number, of normalized shock velocity
M_{cr}	Critical shock velocity below which the Generalized C-J criterion fails
M_{local}	Mach number measured with respect to the local variables
M_{sec}	Shock velocity of the secondary shock (pathological detonations)
M_i	Molar mass of the chemical specie i
NUM	Numerator of the du/dx equation

n_i	Number of moles of chemical specie i
n_T	Total number of moles
p	Pressure
q	Source term in the energy conservation equation
Q	Chemical heat release
Q_{path}	Overshoot in chemical heat release (pathological detonations)
$\dot{Q}$	Chemical heat release rate
R	Tube radius
R_s	Specific gas constant
R_e	Reynold's number
t	Time
T	Temperature
T_w	Wall temperature
T^*	Stagnation temperature
u	Particle velocity
u_{abs}	Particle velocity relative to the laboratory frame
u_{rel}	Particle velocity relative in the shock-attached frame
u_p	Piston velocity
u_w	Particle velocity at the weak detonation state on the equilibrium Hugoniot
u_s	Particle velocity at the strong detonation state on the equilibrium Hugoniot
v	Specific volume
x	Distance
$x_{1/2}$	Half reaction zone length
x_p	Piston location

Greek Symbols

ϕ	Equivalence ratio
γ	Ratio of the specific heats
η	Gas dynamic parameter
κ	Curvature of the shock front
λ	Degree of reaction parameter

$\dot{\lambda}$	Time rate of change of the degree of reaction parameter (chemical rate law)
μ	Numerator of the du/dx equation at the sonic plane
ρ	Density
ψ	Denominator of the du/dx equation at the sonic plane
ζ	Small fractional increase in normalized tube area

Subscripts

CJ	Chapman-Jouguet detonation
o	Reference state
'	Flow variables in the laboratory coordinates
~	Per unit mole
1	Exothermic reactions
2	Endothermic reactions
ext_1	First extinction limit on the M vs k_f curve
ext_2	Second extinction limit on the M vs k_f curve

Chapter 1

Introduction

It has been known from the pioneering studies of Mallard and Le Chatelier [51] and Berthelot and Vieille [4] at the end of the 19th century that detonation waves, once initiated, will propagate with a well-defined constant velocity in a given explosive mixture. Based on this experimental observation, Chapman [10], in his original paper, pointed out that the only unique solution to the conservation laws is the one that corresponds to the minimum detonation velocity when the Rayleigh line is tangent to the Hugoniot curve. He adopted this as the criterion for selecting the steady detonation solution. Later, Jouguet [37] demonstrated that this tangency solution also corresponds to one where the detonation products flow at sonic velocity relative to the shock front. Thus, one can alternatively use the sonic condition as a criterion to determine a steady detonation solution. Following Chapman and Jouguet, the ideal steady-state detonation solution based on the minimum velocity (the tangency solution) or the sonic condition is now referred to as the Chapman-Jouguet (C-J) solution. This ideal C-J solution can be obtained on the basis of the conservation laws and equilibrium thermodynamics without considering the details of the non-equilibrium detonation structure. Hence, the detonation solution depends only on the energetics of the explosive. Consideration of the detailed structure of the reaction zone, which depends on chemical kinetic rate information, is not required in determining the C-J solution. The C-J theory also predicts a detonation velocity independent of initial and boundary conditions since it is based solely on the conservation laws for steady-state, planar, one-dimensional flow and the thermodynamic properties of the reactant and product species (e.g. heat of formation, heat capacity, equilibrium constant) across the wave front. Complete thermal and chemical equilibrium are assumed to occur at the C-J plane (i.e. the sonic condition).

The C-J theory can be considered very successful in combustion theory since, in general, it predicts a detonation velocity within a few percent of the experimental value, especially in smooth tubes when the explosive mixture composition and boundary condition (charge diameter) are far from the limiting values. However, in many situations, the measured experimental detonation velocities can be considerably lower than the equilibrium C-J values and in some chemical systems, the experimental values can even exceed the C-J values significantly. Such large departure from the ideal C-J predictions suggests that different propagation mechanisms are responsible. It is generally accepted that "non-ideal detonations" refer to detonations with propagation velocities that deviate significantly from the ideal C-J solution. In the present work however, non-ideal detonations are defined as detonations that are not governed by the classical C-J theory.

Since the 1940's, various theories have been developed to account for the deviation between the experimentally observed detonation velocities and the theoretically computed values using the ideal C-J theory. Various mechanisms have been proposed to explain these deviations. All these mechanisms involve consideration of the detailed detonation structure in order to arrive at the solution for the steady detonation velocity. A criterion has to be imposed to select the desired steady detonation solution from a spectrum of possible solutions of the conservation equations. In fact, for non-ideal detonation, no general discussion of the criterion for determining a unique (or an "eigenvalue") solution to the conservation laws has been given as yet. Furthermore, it is also not clear that these steady "eigenvalue" detonations, determined from the criterion used, can be realized asymptotically from arbitrary initial condition. Hence, the objective of this thesis is to carry out a general study of non-ideal detonations, bringing together some of the more important mechanisms that can lead to a deviation from the ideal equilibrium C-J theory. The competition and the relative importance of the different mechanisms will be studied and the criterion used for determining the steady eigenvalue detonation solution will be examined. The verification of the existence of these steady solutions necessitates the use of a transient analysis of non-ideal detonations. In a transient computation, no criterion is needed to select the final steady-state solution. The complete flow field is solved from the non-steady conservation equations and the final steady state solution, if it exists, will be approached asymptotically. Comparisons with the steady-state analysis will thus allow a critical examination of the validity of the steady-state criteria used. Emphasis will also be placed on non-ideal detonations that exceed C-J velocities (pathological detonations) since it involves a chemical mechanism for the non-ideal behavior, whereas sub-C-J, non-ideal detonations usually involve loss mechanisms such as friction and heat transfer. The effect of curvature will not be considered in the present study since the steady-state solution has already received significant attention in connection with condensed explosives. A transient study would involve the two-dimensional time-dependent reactive Euler equations which is outside the scope of the present quasi one-dimensional study. Nevertheless, it is appropriate to also consider all investigations where the detonation deviates from the ideal behavior, since the mathematical models used to account for the departure from ideality are mathematically similar to the description for non-ideal detonations. It is just a question of the degree of the deviation itself for non-ideal detonations.

Even in the early investigations of Berthelot and Vieille [4] on gaseous detonations in tubes, it was already observed that the detonation velocity decreases as the tube diameter is reduced, in contrast to the ideal C-J theory where the detonation solution is independent on initial and boundary conditions. For finite size tubes, the detonation velocity is usually below the theoretically predicted value based on equilibrium thermodynamics. Wall effects were thought to be responsible for this dependence of detonation velocity on tube size. Kistiakowsky et al. [38] carried out experiments using various tube sizes, and extrapolated the results to infinite diameter in an attempt to determine a velocity independent of wall effects which could be compared with C-J predictions. Later, Manson and Guénoche [53] found that the detonation limits in gaseous mixtures were also dependent on tube size. They proposed a functional form for the detonation velocity in gases as a function of both the mixture composition and the tube size.

Similar to the results for gaseous explosives, deviations between the experimental observations and the C-J predictions are also observed in condensed explosives (Campbell et al. [8], Nahmani and Manheimer [54]). As the size of the explosive charge is reduced, the detonation velocity is found to drop, and failure occurs at some critical diameter. The relationship between the detonation velocity D and the charge diameter d can be conveniently represented on a D *versus* $1/d$ diagram, also called the diameter effect curve. Extrapolation to $x = 1/d = 0$ gives a detonation velocity for infinite charge diameter. As the detonation velocity decreases, the post-shock temperature is reduced. This increases the induction time of the chemical reactions and, hence, the loss due to the divergence of the curved detonation front. Due to the strong exponential dependence of the induction time on the temperature, failure occurs abruptly at the critical diameter when the velocity deficit is of the order of about 10% for most ideal explosives. For most homogeneous explosives, the diameter-effect curve is thus typically linear, and terminates abruptly at the critical diameter for relatively small velocity deficits.

For gaseous detonations in smooth tubes, detonation velocity deficits are also observed. However, significant deviations from the ideal C-J predictions are observed in very rough tubes (e.g. in obstacle-filled detonation tubes). Using spirals as a way to generate wall roughness, Shchelkin [59] observed steady detonation velocities much less than the C-J values (deficits in excess of 20% in some cases). Such large velocity deficits cause a drop in post-shock temperature that would normally lead to detonation failure. Hence, different mechanisms must be responsible for the self-sustained propagation of the steady detonation with such large velocity deficits. Shchelkin suggested that for low detonation velocities where the temperature downstream of the shock may not be sufficient for autoignition, the leading shock can reflect off the wall protrusions and thus create local hot spots where the chemical reactions can then be triggered. Subsequent to ignition at the hot spots, the chemical reactions then spread from the wall towards the tube axis. This increases the reaction zone length, and thus increases the heat and momentum losses, leading to the low detonation velocities observed. Experiments similar to those of Shchelkin were also carried out by Guénoche and Manson [32], Lee et al. [43], Peraldi et al. [55] and Teodorczyk et al. [63]. Lee et al. [43] inserted spiral coils as well as orifice plates in tubes and observed detonations propagating with velocities as low as 30% of the C-J value in H_2-Air mixtures. They suggested that the ignition of the mixture at such low detonation velocities is possibly due to the reflections of the leading shock from the obstacles, generating temperatures of the order of the auto-ignition limit, a mechanism first suggested by Shchelkin. Peraldi et al. [55] also carried out experiments in tubes with orifice plates as obstacles and observed different combustion regimes including the so-called "choking" regime. The supersonic combustion velocity for this regime is of the order of the sound speed in the burned products, corresponding to large (≈ 50%) velocity deficits, as compared to the ideal C-J value. For such low velocity waves, even the reflection of the shock wave at the wall protrusions may not be sufficient to cause autoignition and this suggests the need to propose new mechanisms to explain the propagation of such waves. In tubes obstructed with thin orifice plates, Teodorczyk et al. also observed high velocity deficits. Moreover, they demonstrated that by eliminating the transverse shocks (damping them out with an acoustic-absorbing liner on the tube wall), such high velocity waves are not possible, thus confirming the importance of the transverse shocks on the propagation of the low-velocity detonations.

Steady-state detonations propagating at velocities significantly below the ideal Chapman-Jouguet predictions were similarly observed in porous media [52], [48], [50]. Mamontov et al. [52] measured very low detonation velocities of the order of 500 m/s in tubes filled with river sand or stainless steel fillings as the porous material. Lyamin et al. [48] observed a continuous spectrum of detonation velocities down to 500 m/s in planar channels, representing a two-dimensional porous medium. In tubes filled with a packed bed of spherical beads, Makris [50] also observed a continuous spectrum of propagation velocities ranging from the C-J value down to nearly sonic velocities (30% C-J) by varying the bead size and the sensitivity of the explosive mixture. In the experiments of Makris [50], the global wave propagation mechanism was found to consist of periodic phases of detonation failure by diffraction around the obstacles.

Recently, a heterogeneous condensed phase explosive analogous to that of Makris [50] was investigated by J.J. Lee [46]. He studied a heterogeneous mixture consisting of a condensed explosive (nitromethane) in a packed-bed of inert spherical glass beads. He measured detonation velocities significantly in excess ($\approx 50\%$) of the ideal equilibrium C-J predictions (pathological detonations) in this porous medium for C-J calculations based on full thermal, mechanical as well as chemical equilibrium. This excess velocity can be attributed to the fact that the breaking up and heating up of the solid beads (mechanical and thermal equilibration) is very slow as compared to the chemical energy release. As a result, a higher than equilibrium energy overshoot is observed to drive the detonation front as the subsequent endothermic heating up and breaking up of the beads is delayed beyond the sonic plane. In the experiments of Makris [50] in the gas phase, the inert material does not participate actively in the process, and hence was not considered in the calculations of the C-J states, even though they could be included as source terms for momentum and heat losses in the detonation zone.

Lee [46] also observed two distinct propagation mechanisms in the nitromethane-inert beads, non-ideal explosive. For sufficiently large bead sizes, the detonation wavelets can successfully propagate in the liquid explosive between the beads. The global detonation front thus consists of a series of these wavelets that propagate in winding paths through the geometric irregularities of the pores. For too small a bead size, such detonation wavelets can no longer propagate in between the beads, since the chemical length scale of the liquid explosive becomes comparable to the characteristic dimension of the pores. Thus, the liquid nitromethane is effectively isolated in individual pockets separated by inert solid material. A global detonation propagation is obtained in this case due to the transmission of shock waves through the inert material. When the shock is transmitted to other explosive pockets, the shocks trigger the chemical reactions and ignite the liquid explosive. In turn, the explosions in the liquid pockets generate more shocks in the neighboring inert beads ahead. This results in a sustained detonation propagation through the heterogeneous explosive medium. Thus, there are cases of non-ideal detonations where the observed detonation velocity can be in excess or below the equilibrium C-J value due to different propagation mechanisms operating in the detonation zone.

The experimental observations of Lee [46] are in agreement with the qualitative hot spot model of Rybanin [56]. According to Rybanin, inhomogeneities, referred to as hot spots, are the centers of reaction behind the detonation front. He describes two types of hot spots. The natural hot spots arise from the inherent instability of the detonation front, whereas the inert solid particles play the role of artificial hot spots. After some chemical induction time, the chemical reactions spread from the hot spots to the rest of the explosive. Thus, this reaction rate does not depend on the post-shock temperature, but rather on the very high local hot spot temperature. As a result, the diameter-effect curve of heterogeneous explosives differs significantly from that of ideal explosives. Much higher velocity deficits are allowed, owing to the weak dependence of the decomposition rate of the explosive on the post-shock temperature. Based on this hot spot model, Rybanin investigated the effect of particle size and density on the critical diameter of heterogeneous explosives. Johnson et al. [35], and Son et al. [60] among many others, later suggested mathematical formulations for the hot spot-based reaction rate modeling, taking parameters such as the mass fraction, average temperature, and degree of reaction of the hot spots into account.

Although highly empirical, these hot spots models give good qualitative agreement with experimental data.

Although the physical mechanisms responsible for the non-ideal behavior are quite complex (shock reflection, diffraction, and transmission, turbulent mixing, shock-vortex interactions, hot spots, etc.), it is perhaps possible to model them by suitable source terms for momentum and heat losses within the framework of a one-dimensional model. In the case of the heterogeneous explosives of Lee [46], a fraction of the velocity deficit can also be attributed to the divergence of the detonation products, since the curvature of the shock front plays a role in addition to the loss mechanisms. Although these mechanisms are multi-dimensional and very complex, their effect can be averaged out across the cross section of the explosive. More realistic modeling would require the use of two or three-dimensional geometry. In this case, the computer simulations become lengthy, and it is difficult to extract any physics from them. Accurately modeling the non-ideal effects by appropriate friction and heat transfer functions may also represent a considerable task. However, when investigating the existence of solutions to non-ideal detonations, simple arbitrary loss functions can be used. The qualitative features of the flow field should not be too dependent on the model used to get the non-ideal behavior. Thus, the effect of external friction and heat transfer shall be investigated, as well as flow divergence, in the propagation of non-ideal detonations.

From elementary compressible gas dynamics [14], it is well known that area increase or heat removal reduces the Mach number in a subsonic flow, whereas heat addition and friction will accelerate subsonic flow towards Mach 1. Similarly, within the reaction zone of an explosive, flow divergence and endothermic chemical reactions both tend to reduce the subsonic Mach number, whereas exothermic reactions increase the flow Mach number towards unity. The effect of friction, however, is not that obvious, since the relevant Mach number is that of the flow relative to the walls, and not to the shock front. Nevertheless, in the later part of the reaction zone, friction is found to increase the Mach number of the flow. These non-ideal effects can be taken into account by introducing source terms in the conservation equations. Area change (expansion of the products) requires a source term in the conservation of mass, friction requires a source term in the momentum equation, and heat transfer is taken into account by a source term in the conservation of energy. The three conservation equations with source terms can then be integrated to obtain the detonation structure of the non-ideal detonations.

Due to the presence of source terms in the conservation equations, the flow may become sonic prior to the complete equilibration of the flow. Hence, the ideal C-J criterion is no longer valid. An alternative criterion that relaxes the equilibrium requirement of the ideal C-J theory has to be used. Eyring et al. [24] were among the first to propose a criterion to determine a unique detonation solution when a source term is present in the conservation of mass due to the effect of the divergence of the flow behind a curved detonation front. However, they erroneously assumed complete reaction of the reactants at the sonic plane. A few years later, inspired by the work of Eyring et al. [24] and Devonshire [16], Wood and Kirkwood [66] correctly suggested the use of what is now referred to as the "Generalized C-J criterion" to determine a steady detonation solution. This Generalized C-J criterion states that the effective heat release rate must vanish as the flow becomes sonic relative to the shock front. This is equivalent to stating that the numerator and the denominator of the differential equation for the particle velocity must vanish simultaneously for a regular solution. For such a regular solution, the subsonic flow (relative to the shock front) becomes supersonic and eventually reaches the supersonic or the weak detonation branch of the Hugoniot. This is physically analogous to a converging-diverging nozzle in which the flow can undergo a transition from the subsonic to supersonic regimes at the throat. The particular solution is found by iterating for the detonation velocity that satisfies the aforementioned criterion while integrating the conservation equations for the detonation structure.

In the model of Wood and Kirkwood [66], the exothermic energy release competes with an effective "energy loss" in the direction of propagation, due to the lateral expansion of the flow behind a curved front. The energy associated with the diverging flow in the radial direction is considered not to contribute to driving the shock front. Therefore, only a fraction of the total energy release is available to support the detonation front. This apparent loss will cause a reduction in the detonation velocity for finite diameter charges. If the curvature is too severe, the detonation can even be quenched and fail. Jones [36] referred to this as a "lateral loss" effect. By modeling appropriately the shock curvature, Wood and Kirkwood [66] were able to reproduce qualitatively the so-called diameter-effect curve, and could thus provide a physical explanation for the existence of a critical failure diameter.

As early as 1940, Zel'dovich [71] investigated wall effects such as frictional drag and heat loss, assumed to be uniformly distributed (or averaged) across each plane normal to the shock front, in accordance with a quasi 1-D model. The Generalized C-J criterion was also used to determine the solution. Zel'dovich obtained velocity deficits proportional to the thickness of the reaction zone and inversely proportional to the tube diameter, in agreement with basic physical considerations. From the one-dimensional model of Zel'dovich, it is found that there is a maximum amount of friction above which no solution to the conservation equations can be found (as in the case of curvature in condensed explosives). This maximum friction solution is referred to as the "extinction limit", and is related to the critical tube diameter for a detonation propagation. Gelfand et al. [31] carried out an extensive review of friction effects in tubes. They suggested various expressions for the appropriate friction model to be used, which depend on the tube material and roughness, to predict the extinction limits.

Liu [47] suggested an alternative criterion to determine the unique detonation velocity. He suggested that a criterion based on maximum entropy along the Rayleigh line should be used, instead of a criterion based on the sonic flow condition. For ideal detonations without losses, Liu's criterion is exactly equivalent to the ideal C-J criterion. Liu verified his model for the analysis of quasi 1-D gaseous detonation waves, with a well-defined flow divergence term. He found that by using the maximum entropy condition, the Rayleigh line on a $p\ vs.\ v/(\xi+1)$ plane just tangent to the equilibrium Hugoniot gives the correct solution (ξ represents the small fractional change in area). This solution differs only slightly from the generally accepted solutions based on sonic outflow. However, it is not obvious how to extend Liu's criterion to non-ideal detonations subject to momentum and heat transfer losses. Moreover, Liu did not perform transient detonation simulations to verify the validity of the maximum entropy criterion and only considered small deviations from ideal behavior.

In the studies of Wood and Kirkwood [66], Zel'dovich [71], Gelfand [31], and others, the steady ZND equations for the detonation structure are integrated and the Generalized C-J criterion is used to iterate for the unique detonation solution. However, they did not extend their studies to investigate the non-ideal detonation regime with very high velocity deficits. Recently, Stewart and Yao

[61] carried out a further study of curved detonation fronts and obtained a continuous range of solutions for increasing curvature down to shock Mach numbers equal to unity. However, no similar studies have been made for non-ideal detonations in porous media and obstacle-filled tubes. In this thesis, the aforementioned non-ideal, low-velocity detonations will be studied by including source terms in the momentum and energy equations to model the propagation mechanism due to friction and heat transfer.

The large deviations from the ideal C-J predictions discussed above are credited to the presence of different loss mechanisms. However, on the other hand, there exists a class of non-ideal explosives whose deviations from the ideal C-J predictions can be thought of as due to a chemical mechanism. These gaseous explosive mixtures, where the detonation velocities are found to be in excess of the C-J value, are generally referred to as "pathological" mixtures. Pathological detonations were first experimentally observed in hydrogen-chlorine mixtures by Zel'dovich and Ratner [72], and later by Lee et al. [41], [42], Knystautas et al. [39] and Akyurtlu [1]. Pathological detonations were also observed in HN_3 by Dupré [21]. In this mixture, an excess in detonation velocity of 7.5% was observed at an initial pressure as low as 5 Torr, and nearly constant detonation velocities were measured irrespective of the initial pressure. In the $H_2 - Cl_2$ case, Zel'dovich and Ratner also found that the detonation velocities were independent of the initial pressure. In other explosive mixtures, the detonation velocity is found to decrease as the initial pressure is lowered, due to an increase in dissociation of the molecules at low pressure. Since they did not observe such a reduction in detonation velocity in the $H_2 - Cl_2$ mixture with decreasing pressure, Zel'dovich and Ratner concluded that the dissociation of H_2 and Cl_2 into H and Cl radicals must be delayed after an equilibrium amount of HCl is formed. This delayed dissociation probably occurs far from the shock front and does not influence its propagation velocity. The formation of H and Cl radicals from the Nernst chain would thus be responsible for the exothermic reaction to form the product HCl, rather than the endothermic dissociation reaction to form the H and Cl radical. Thus the exothermic reaction overshoot gives rise to a detonation velocity in excess of the C-J predictions. In the HN_3 mixture, among the hypotheses to account for the detonation velocity in excess of the ideal equilibrium value, Dupré [21] also pointed out the possible delay in the endothermic formation of radicals.

Von Neumann [64] first pointed out the existence of a possible thermodynamic path that can lead to the weak detonation branch of the equilibrium Hugoniot. He showed that detonation velocities in excess of C-J values could be observed in a system that exhibits a large mole decrement from reactant to product. In such a case, the energy release function includes a volume term that gives rise to a negative contribution to the overall energy release rate when the number of moles is reduced. A vanishing heat release rate can thus be obtained prior to complete chemical equilibration, as a result of the competition between the positive chemical energy release rate and this negative volume change rate. In the case of ideal detonations, the vanishing heat release rate occurs at the sonic plane where the flow is in chemical equilibrium. For pathological detonations, on the other hand, the vanishing heat release also occurs at the sonic plane, but prior to the complete chemical equilibrium of the detonation products. As a result, the ideal C-J criterion cannot be used to determine a unique detonation velocity for "pathological" mixtures. The Generalized C-J criterion must be used instead.

A maximum in the integrated heat release function is observed at the sonic point. This overshoot in chemical energy release is responsible for the detonation velocity being in excess of the ideal C-J value. Von Neumann used a single irreversible chemical reaction with mole decrement to obtain a pathological detonation. Wood and Kirkwood [65] also pointed out the possibility of pathological detonations in multiple reaction systems where the energy release rate vanishes within the reaction zone before complete chemical equilibrium is achieved, a consequence due to the competition between exothermic and endothermic chemical reactions. Unaware of the existence of actual mixtures exhibiting this behavior, Wood and Salsburg [70] even questioned the physical significance of pathological detonations. Long after pathological detonations were first observed experimentally by Zel'dovich and Ratner [72], Guénoche et al. [33] performed a detailed chemical kinetics study of the $H_2 - Cl_2$ mixture. They indeed showed that the heat release function in this mixture exhibits an overshoot prior to chemical equilibrium. Thus this overshoot in energy release caused by the highly exothermic reaction of HCl formation in the Nernst chain is subsequently absorbed only downstream of the sonic plane, when dissociative equilibration is effected. The detonation velocity is thus governed by this maximum heat release, and not by the equilibrium value, and the final state lies on the supersonic branch of the Hugoniot curve. Using the Generalized C-J criterion, Guénoche et al. [33] iterated for the detonation velocity (eigenvalue) and obtained a value 15% above the equilibrium predictions based on the ideal C-J condition. As a result, unlike ideal detonations, pathological detonations are found to be dependent on the rate of the competing exothermic and endothermic reactions.

The above pathological detonations are examples of non-ideal detonations where no source terms are needed in the conservation equations, since it is a chemical mechanism, appearing implicitly in the chemical kinetic rates, which may be responsible for significant deviations from the C-J predictions. Despite the absence of source terms, the Generalized C-J criterion is still needed to solve for the unique detonation solution. The detonation velocities in excess of the C-J predictions observed in the heterogeneous condensed phase explosives studied by Lee [46] were due to loss mechanisms. The detonation mechanism in this explosive can nevertheless be viewed as a competition between the exothermic decomposition of nitromethane, and the endothermic mechanical and thermal relaxation of the solid beads. Pathological detonations thus generally occur as a result of a competition between exothermic and endothermic processes.

The Generalized C-J criterion has been used extensively to determine the eigenvalue detonation solution of explosive systems including the presence of any source term or combination of source terms. The effective heat release rate incorporates the effect of all source terms. This criterion has been used, for instance, to calculate the detonation properties of pathological detonations (Guénoche et al. [33]), condensed explosives detonations (Bdzil [2], Chan [9], Braithwaite [7], Huerta [34]) and two-phase detonations (Fedorov and Khmel' [27], Dionne [17]).

The use of the Generalized C-J criterion in the above studies involved the consideration of the steady flow from the von Neumann state down to the sonic plane. For these non-ideal detonations, the flow is in a non-equilibrium state at the sonic plane. As a result, chemical reactions and other types of mass, energy and momentum transfers are still occurring downstream of the sonic plane, while the flow proceeds towards complete equilibrium in a non-steady manner. According to the Generalized C-J criterion (steady-state ZND analysis), these events behind the sonic plane cannot have any influence on the propagation of the detonation wave, since the sonic plane acts somewhat as a physical barrier, isolating the front from the transient flow in the products. The physical barrier analogy was also used in the work of Jouguet as an additional justification for the minimum (tangency) solution, chosen by Chapman solely on account of its uniqueness. However, Jouguet did not consider the flow downstream of the sonic plane. Taylor [62], however, was the first to point out the necessity of verifying whether the steady boundary condition at the sonic plane can be matched with the unsteady flow downstream of the detonation wave. Following Taylor, an alternative criterion for determining the detonation solution can also be formulated based on whether a detonation solution can allow the steady reaction zone to be matched to the unsteady flow downstream. It turns out that the sonic plane corresponds to a characteristic line, so that the centered expansion fan for the products can be connected to the sonic plane of an ideal detonation. In this sense, Taylor's criterion is equivalent to the ideal C-J condition in the case of ideal detonations. In the presence of source terms (or delayed endothermic reactions), the steady-state solution no longer corresponds to the tangency (minimum) solution. The Generalized C-J criterion has to be used. Similar to the ideal C-J condition, this criterion does not take the flow downstream of the sonic plane into account. However, it is worth investigating if the unsteady flow can still be matched with the steady boundary condition at the sonic plane, in cases where the sonic state is a non-equilibrium state, since this matching is necessary for a stable solution to exist.

The most convenient approach to verify the validity of a steady-state criterion is to carry out a transient analysis of the development of a detonation from initial conditions. In transient calculations, the unsteady Euler reactive equations are used. In a transient analysis, no criterion is necessary to determine a detonation solution, thus an independent check of the validity of a steady-state criterion can be made by comparing the results from the transient calculations and the steady-state analysis of the ZND structure. Transient calculations for ideal detonations have already been performed [28]. Even for one-dimensional detonations without losses, the Generalized C-J criterion (sonic matching) may not be satisfied. For high activation energy, the detonation wave can execute an oscillatory or even chaotic behavior. For low enough activation energies, on the other hand, the asymptotically stable solutions are found to agree with the steady-state results based on the ideal C-J criterion. The existence of a steady wave solution when source terms are included is not guaranteed. It must be examined whether the addition of losses leads to compatibility of the rear transient flow with the sonic condition of the Generalized C-J criterion. If the flow field of the detonation products is not compatible with the steady Generalized C-J criterion, oscillatory solutions may result. Moreover, it must be verified whether the asymptotically stable detonation solution indeed corresponds to the steady-state non-ideal detonation predictions. One of the main objectives of this thesis is therefore to investigate the validity of the Generalized C-J criterion by carrying out steady-state as well as transient numerical simulations of non-ideal detonations and compare their results.

The use of the ZND conservation equations for the ideal detonation case shall first be introduced, where the sound speed problem is discussed and the failure of the Generalized C-J criterion to determine the ideal detonation solution is pointed out (Chapter 2). The Generalized C-J criterion is then applied to seek a steady-state pathological detonation solution for a real explosive system known to exhibit excess in detonation velocity (Chapter 3). It is then verify whether the excess in detonation velocity can indeed be attributed to the overshoot in energy release typical of pathological detonations. The numerical experiments of Guénoche et al. [33] are thus extended to various stoichiometries and initial pressures for the $H_2 - Cl_2$ system, with emphasis on the chemical processes within the reaction zone. The hypothesis of Zel'dovich and Ratner [72] (delayed dissociation of Cl_2) can thus be verified by these numerical experiments.

An analysis of the transient development of pathological detonations shall then be carried out to verify both the existence and the stability of such systems exhibiting detonation velocities in excess of the C-J value. It is not clear that when the steady-state assumption is relaxed (i.e. the sonic condition from the Generalized C-J criterion is removed by doing a transient calculation) a detonation will eventually asymptotically reach the stable solution predicted by the steady-state analysis. Moreover, if an oscillatory solution is obtained, similar to the ideal detonation case with high activation energy, it is obvious that there cannot be any stationary sonic plane (relative to the shock) imbedded in the reaction zone where the effective energy release vanishes. It is thus worthwhile to verify whether the averaged properties of oscillatory pathological detonations can nevertheless be correlated with the steady-state predictions obtained assuming the existence of such a sonic plane.

The role of source terms in the conservation equations is then investigated for the modeling of non-ideal detonations (Chapter 4). A source term is introduced in the momentum equation to account for the effect of friction, and a source term in the energy equation accounts for heat transfer to the walls. It is again interesting to compare the results from the steady state analysis to the transient calculations where the detonation is initiated from arbitrary initiation conditions. Lee and Zhang [44] performed such a comparison and have shown that friction induces instability in the flow, and that the averaged properties of oscillatory detonations with friction correspond to the steady state predictions. Unlike the pathological detonation case, where there exists a well-defined range of possible solutions above the C-J value, the detonation velocities when friction and heat transfer are introduced are below the C-J predictions, and defining a lower bound for the possible solutions is not obvious. Lee and Zhang [44] did not investigate the case of low-velocity detonations, below the validity range of the Generalized C-J criterion. These low-velocity solutions could possibly simulate the effect of very high friction caused by large arrays of obstacles (porous medium). In this thesis, the low-velocity regime is investigated and a new criterion to determine the steady state solutions will be sought. A qualitative comparison will be made with the experimental results of Lyamin [48] and Makris [50] to verify if the present model successfully reproduces the main qualitative features observed experimentally.

Based on the above discussions, the validity of the Generalized C-J criterion in the steady-state analysis of non-ideal detonations shall be critically examined (Chapter 5). The limitations of this criterion will be discussed, and an alternative criterion will be suggested.

Chapter 2

The Detonation Structure Equations

A model for the structure of detonation waves was first introduced in the 1940's independently by Zel'dovich [71], von Neumann [64] and Döring [19], now generally referred to as the ZND model. When applied to non-ideal detonations, the ZND model requires not only knowledge of the rates of the chemical reactions, but also the mechanisms responsible for the non-ideal behavior. These mechanisms can be modeled as source terms in the conservation equations. Although the ZND model is well established for ideal detonations, it has not been discussed in a unified way for non-ideal detonations. Thus, a general formulation of the basic equations for the structure of non-ideal detonations shall be presented with emphasis on the important concepts regarding the criterion for determining a steady-state solution to these equations. The present chapter serves to introduce the ZND equations for the detonation structure and discuss the issue of choosing an appropriate criterion to determine the steady-state solution, thus paving the way for the analysis given in the subsequent chapters of the thesis.

2.1 – CONSERVATION EQUATIONS FOR THE STRUCTURE OF NON-IDEAL DETONATIONS

The ZND equations for non-ideal detonations can be derived starting from the unsteady Euler equations with source terms (fixed laboratory frame):

$$\frac{\partial\rho}{\partial t'}+\frac{\partial(\rho u')}{\partial x'}=m$$

$$\frac{\partial(\rho u')}{\partial t'}+\frac{\partial}{\partial x'}\left(\rho u'^2+p\right)=f$$

$$\frac{\partial(\rho e')}{\partial t'}+\frac{\partial}{\partial x'}\left[u'(\rho e'+p)\right]=q$$

$$e'=\frac{p}{\rho(\gamma-1)}-\lambda Q+\frac{1}{2}u'^2 \tag{2.1}$$

where m, f and q account respectively for the source terms in the mass, momentum and energy equations. The variables ρ, u, p, x, t, Q, γ, and e respectively stand for the density, particle velocity, pressure, distance, time, chemical heat release, ratio of specific heats, and the sum of the internal and kinetic energies. The primes indicate values relative to the fixed laboratory frame. In the present study, a polytropic equation of state (EOS) is assumed for simplicity. The parameter λ denotes the degree of reaction ($\lambda=0$ corresponds to unreacted explosive, $\lambda=1$ corresponds to fully reacted products). Equations 2.1 can be rewritten in terms of a reference frame attached to the moving shock, and when the time derivatives are equated to zero for a steadily propagating wave, one obtains:

$$\frac{d(\rho u)}{dx}=m$$

$$\frac{d}{dx}\left(\rho u^2+p\right)=Dm-f$$

$$\frac{d}{dx}\left[u(\rho e+p)\right]=\frac{1}{2}D^2m-Df+q$$

$$e=\frac{p}{\rho(\gamma-1)}-\lambda Q+\frac{1}{2}u^2 \tag{2.2}$$

This coupled set of ordinary differential equations (ODE) can be reduced to a single differential equation with the particle velocity u as the dependent variable by performing a series of algebraic manipulations (Appendix I). The resultant equation is:

$$\frac{du}{dx}=\frac{(\gamma-1)\left[\rho\dot{\lambda}Q+q\right]+m\left[-\gamma u(D-u)+c^2\right]+f\left[\gamma u-D(\gamma-1)\right]}{\rho\left(c^2-u^2\right)} \tag{2.3}$$

where $\dot{\lambda}=d\lambda/dt$ is the chemical heat release rate. For a given shock strength, the state behind the shock can be determined from the Rankine-Hugoniot relationships which serve as initial conditions for the integration of Eqn. 2.3 for the thermodynamic profiles within the detonation structure.

2.1.1 – The Source Terms

In this section, examples of functional forms of source terms used to model non-ideal detonation within the framework of a 1-D (or quasi 1-D) model are presented. Frictional losses in tubes are modeled by introducing a source term f in the momentum equation. For instance, Zel'dovich et al. [73] suggested the following form:

$$f=k_f\,\rho\,u_{abs}\left|u_{abs}\right| \tag{2.4}$$

where u_{abs} is the particle velocity in the laboratory frame, and k_f is a friction factor given by Schlichting's formula, i.e.:

$$k_f=2\left[2\log(R/k_s)+1.74\right]^{-2}$$

where k_s is the equivalent sand roughness and R is the tube radius. This friction factor is valid for flow regimes with full exposure of roughness, and for Reynolds numbers based on the height of the roughness elements above 530. The absolute value in Eqn. 2.4 accounts for the fact that friction always tends to oppose the motion of the flow. Lee and Zhang [44] used a very similar function where they included the effect of the tube diameter independently from k_f, i.e.:

$$f = \left(\frac{2}{D_h}\right) k_f \rho u_{abs} |u_{abs}|$$

where k_f is assumed to obey the Blasius formula, i.e.:

$$k_f = \frac{0.3164}{\mathrm{Re}^{0.25}}$$

The Reynolds number Re is based on the hydraulic diameter of the tube D_h. In the present study, only the qualitative behavior of non-ideal detonation is investigated. Therefore, Eqn. 2.4 with a constant value of k_f will be used to model frictional losses.

External heat losses are modeled by introducing a source term q in the conservation of energy equation. For example, Zel'dovich et al. [73] used the following form to account for heat losses to the tube walls, i.e.:

$$q = \gamma C_h^{sm} \rho u_{rel} C_p \left(T^* - T_w\right)$$

where C_h^{sm} is the coefficient of heat transfer for a smooth tube, u_{rel} is the particle velocity relative to the shock, T^* is the stagnation temperature and T_w is the wall temperature. An alternative approach to model heat losses in tubes with friction is to use Reynolds analogy. This analogy relates the heat losses to the frictional losses:

$$\frac{h_c}{\rho u_{rel} C_p} = \frac{f}{2}$$

where h_c is the heat transfer coefficient, and f is the source term for friction, as given in Eqn. 2.4, for example. This relation is then used to obtain a functional form for the source term q, i.e.:

$$q = \frac{\gamma}{\gamma - 1} \frac{f}{u_{rel}} \left(T - T_w\right) \tag{2.5}$$

where T is the local temperature of the detonation products. In the present study, Eqn. 2.5 will be used to account for heat losses in the presence of friction. The advantage of using this formulation in the context of a qualitative parametric study is that no additional coefficient is necessary to account for heat losses.

A source term m in the conservation of mass equation is present when there is an area change due to the curvature of the shock front. Even if friction and heat losses are assumed to be negligible, source terms due to area change must be included in the three conservation equations. This can be explained by the fact that in a quasi 1-D model, the momentum and energy carried by the gas flowing in the radial direction are considered as effective losses in the axial direction. As a result, the conservation equations in the laboratory frame (Eqn. 2.1) where the stream tube area is given by $A = A(x')$ become [45]:

$$\frac{\partial \rho}{\partial t'} + \frac{\partial(\rho u')}{\partial x'} = -\frac{1}{A}\frac{dA}{dx'}\rho u$$

$$\frac{\partial(\rho u')}{\partial t'} + \frac{\partial}{\partial x'}\left(p + \rho u'^2\right) = -\frac{1}{A}\frac{dA}{dx'}\rho u'^2$$

$$\frac{\partial(\rho e')}{\partial t'} + \frac{\partial}{\partial x'}\left[u'(\rho e' + p)\right] = -\frac{1}{A}\frac{dA}{dx'}u'(\rho e' + p)$$

In the present study, area change is not considered, since it has already received significant attention in the literature in considering failure diameter in condensed explosives [66], [7], [61], [2], [9], [34]. Therefore, only the source terms f and q accounting for frictional and heat loss rates will be considered.

2.1.2 – The Criterion to Determine the Detonation Solution

With the presence of source terms in Eqns. 2.2, the classical C-J criterion can no longer be used to select the unique detonation solution. Chapman's minimum velocity solution does not apply, since the integral curve is no longer a straight line (Rayleigh line) to permit a solution tangent to the equilibrium Hugoniot to be found directly. Jouguet's criterion is also invalid, since the detonation products are no longer in equilibrium within the reaction zone when the sonic plane is reached. Hence, an alternative criterion has to be defined to seek a unique solution to the conservation equations for the detonation structure. When the particle velocity becomes sonic (i.e. $M = u/c = 1$) in Eqn. 2.3, the denominator vanishes. Hence, for an arbitrary value of the numerator, the solution becomes singular at the sonic plane. The derivatives of the thermodynamic variables then become infinite. This singularity can be removed if one seeks a particular integral curve in which the numerator also vanishes simultaneously with the denominator. This results in an indeterminate value for the derivative du/dx and permits a smooth transition through the sonic point. The condition of requiring that the numerator vanishes when the sonic condition is reached is often referred to as the "Generalized C-J criterion" in the literature, even though both of the classical Chapman and Jouguet's criteria do not involve the analysis of the non-equilibrium detonation structure. This criterion provides a means of seeking a particular integral curve to the conservation law for the detonation structure that is regular. This particular solution is sometimes also referred to as an "eigenvalue" solution.

Expressions for the source terms m, f, and q in the numerator of the du/dx equation depend on the models used to describe the physical processes. The different source terms also compete with the chemical energy release to drive the flow towards Mach 1. At the sonic plane, all these effects are balanced out, so that the effective heat release rate is zero there. The Generalized C-J criterion can therefore be written as:

$$(\gamma-1)\left[\rho\dot{\lambda}Q+q\right]+m\left[-\gamma u(D-u)+c^2\right]+f\left[\gamma u-D(\gamma-1)\right]=0$$

$$\text{when} \quad u = c$$

The differential equation for *du/dx* (Eqn. 2.3) will be used in the subsequent chapters to model non-ideal detonations due to different mechanisms. Generally, non-ideal detonations have velocities *less* than the ideal C-J values. However, detonations with velocities in *excess* of the ideal equilibrium C-J values are also possible when there is an overshoot in the energy release function. These detonations are referred to as "pathological detonations" and will be investigated. The overshoot is due to a rapid exothermic process and a slower endothermic one. The endothermic process can be accounted for by adding a source term q in the energy equation (Chapter 3). In order to study non-ideal detonations with velocities below the equilibrium C-J value (e.g. gaseous detonations propagating with very low velocities in porous medium or in obstacle-filled tubes) the source terms f and q will be introduced in the momentum and energy equations (Chapter 4). Note that the Generalized C-J criterion for non-ideal detonations reduces to the classical C-J criterion for ideal detonations when all the source terms m, f, and q vanish. The equivalence of the Generalized C-J criterion to the classical C-J criterion for ideal explosives will be discussed in more detail in the next section.

2.2 – THE CLASSICAL CHAPMAN-JOUGUET CRITERION FOR IDEAL DETONATIONS

In view of the existence of separate criteria that can be used to determine a detonation solution, it is worthwhile to discuss their equivalence or similarity. Based on the experimental observation that the detonation velocity for a given mixture is unique, Chapman [10] proposed that the appropriate detonation solution to the conservation equations should correspond to the minimum velocity solution when the Rayleigh line is just tangent to the equilibrium Hugoniot curve. This tangency requirement then leads to a unique solution of the conservation equations across the detonation wave. Jouguet later demonstrated [37] that Chapman's tangency solution corresponds to a sonic particle velocity of the detonation products (relative to the shock front) at the equilibrium plane. Thus, it is possible to define an alternate criterion based on Jouguet stating that the desired detonation solution should be one where the velocity at the end of the reaction zone is sonic. Jouguet also presented the physical argument that on account of this sonic condition, the detonation wave is not affected by the perturbations downstream, and is thus independent of the initial conditions. Chapman's tangency criterion and Jouguet's sonic condition are equivalent in that they both give the same result. They can be used independently to determine the ideal detonation solution (i.e. without source terms). However, the actual procedure of iteration for the detonation solution is different using Chapman's criterion of minimum velocity or Jouguet's criterion of sonic condition at the end of the reaction zone. To solve for the detonation solution using Jouguet's criterion, one must find the point along the equilibrium Hugoniot where the particle velocity is equal to the sound speed. When using Chapman's criterion, one must find the point along the equilibrium Hugoniot that is tangent to the Rayleigh line. In both cases, one does not need to consider the actual path of the chemical reaction with the detonation structure. The solution can be obtained by considering only the global conservation laws for a control volume across the entire detonation zone.

In Jouguet's original work, the model used was idealized and the possibility of two sound speeds did not arise until more detailed chemical reaction processes were later considered. When considering mixtures of gases in which reversible chemical reactions can occur, Jouguet's criterion posed a problem, since two sound speeds could be defined. The frozen sound speed corresponds to one where the composition of the mixture across the sound wave is constant. This occurs when the characteristic chemical reaction time is long with respect to the characteristic time for the variation of the thermodynamic variables across the sound wave (high frequency sound waves). The equilibrium sound speed is the other limit of very fast chemical reactions (low frequency sound waves) where the composition varies across the sound wave. In reality, the sound waves may propagate at a velocity somewhere between these two limits. If one uses the sonic criterion of Jouguet, then the existence of two sound speeds can lead to two distinct detonation solutions and thus creates a problem regarding the correct sound speed to use in solving for the detonation solution.

Wood and Kirkwood [65] were among the first to address this difficulty of the two sound speeds. They first argued that the appropriate sound speed to use in the detonation calculations should be the frozen one, since the frozen sound speed naturally appears in the formulation of the ZND structure equations. This would then lead to a weak detonation solution on the equilibrium Hugoniot. Although it appears that weak detonations seem to explain the experimental observations of Fay and Opel [25] who measured supersonic Mach numbers behind the detonation front ($40\%\ C_2H_2 - 60\%\ O_2$) from the Mach angle, there is a problem as to how the weak detonation point on the equilibrium Hugoniot can be reached. Wood and Kirkwood [67] later reversed their view. They found that the weak detonation solution based on the sonic point using the frozen sound speed could not be reached if the integral curves start from the von Neumann state behind the shock (at least in the case of using a single irreversible reaction). This is due to the fact that the flow proceeding down the Rayleigh line must first intersect the strong detonation solution on the subsonic branch of the Hugoniot and stop there, since further changes along the Rayleigh line from the strong to the weak solution correspond to an expansion shock and thus violates the 2nd law of thermodynamics. Wood and Kirkwood [67] could not generalize their result to more than one reaction, but this argument was sufficient to raise some serious doubts about the existence of a weak detonation solution based on the frozen sonic condition. Duff [20] later performed a detailed numerical calculation of the ZND detonation structure of the $H_2 - O_2$ system by integrating the ZND structure equations with detailed chemistry. He used the detonation velocity based on the frozen sonic condition. Similar to the single-irreversible reaction case discussed by Wood and Kirkwood, the results from Duff's calculations also indicate that the final point must correspond to the strong solution on the subsonic branch of the equilibrium Hugoniot. Hence, the C-J solution cannot be reached if the frozen sound speed is used to determine the solution using Jouguet's criterion. Analytical studies with multiple reactions were later carried out by Wood and Kirkwood [68], Wood and Parker [69], and Wood and Salsburg [70]. Eventually, the conclusion was that the correct solution should be the one based on the equilibrium sound speed. Chapman's tangency solution is thus equivalent to Jouguet's sonic criterion, only when the equilibrium sound speed is considered. For an ideal detonation calculation, one does not have to resolve the structure, so one can freely choose to use the equilibrium sound speed for the Jouguet criterion.

For a non-ideal detonation, one can no longer obtain the detonation state based on the conservation laws for a control volume encompassing the entire detonation zone. Due to the presence of source terms, the conservation equations in differential form have to be integrated, and the Generalized C-J criterion is then used to determine the particular integral curve that is regular when the flow is sonic. One can think of an ideal detonation as the limiting case of non-ideal detonation where all source terms are zero. It should therefore be possible to apply the Generalized C-J criterion to determine a unique solution for ideal detonations also by considering the structure rather than just the global conservation laws. When equating m, f, and q to zero, Eqn. 2.3 reduces to:

$$\frac{du}{dx}=\frac{(\gamma-1)\dot{\lambda}Q}{c_f^2-u^2} \qquad (2.6)$$

When chemical equilibrium occurs, the overall chemical reaction rate vanishes (forward and backward rates cancel each other out) so that the numerator of Eqn. 2.6 vanishes as in the Generalized C-J criterion. Hence, chemical equilibrium at the sonic plane is equivalent to the vanishing numerator requirement. The denominator of the *du/dx* equation (Eqn. 2.6) vanishes when the particle velocity is equal to the frozen sound speed. This is a consequence of the conservation equations (not based on any particular assumption). Thus, for an ideal detonation, the use of the Generalized C-J criterion will lead to a solution if at chemical equilibrium, the sonic condition is based on the *frozen* sound speed. As discussed previously, the conclusions of Wood and Salzburg [70] were that the particle velocity at the end of the reaction zone should be equal to the *equilibrium* sound speed. Thus, the Generalized C-J criterion does not lead to the classical Chapman-Jouguet solution for the case of ideal detonations. However, when there is no distinction between the frozen and equilibrium sound speeds, the Generalized C-J criterion then becomes equivalent to the classical Chapman and Jouguet's criteria.

To compute the detailed structure of an ideal detonation, one must select a detonation velocity corresponding to the equilibrium sound speed solution first using either Chapman or Jouguet's criterion. Then, the thermodynamic profiles within the structure are obtained through the integration of Eqn. 2.6. When the flow reaches chemical equilibrium, the particle velocity is now equal to the equilibrium sound speed, since the detonation velocity is determined from the Chapman or the Jouguet criterion using the equilibrium sound speed. Since the equilibrium sound speed is always less than the frozen one, the denominator of the du/dx equation never vanishes (no singularity) within the reaction zone. Thus, the derivative du/dx is equal to zero at the sonic plane since chemical equilibrium ensures that the numerator vanishes.

On the other hand, the sound speed problem does not arise when considering non-ideal detonations. This is due to the fact that the detonation products at the sonic plane are not in equilibrium. Hence the equilibrium sound speed cannot be defined. The Generalized C-J criterion will therefore be used for the study of pathological detonations (Chapter 3), where an overshoot in the chemical energy release is observed, and also for detonations in rough tubes (Chapter 4). In the latter case, it will be shown that the Generalized C-J criterion is not applicable for very low detonation velocity solutions, because the flow becomes entirely subsonic relative to the shock.

Chapter 3

Pathological Detonations

Although the possibility of pathological detonations was first suggested by von Neumann [64], it was Guénoche et al. [33] who first integrated the steady ZND structure equations with detailed chemical kinetics and obtained detonation velocities in excess of the C-J predictions for the H_2-Cl_2 system. Their computations were restricted to the stoichiometric case at one atmosphere and hence their work is extended in the present study over a wider range of conditions to investigate the effect of equivalence ratio and initial pressure on the pathological behavior more thoroughly. More extensive experimental data is also obtained to compare with the numerical results. The present experiments in the H_2-Cl_2 mixture have been carried out in a much longer tube than those used in previous studies in order to ensure that truly steady detonations were observed [18].

In steady-state analysis, only the structure has to be considered and one does not have to worry about the back boundary conditions past the sonic plane ($u=0$ at $x=0$, or $u=u_p$ at the piston surface $x=x_p$). Hence, it is not obvious that the solution is valid in the case of pathological detonations, since chemical reactions are still going on downstream of the sonic plane. Therefore, to verify the existence of the steady-state pathological detonation solutions, one must examine the non-steady development of the detonation and solve for the entire flow field from the back boundary to the leading shock front to determine if a steady-state solution can be approached asymptotically. An unsteady one-dimensional numerical computation of the transient development of a pathological detonation is thus carried out to verify if the steady pathological detonation can be realized under arbitrary initial conditions of the initiation process.

3.1 - STEADY-STATE DETONATION STRUCTURE OF H_2-Cl_2

In the $H_2 - Cl_2$ system, Zel'dovich and Ratner [72] pointed out that on the basis of the Nernst chain for the $H_2 - Cl_2$ reaction, two molecules of HCl can be produced from H_2 and Cl_2 without a change in radical concentration of H and Cl, i.e.

a) $H_2 + M \leftrightarrow 2H + M$

b) $Cl_2 + M \leftrightarrow 2Cl + M$

c) $H_2 + Cl \leftrightarrow HCl + H$

d) $H + Cl_2 \leftrightarrow HCl + Cl$

The vibrationally-excited molecules are not considered in the above simplified model, since they do not affect the qualitative behavior of the mixture. The reactions a) and b), referred to as the chain initiation, are responsible for the formation of the H and Cl radicals (H_2 goes into $2H$, and Cl_2 goes into $2Cl$). These two equations are endothermic. The reactions c) and d), referred to as the chain reaction, are responsible for the formation of the main product, HCl. Globally, these two reactions are exothermic. A closer look at the chain reactions shows that the Cl radical required by reaction c) is provided by reaction d).

Similarly, the H radical required by the reaction d) is provided by the reaction c). As a result, the chain reaction can be rewritten as an overall reaction $H_2 + Cl_2 \rightarrow 2HCl$. Thus the global reaction can proceed at any concentration of the radicals H and Cl, since the concentrations of H and Cl remain unaffected by the chain reaction. Moreover, the activation energy of the chain reaction is relatively small as compared to the activation energy of the dissociation of the Cl_2 molecules. As a result, the dissociation of Cl_2 is delayed after an equilibrium amount of HCl has already been produced. And since the dissociation of Cl_2 is endothermic, this means that the heat release for this mixture will proceed in two steps: first the exothermic step (formation of the HCl product), followed by an endothermic step of Cl_2 dissociation afterwards. Thus the highly exothermic reaction of HCl formation from $H_2 + Cl \rightarrow HCl + H$ can lead to an overshoot in the energy release in the reaction zone which is subsequently absorbed in the endothermic dissociation reaction of Cl_2. As a result, the detonation velocity in this mixture is governed by the overshoot in the energy release occurring before the complete endothermic formation of Cl radicals from the dissociation of Cl_2.

The $H_2 - Cl_2$ mixture is convenient to use in a numerical study, since its detailed chemical kinetics are relatively simple and the rate constants are fairly well known. In the present section, the numerical simulations of Guénoche et al. are thus extended to different initial compositions and initial pressures, to verify the hypothesis of Zel'dovich and Ratner regarding the delayed dissociation of the Cl_2 molecule downstream of the sonic plane. The ZND structure equations with detailed chemistry shall first be derived.

3.1.1 – The ZND Equations with Detailed Chemistry

The detailed chemical kinetics of the $H_2 - Cl_2$ mixture is now used in the analysis of the ZND detonation structure. The ZND structure equations, derived previously in Chapter 2, shall now be used. No source terms are necessary, since the reasons for pathological behavior are implicit in the particular chemical kinetics scheme used. Instead of using a polytropic gas equation of state with constant specific heats, the ideal gas equation of state, coupled with a caloric equation of state shall now be used. After algebraic manipulations, one obtains the following expression for the du/dx derivative:

$$\frac{du}{dx} = -\frac{\frac{\rho}{m}\sum_i \frac{dn_i}{dt}\left\{\bar{h}_i - \frac{\partial R_s}{\partial n_i}\frac{T}{R_s}\sum_j n_j \frac{d\bar{h}_j}{dT}\right\}}{\rho u^2 + \frac{1}{mR_s}\sum_i n_i \frac{d\bar{h}_i}{dT}\left[P - \rho u^2\right]} \tag{3.1}$$

The complete derivation is shown in Appendix IV. Kinetic rate equations have to be provided for each elementary reaction to get the molar change rates dn_i/dt. Through these rates, the conservation of atoms is automatically taken care of. In the present study, the same chemical kinetics scheme as suggested by Guénoche is used (Table 3.1).

Although Eqn. 3.1 is very convenient for computational purposes, it is easier to interpret when written in a different form. By substituting expressions for the specific heat at constant pressure c_p, the ratio of the specific heats γ, and the frozen sound speed c_f for the mixture, one can write the du/dx derivative as:

$$\frac{du}{dx} = \frac{\gamma\dot{Q}}{\left(c_f^2 - u^2\right)}$$

This simplified expression is also derived in Appendix IV. The denominator of the du/dx derivative vanishes when the particle velocity becomes sonic ($u = c_f$) during the course of the integration. To avoid a singular point, the numerator has to go to zero simultaneously (Generalized C-J criterion). For the numerator to vanish, the heat release rate $\dot{Q}$ has to go to zero when the flow becomes sonic relative to the shock front.

The equation *du/dx* used for pathological detonation is the same as that for ideal detonations. For ideal detonations, the heat release rate vanishes when the flow reaches chemical equilibrium. However, in the case of pathological detonations, the heat release rate $\dot{Q}$ becomes zero at the transition from exothermic to endothermic reactions. As a result, the value of the heat release function Q at the sonic plane reaches a maximum (overshoot value) above the equilibrium C-J value. This will result in an excess in the detonation velocity over the equilibrium C-J value. It is the parameters in the chemical kinetics equations that determine whether the detonation is pathological or not.

3.1.2 – Steady-State H_2-Cl_2 Numerical Results

The eigenvalue solution (i.e. the particular solution where the numerator and denominator vanish simultaneously) is found by iterating for the detonation velocity that satisfies the Generalized C-J criterion. An initial detonation velocity is assumed. The *du/dx* equation (Eqn. 3.1) is integrated from the von Neumann point until either the numerator (effective energy release rate) or the denominator vanishes (at the sonic plane). If the numerator vanishes prior to the sonic plane, a lower shock velocity is then assumed. If the sonic plane is reached prior to a net vanishing heat release rate, a higher shock velocity is assumed instead. The iterations are repeated until the shock velocity is determined within six decimal places. The profiles of the thermodynamic variables can be obtained for the whole reaction zone, even beyond the sonic plane. When the derivative *du/dx* is indeterminate (i.e. when $u = c_f$), L'Hospital's rule is used to obtain the slope of the thermodynamic functions there.

The eigenvalue detonation propagates with a velocity above the equilibrium C-J value, corresponding to a steeper Rayleigh line on the $p-v$ diagram. As the flow proceeds down this steeper Rayleigh line (Fig. 3.1), it appears to intersect the equilibrium Hugoniot above the C-J value in the $p-v$ plane. However, this intersection point does not correspond to the equilibrium strong detonation state. This is due to the fact that the flow is not at equilibrium yet, so the temperature and composition of the mixture are not the same as the equilibrium strong detonation state (even though the pressure and specific volumes are the same). The flow can keep proceeding down the Rayleigh line as the chemical reactions continue. Eventually, the particle velocity becomes sonic (relative to the shock front) and the chemical energy release rate in Eqn. 3.1 simultaneously vanishes, if the particular solution as dictated by the Generalized C-J criterion is chosen. Since the flow is not yet at equilibrium when the sonic condition is reached, chemical reactions continue further downstream of the sonic plane. For an unsupported detonation, when the chemical reactions are completed (equilibrium) along the Rayleigh line, the state corresponds to the weak detonation state on the equilibrium Hugoniot. The competition between exothermic and endothermic reactions thus provides a path to the weak detonation branch of the equilibrium Hugoniot without violating the 2nd law of thermodynamics. Hence, pathological detonations are weak detonations if one considers the final state being on the weak branch of the equilibrium Hugoniot. However, the detonation velocity is determined by the non-equilibrium energy release at the sonic plane.

The ZND structure calculations permit us to plot the chemical species profile downstream of the shock front. For a detonation wave moving towards the right, Fig.3.2 indicates the number of moles of various species with respect to the local Mach number of the flow, for the H_2-Cl_2 mixture, $\phi=0.667$ and $p_o=6\,kPa$. Immediately downstream of the shock front, the flow is subsonic. The flow Mach number then increases to a value of 1, corresponding to the sonic plane, and eventually reaches supersonic values, which is typical behavior of weak detonations that have a sonic plane embedded within the reaction zone. The amount of HCl molecules produced at the sonic plane (dotted line) is found to be very close to the equilibrium value HCl^o corresponding to the final equilibrium state on the equilibrium Hugoniot. The concentrations of Cl_2 and Cl at the sonic plane are still far from their respective equilibrium values Cl_2^o and Cl^o. Fig. 3.2 therefore clearly demonstrates that the dissociation of Cl_2 molecules is not yet complete at the sonic plane, even though an equilibrium amount of HCl has already been produced. This confirms the suggestion of Zeldovich and Ratner [72], i.e. the delayed dissociation of Cl_2 beyond the sonic plane.

The heat release as a function of the local Mach number for the same case is shown on Fig. 3.3. The increasing part of the curve corresponds to the exothermic formation of HCl molecules. The second part corresponds to the endothermic dissociation of Cl_2. The overshoot in heat release observed at the sonic plane is in agreement with the Generalized C-J criterion that states that the net heat release rate has to vanish there (a zero rate corresponds to a maximum in the function). As a result, the detonation state is governed by this overshoot value, rather than by the equilibrium C-J prediction. This overshoot, which is the main characteristic of pathological detonations, is responsible for the detonation velocities being in excess of the C-J predictions. In the ideal detonation case, the heat release function would monotonically increase to the C-J value. No overshoot would be observed.

The theoretical values for the detonation velocity for pathological detonations are now computed for various compositions and initial pressures. The predicted detonation velocities are found to be independent of the initial pressure for all 3 equivalence ratios (Fig. 3.4). This is in agreement with Zeldovich and Ratner's hypothesis that the Cl_2 dissociation occurs beyond the sonic plane, and hence does not influence the detonation velocity. The present theoretical ZND calculation also confirms the existence of pathological detonations in $H_2 - Cl_2$ mixtures, as can be readily observed in Fig. 3.5, where the detonation velocities are found to be greater than the equilibrium C-J values. The velocities have been normalized with the C-J values and the largest pathological behaviors are observed at low initial pressures, in mixtures with a low equivalence ratio, where dissociation of Cl_2 molecules is important.

The present analysis using a detailed chemical kinetics scheme thus succeeds in demonstrating qualitatively the existence of pathological detonations in $H_2 - Cl_2$ mixtures. The independence of the detonation velocity on the initial pressure as first suggested by Zel'dovich and Ratner is also confirmed. These numerical results will now be compared with new accurate experimental data on $H_2 - Cl_2$ detonations.

3.2 – EXPERIMENTAL INVESTIGATION OF H_2-Cl_2 DETONATIONS

Although previous experimental studies have appeared to indicate the existence of pathological detonations in $H_2 - Cl_2$ mixtures (Fig. 3.6), the results are not conclusive. Hence, it is of value to carry out more precise measurements of detonation velocities in H_2-Cl_2 mixtures to confirm experimentally the existence of pathological detonations.

3.2.1 – Experimental Details

Measurements of the detonation velocity were carried out in a 12 m long cylindrical tube, with a diameter of 50.8 mm. The long length of the tube used (200 diameters) is sufficient to ensure that steady-state detonation can be achieved. Detonations were initiated via a high-energy electric spark from a 0.9 μF - 40 kV discharge. Four pressure transducers (PCB-113A24 and PCB-401A25) were used to measure the detonation pressure and the time of arrival of the detonation front at different locations in the final 8 meters of the tube. The detonation velocities were found to be stable within 1% according to the $x-t$ diagrams (Fig. 3.7). Explosive mixtures of H_2-Cl_2 of desired composition are prepared by a partial pressure technique and allowed to mix by diffusion for at least 3 days prior to use. The error in the mixture composition is found to be less than 0.1% and this limitation is due to the accuracy in reading the pressure gauges. The initial pressure of the mixtures studied is in the range of 3 kPa to 25 kPa.

3.2.2 – Experimental Results

Detonation velocities are first determined in a mixture that has the normal ideal behavior in accord with equilibrium C-J theory. Stoichiometric $C_2H_2-O_2$ mixtures at initial pressures p_o ranging from 3 kPa to 25 kPa are used. These experimental results are shown in Fig. 3.8 together with the theoretical C-J values for comparison. One notes that the experimental values are typically 1% to 3% below the theoretical C-J predictions, and this velocity deficit is due to the fact that the velocities have not been corrected for the boundary layer effects.

Three compositions of $H_2 - Cl_2$ with equivalence ratios of $\phi = 0.667$, $\phi = 1.0$, and $\phi = 1.5$, representing lean, stoichiometric and rich mixtures, are investigated. The experimental detonation velocities have been corrected for boundary layer effects using the Fay-Dabora theory [25], [15] to offer a better comparison with theory. The complete experimental results are shown in Table 3.2, together with the theoretical predictions. According to these experimental results, one first notes that, for the three mixtures investigated, the detonation velocities are practically independent of the initial pressure in accord with the theoretical steady-state analysis and this confirms the explanation given by Zel'dovich and Ratner, i.e. HCl production independent of Cl_2 dissociation (Fig. 3.9). These results are also found to differ from the equilibrium C-J theory, based on complete chemical equilibrium at the sonic plane. The experimental and ideal C-J detonation velocities are compared for the stoichiometric mixture in Fig. 3.10. The equilibrium C-J detonation velocity in $H_2 - Cl_2$ decreases with decreasing initial pressure of the mixture, due to increased endothermic dissociation and also due to the internal energy being partitioned among a larger number of species molecules in the detonation products. However, the experimental results do not show the same trend as the equilibrium C-J theory, due to the fact that the dissociation occurs mostly beyond the sonic plane where it no longer affects the propagation of the detonation front. From Fig. 3.10, one can conclude that the detonations in the $H_2 - Cl_2$ mixture are pathological. The experimental detonation velocities for the three mixtures normalized with respect to the ideal C-J values are shown in Fig. 3.11. The greatest pathological effects are observed at low initial pressures, where Cl_2 dissociation becomes more important, thus lowering the equilibrium C-J velocity. Below initial pressures of 6 kPa, the experimental detonation velocities are at least 2% above the ideal C-J predictions for all mixtures. The pathological effect is enhanced for mixtures with equivalence ratio below unity (excess Cl_2). For $\phi = 0.667$ and $p_o = 3.33$ kPa, the experimental detonation velocity exceeds the C-J value by as high as 10%. This is an additional indication of the important role of Cl_2 dissociation, as the concentration of this molecule is larger for mixtures with low equivalence ratios where the Cl_2 concentration is higher.

Although the steady-state analysis with detailed chemistry successfully reproduced the essential features observed experimentally (i.e. detonation velocity independent of the initial pressure, higher pathological effect for lean mixtures), large deviations are observed between the theoretical pathological detonation velocities and the experimental values. For instance, for the $\phi = 0.667$ mixture, the theoretical and experimental detonation velocities are shown in Fig. 3.12. Unlike ideal detonations, pathological detonations are rate dependent, and thus are more sensitive to temperature variations due to the boundary layer or multi-dimensional shock front. This could account for the deviations observed between the numerical and experimental results.

The present study confirms both experimentally and theoretically the existence of pathological detonations in $H_2 - Cl_2$ mixtures and that the effects are more pronounced at low initial pressures and low equivalence ratios where the dissociation of Cl_2 becomes important. The kinetic mechanism as proposed by Zel'dovich and Ratner [72] responsible for pathological detonations is confirmed by the present experimental results. The current kinetic scheme used in the ZND structure leads to predictions that are in reasonable agreement with the experimental results.

3.3 – SIMPLIFIED MODEL FOR PATHOLOGICAL DETONATIONS

In the previous section, the steady ZND structure of $H_2 - Cl_2$ detonations was solved to obtain the steady-state pathological detonation solution. However, it is not clear that this steady-state solution can be realized asymptotically from arbitrary initiation conditions. A transient study is thus carried out to verify if steady pathological detonations can be achieved from a transient development. Performing a non-steady analysis of pathological detonations with detailed chemistry would require enormous computer time. Hence, a simplified two-rate chemical reaction model (suggested by Fickett and Davis [29]) will be used instead. A parametric study can also be easily performed with this simple model, by varying the activation energies and the magnitude of the chemical heat release associated with each of the two reactions. Prior to the transient computation of pathological detonations, the steady-state structure of pathological detonations shall first be investigated based on this simpler two-rate model of Fickett and Davis [29] to provide a basis of comparison for the transient computations.

3.3.1 – Steady-State Structure with a Two-Rate Law

The simple two-step chemical rate law suggested by Fickett and Davis [29] consists of two consecutive irreversible reactions. An irreversible exothermic reaction changes molecule A into molecule B. It is followed by an irreversible endothermic reaction that changes the molecule B into molecule C:

$$A \rightarrow B \ \ (exothermic)$$

$$B \rightarrow C \ \ (endothermic)$$

For both reactions, an Arrhenius rate law is used, i.e.:

$$\frac{d\lambda_1}{dt} = k_1(1-\lambda_1)\exp\left(\frac{-E_{a_1}}{RT}\right) \qquad \frac{d\lambda_2}{dt} = k_2(\lambda_1-\lambda_2)\exp\left(\frac{-E_{a_2}}{RT}\right)$$

The parameters E_{a_1} and E_{a_2} denote the activation energies of the exothermic and endothermic reactions respectively, and k_1 and k_2 are the pre-exponential factors, assumed to be equal throughout this study. The progress variables can be related to the mass fractions of molecules A and C by the following equations:

$$\lambda_1 = 1 - x_A \qquad \lambda_2 = x_C$$

With the above reaction scheme, the net chemical energy release Q is given by:

$$Q = \lambda_1 Q_1 + \lambda_2 Q_2$$

where Q_1 and Q_2 represent the heat release by the exothermic and the endothermic reactions respectively. If the first reaction is much faster than the second one, in other words, if the heat release rate by the exothermic reaction is fast as compared to the heat absorbed by the endothermic reaction, an overshoot is observed in the chemical heat release profile for Q. The differential equation for du/dx involving the two chemical energy release terms is given by:

$$\frac{du}{dx} = \frac{(\gamma-1)\left[\dot{\lambda}_1 Q_1 + \dot{\lambda}_2 Q_2\right]}{c^2-u^2}$$

where the distance x is normalized with respect to the half reaction distance, i.e. the value of x when:

$$\frac{\lambda_1 Q_1 + \lambda_2 Q_2}{Q_1 + Q_2} = 0.5$$

The detailed derivation is given in Appendix II. To obtain a solution, the above differential equation is integrated from the von Neumann (V-N) state just downstream of the shock front, together with the chemical rate law equations. The Generalized C-J criterion is then used to select the desired regular solution for the detonation structure. This criterion can be represented in the present case by the following conditions:

$$u = c = \sqrt{pv} \quad \text{and} \quad \dot{\lambda}_1 Q_1 + \dot{\lambda}_2 Q_2 = 0$$

Through this sonic plane, the flow can now smoothly transit from subsonic to supersonic velocities (relative to the shock). It is then possible to continue the integration of the ZND equations further downstream, until the flow has reached complete equilibrium where both $\lambda_1 = 1$ and $\lambda_2 = 1$. The same solving method as for the detailed chemistry case is used.

For given values of the other mixture parameters (i.e. Q_1, Q_2, k_1, k_2), the pathological solution is found to depend on the difference in the activation energies $E_{a_1} - E_{a_2}$, or alternatively on the ratio of their exponentials $\exp(E_{a_1})/\exp(E_{a_2})$. For example, exothermic and endothermic activation energies of 25 and 22 respectively, lead to the same detonation state as activation energies of 28 and 25. Only the time and length scales are different. In the limiting case of a very low endothermic activation energy ($E_{a_2} \to 0$), the endothermic reactions are so fast that complete equilibrium is reached at the sonic point, leading to the ideal C-J solution ($Q = Q_1 + Q_2$) and no pathological behavior is obtained. In the limiting case of very high endothermic activation energy ($E_{a_2} \to \infty$), the endothermic reactions are now so slow that the detonation is solely governed by the exothermic heat release ($Q = Q_1$). This corresponds to the maximum achievable pathological detonation velocity. Thus, there is a limited range of pathological detonation velocities corresponding to a heat release ranging from $Q_1 + Q_2$ (with Q_2 negative) up to Q_1. Fig. 3.13 shows the normalized detonation velocity M as a function of the endothermic activation energy E_{a_2} for the case $Q_1 = 50$, $Q_2 = -10$, $\gamma = 1.2$, $k_1 = k_2 = 100$ and $E_{a_1} = 22$. One can clearly see the two asymptotes for the high and low values of E_{a_2} respectively, between which lies the range of possible pathological solutions.

The main characteristics of pathological detonations are the sonic plane embedded within the reaction zone and the overshoot in chemical energy release. For an unsupported pathological detonation, the steady particle velocity relative to the shock, together with the local sound speed with respect to the distance behind the shock is shown on Fig. 3.14a. It is clear from Fig. 3.14a that the flow transits from subsonic to supersonic velocity within the reaction zone and a maximum in the sound speed is observed in the reaction zone, corresponding to a temperature maximum. The values of the degree of reaction variables λ_1 and λ_2 within the reaction zone are shown in Fig. 3.14b. This figure clearly indicates that chemical equilibrium is not reached at the sonic plane. The heat release function ($Q = \lambda_1 Q_1 + \lambda_2 Q_2$) is shown on Fig. 3.14c for the same mixture. The overshoot in heat release is clearly visible and the maximum is reached exactly at the sonic point, as dictated by the Generalized C-J criterion. At the end of the reaction zone, where the flow reaches the weak state, the value of Q is now equal to the equilibrium C-J value ($Q = Q_1 + Q_2$), but all the energy release occurring downstream of the sonic plane does not affect the propagation of the detonation front. Fig. 3.14d shows again the heat release function Q, but this time with respect to the local Mach number $M_{local} = u/c$. Immediately downstream of the shock, the value of M_{local} is subsonic and reaches unity when Q is maximum, as dictated by the Generalized C-J criterion. The terminal state on the equilibrium Hugoniot corresponds to a weak detonation with a local Mach number $M_{local} = 1.2302$.

Hence, the two-rate law model of Fickett and Davis [29] is shown to be successful in reproducing the essential features of the pathological detonations in a real system like the $H_2 - Cl_2$. The transient development of pathological detonations in a mixture with the chemical reaction governed by this simplified two-rate law model shall now be investigated.

3.3.2 – Unsteady Solution

For the present numerical calculations, the detonations are initiated by the motion of a piston. Two types of initiation processes by the piston are considered in the present study. In the first type of initiation, a piston is driven at a high velocity for only a short period of time sufficient to initiate the detonation (i.e. approximately two reaction zone lengths), and is then abruptly stopped thereafter. The impulsive motion of the piston generates a strong shock wave that eventually develops into a detonation, but the abrupt stopping of the piston generates an expansion flow. In the limit when the piston velocity approaches infinity but the duration tends to zero, this impulsive motion generates a shock process approaching that of an ideal blast wave. The work done by the piston can then be correlated to the amount of energy deposited into the reactive mixture by the blast wave. In the present study, the piston velocity is chosen so as to generate a shock wave of the same strength as the von Neumann shock of the detonation front (as predicted by the steady-state analysis). This initially results in a highly overdriven detonation, until the piston is eventually stopped and the overdriven detonation decays. This method of initiation is referred to subsequently as the "impulsive piston initiation."

In the second type of initiation, the detonation is assumed to be initiated by a piston moving at constant velocity throughout. The detonation is thus supported by the motion of the piston and the rear boundary condition in the detonation products is governed by the boundary condition at the piston interface, i.e. particle velocity equal to the piston velocity. This method of initiation is referred to as the "constant velocity piston initiation."

In the transient analysis, the one-dimensional unsteady reactive Euler equations are solved numerically. An unsteady 1-D Lagrangian code is used for the computation. One of the advantages of the present Lagrangian coordinate system are that it is more convenient to handle piston-driven detonations since the distance is defined with respect to the piston location. Also, it provides a natural adaptative grid refinement around shock waves and regions of high-pressure gradient, since each cell contains the same amount of mass, rather than being equally spaced. The reactive Euler equations are solved by a combination of a 2nd order two-step predictor-corrector MacCormack scheme [49] and the Fluid Corrected Transport (FCT) scheme of Boris and Book [5] which is applied to the conservation equations to improve the accuracy of the solution near the shock. The grid size is chosen such that there are 50 numerical cells in the half reaction zone for the steady ZND detonation profile. This resolution is found to be adequate and the results are grid independent. Numerical calculations made with more than 50 numerical cells are found to yield the same results. For example, the results obtained for an oscillatory pathological detonation ($Q_1 = 50$, $Q_2 = -10$, $\gamma = 1.2$, $E_{a_1} = 26$, $E_{a_2} = 32$ and $k_1 = k_2$) with respectively 50 and 100 numerical cells in the half reaction zone length are compared in Figs. 3.15a and 3.15b. The two curves are found to be in almost perfect agreement. This code was initially developed by Chue [12] and extended to a two-rate mechanism for the present study.

3.3.3 – Impulsive Piston Initiation

The first set of calculations simulates closely the blast wave initiation. The initiation energy is varied by changing the duration of the piston motion. For a sufficiently long piston duration (high initiation energy), the detonation is said to be supercritical. For low enough activation energy of the exothermic reaction, the detonation is initially highly overdriven, and asymptotically decays towards a steady pathological detonation when the piston stops (Fig. 3.16). The pressure profiles for the transient development of the steady detonation are shown on Fig. 3.17. After the initial transient development, a stable structure is observed.

Near the critical initiation energy (shorter piston duration, decrease in the initiation energy), the initially overdriven detonation first decays to a value below the final steady-state solution. Similar to blast initiation of ideal detonations, a quasi-steady period is observed prior to the onset of the detonation. At the end of this quasi-steady period, the shock abruptly re-accelerates to an overdriven state and then decays subsequently towards a final steady value (Fig. 3.18). The pressure profiles for the transient development of a near-critical steady detonation are shown in Fig. 3.19. The re-acceleration of the shock that causes the increase in the pressure at the shock front is clearly visible on this figure. The asymptotically stable supercritical and critical detonations obtained above are both in agreement with the steady-state analysis based on the Generalized C-J criterion, despite the fact that no criterion is used in the transient analysis.

The profiles of the thermodynamic variables for the asymptotically stable solution shall now be investigated ($Q_1 = 50$, $Q_2 = -10$, $\gamma = 1.2$, $E_{a_1} = 22$, $E_{a_2} = 32$ and $k_1 = k_2$). The heat release function curve ($Q = \lambda_1 Q_1 + \lambda_2 Q_2$) is first shown on Figs. 3.20a and 3.20b. As predicted by the steady-state theory, an overshoot is observed in the heat release function, before Q eventually drops down to the Chapman-Jouguet value further downstream. Moreover, this maximum value of Q is found to be in agreement with the steady-state predictions based on the Generalized C-J criterion. The particle velocity relative to the shock can only be approximated at that point, since the present Lagrangian code does not keep track of the detonation velocity. Using the value of the shock Mach number corresponding to the steady pressure value (through the Rankine-Hugoniot equations) and the absolute particle velocity obtained at the point where $dQ/dt = 0$, it is found that the local Mach number there is equal to $M_{local} = 1.005$. This value is indeed very close to unity in accord with the Generalized C-J criterion used in the steady calculations which requires the flow to be sonic when the maximum Q is reached. Moreover, the profiles of the degree of reaction variables λ_1 and λ_2 (Fig. 3.20b) also indicate that chemical equilibrium is not achieved at the point where $dQ/dt = 0$, in agreement with the Generalized C-J criterion. The pressure profile (Fig. 3.20c) for the complete flow field indicates that the steady reaction zone is matched to the unsteady flow downstream through an expansion wave, in agreement with Taylor's criterion for a stable detonation.

For low activation energy of the exothermic equation, asymptotically stable pathological solutions are thus possible from an impulsive piston initiation, and the results are found to be in agreement with the steady-state analysis based on the Generalized C-J criterion. Even though no criterion is necessary in the transient calculations, the same pathological features (overshoot in heat release at the sonic plane and excess in detonation velocity) are observed in the asymptotic steady-state wave.

3.3.4 – Constant Velocity Piston Initiation

The profiles in the previous section were obtained for an impulsive piston initiation, where the piston is brought back to rest after a short duration. In the present section, the piston is allowed to continue to move with constant velocity u_p throughout. This permits us to investigate the effect of having to match the solution to a back boundary condition. Fickett and Davis [29] have discussed previously piston-driven pathological detonations, but did not carry out a non-steady analysis.

The variables u_s and u_w correspond respectively to the absolute particle velocities at the strong and weak states on the equilibrium Hugoniot for the pathological detonation. For piston velocities above the strong value ($u_p > u_s$), the detonation is overdriven, and the flow is subsonic throughout. As a result, the detonation is no longer pathological and the solution is governed by the piston velocity, i.e. the particle velocity becomes equal to the piston velocity u_p at the piston face $x = x_p$ (Fig. 3.21). For piston velocities below the strong value ($u_p < u_s$), the detonation velocity is the same as in the unsupported case, since the thermodynamic profiles are not modified in the region between the shock front and the sonic plane. However, the complete flow field is now affected.

For the unsupported case $u_p = 0$, the process is equivalent to the impulsive piston initiation case already shown in Figs. 3.20. Pressure profiles for the

$0 < u_p < u_w$ case are shown in Figs. 3.22a and 3.22b, corresponding to two different times. The flow first proceeds towards the weak detonation state, and a receding expansion wave then connects an ever-widening region of constant weak detonation state to the piston state. For the $u_p = u_w$ case, there is no expansion wave, and the weak state expands all the way back to the piston, as shown in Fig. 3.23. For intermediate values of u_p between u_w and u_s, the steady-state analysis predicts that the flow first reaches the weak detonation state, followed by an ever-widening region of constant state (weak detonation state). A receding secondary shock wave then connects the weak detonation state to the piston (Figs. 3.24a and 3.24b). The strength of this secondary shock must be such that the pressure increase across it corresponds to the transition from the weak detonation state to the state at the piston interface. The existence of a secondary shock in the products is similar to the case considered by Lee [40] for piston-driven diverging detonations. The detailed method to predict the secondary shock velocity from steady-state considerations is shown in Appendix V. The shock velocity measured in the transient calculation ($M_{sec} = 5.96$) is found to be in agreement with the steady-state calculations based on a control volume analysis ($M_{sec} = 5.99$). In the case $u_p = u_s$, a secondary shock wave is coupled to the end of the reaction zone, connecting the weak and the strong detonation states (Figs. 3.25). The velocity of this secondary shock wave is equal to that of the detonation front, since it joins the weak and strong points, which both lie on the detonation Rayleigh line.

There is a very good agreement between the profiles for the asymptotically stable transient solution and the steady-state predictions of Fickett and Davis [29] based on the Generalized C-J criterion. Hence the present transient study confirms the validity of the steady-state analysis based on the Generalized C-J criterion for piston-supported pathological detonations. These results also demonstrate the importance of Taylor's criterion of matching the steady reaction zone to the unsteady flow downstream.

3.3.5 – High Activation Energy (Unstable Pathological Detonations)

The existence of asymptotically stable pathological detonations has been demonstrated in the previous section for low activation energy values of the exothermic reaction. Even for ideal detonations, asymptotically stable solutions can not always be achieved and this depends on the activation energy. High activation energies increase the temperature sensitivity of the explosive mixture to perturbations. From both linear stability analysis [22] and transient numerical simulations [28], it was shown that above some limiting value of the activation energy, the detonation is unstable and an oscillatory behavior is observed. However, even for unstable detonations, the velocity is found to oscillate around a mean value corresponding to the ideal detonation solution. The influence of the activation energy on the stability of pathological detonations will now be investigated.

Recently, Sharpe [57] performed a one-dimensional stability analysis of pathological detonations and found that the linear response of these detonations to perturbations is very similar to the ideal C-J detonation case. However, in the linear stability analysis, the complete flow field downstream of the reaction zone need not be considered. Moreover, only small perturbations can be considered in a linear stability analysis. Since chemical reactions are still proceeding downstream of the sonic plane for the case of pathological detonations, it is worthwhile to carry out a non-steady numerical simulation of a pathological detonation to see if the energy release downstream of the sonic plane can influence the stability. Sharpe et al. [58] have also performed a numerical simulation of pathological detonations recently to study the non-linear stability of the structure of pathological detonations. However, they assumed a stable ZND structure first based on the steady-state solution using the Generalized C-J criterion, and then subjected this stable solution to a perturbation. They found that the non-linear response of pathological detonations can be very different in the supported and unsupported cases. They investigated the periods and amplitudes of the oscillations and observed both oscillatory and irregular detonation propagations. It is not obvious that the stable ZND profile imposed by Sharpe et al. as a starting condition in their simulations can in fact be reached during the transient development of the pathological wave from an arbitrary initiation condition. In the present study, the detonation wave is initiated by a strong blast wave (impulsive piston initiation). It is therefore possible to investigate the stability of pathological detonations from the complete history of the transient development of the detonation. The next paragraphs therefore focus on the existence and the stability of a pathological detonation wave initiated from a strong blast wave.

For the present pathological system studied, the exothermic activation energy is first varied, keeping everything else constant ($Q_1 = 50$, $Q_2 = -10$, $\gamma = 1.2$, $E_{a_2} = 32$, and $k_1 = k_2$). For a low exothermic activation energy $E_{a_1} = 22$, the shock pressure profile is very stable. As E_{a_1} is increased, the oscillations are found to shift from regular periodic to quasi-periodic and eventually to highly irregular or even chaotic structures (Figs. 3.26a to 3.26d). This effect is similar to what had been observed for ideal C-J detonations. The unstable oscillatory and chaotic solutions cannot be predicted from the steady-state analysis based on the

Generalized C-J criterion. In this unstable case, there is no stable sonic point in the flow where a steady-state boundary at the detonation front can be matched to the unsteady flow downstream. Nevertheless, it is found that the time-averaged value around which the shock pressure oscillates corresponds to the steady-state solution obtained with the Generalized C-J criterion. The average pressures measured over a few cycles are compared with the steady-state predictions and the ideal C-J solution in Table 3.3. Deviations of no more than 1.4% are obtained between the unsteady results and the steady-state predictions, even when the departure from stability is large.

The effect of the endothermic activation energy shall now be investigated by varying E_{a_2} keeping all other parameters the same, and using $E_{a_1} = 24$ as a reference. For this value of the exothermic activation energy, the ideal C-J detonation is found to oscillate regularly (Fig. 3.27a). For a low value of the endothermic activation energy E_{a_2}, the detonation velocity is close to the ideal C-J value. Once again, the mean value of the pressure oscillations corresponds to the steady-state predicted value. As E_{a_2} is increased, the endothermic reactions are further delayed, and the pathological effect is increased. The amplitude of the oscillations is found to decay, but this decay is almost not perceptible (Figs. 3.27b and 3.27c), indicating that the stability of the pathological detonations is practically independent of the endothermic activation energy.

The activation energy can also be varied in such a way that the steady detonation velocity remains the same. By keeping the difference between the activation energies constant ($E_{a_2} - E_{a_1}$), the steady-state solution is always the same. The transient solution, on the other hand, will become increasingly unstable as the values of the activation energies are increased. The shock pressure profiles for increasing values of the activation energies keeping their difference constant are shown on Fig. 3.28a to 3.28c. The average shock pressure is indeed found to be the same in all cases.

The pathological effect can also be investigated by varying the endothermic chemical heat release Q_2. When $Q_2 = 0$, an ideal C-J detonation is obtained. For finite negative values of Q_2, a pathological effect is introduced. The pathological detonation solution always lies in the range $Q_{CJ} < Q_{path} < Q_1$ as was shown on Fig. 3.13. By introducing a finite negative value of Q_2, the detonation velocity is thus lowered, since Q_{path} is less than Q_1 (or exactly equal in the limiting case $E_{a_2} \to \infty$). A decrease in the detonation velocity causes a reduction in the post-shock temperature (von Neumann temperature), thereby causing an increase in the (E_a/T) term. This results in a higher effective exothermic activation energy (E_{a_1}/T) and thus a less stable solution. It is expected that the shock pressure profile grows unstable as $|Q_2|$ is increased, based on the above consideration of the shock temperature. Indeed, Figs. 3.29a to 3.29c, where Q_2 is varied form 0 to –30, indicate the destabilizing effect of the endothermic heat release Q_2. This effect was also observed by Sharpe et al. [58] in their simulations where they imposed a steady ZND profile to initiate the calculations. Once again, the mean value around which unstable solutions are found to oscillate corresponds to the steady-state predictions based on the Generalized C-J criterion.

Another parameter that can be varied is the supporting piston velocity, in the case of constant velocity piston initiation. In the linear stability analysis, only the state at the sonic plane is considered, and the entire flow need not be considered. This implies that according to the linear stability analysis, a supporting piston should not have an effect on the stability of the detonation wave. This has been verified in the present study by investigating the case of an oscillatory pathological detonation ($Q_1 = 50$, $Q_2 = -10$, $\gamma = 1.2$, $E_{a_1} = 26$, $E_{a_2} = 32$ and $k_1 = k_2$) supported by constant velocity pistons with velocities $u_p = 0$, $u_p = u_w$, and $u_p = u_s$ (the $u_p = 0$ case corresponds to the impulsive piston initiation). The shock pressure profiles for the three cases are shown in Figs. 3.30a to 3.30c. The three curves match almost exactly, thus confirming that in accordance with the linear stability analysis, the supporting piston does not influence the stability of pathological detonation waves. This indicates that the source of instability does not originate from the far field, but rather from the near shock flow conditions.

In summary, it is the ratio E_{a_1}/T that determines the stability of pathological detonations. This ratio depends on the activation energy of the exothermic reaction itself, as well as the detonation velocity, since higher detonation velocities imply higher temperatures. Parameters such as the chemical heat releases Q_1 and Q_2 or the activation energy of the endothermic reaction E_{a_2} can thus indirectly affect the stability of the detonation through their effect on the detonation velocity. On the other hand, supporting constant velocity pistons do not affect the stability of pathological detonation waves, provided that the piston velocity remains below the strong value u_s.

3.4 – CONCLUSION

The classical criteria of Chapman and Jouguet fails to predict the steady detonation solution for cases where there is an overshoot in the energy release function (e.g. $H_2 - Cl_2$ mixtures and mixtures governed by the simplified two-rate law model of Fickett and Davis [29]). In both cases, if one integrates along the Rayleigh line that corresponds to the equilibrium C-J value, a singular point is eventually encountered, i.e. infinite value of the derivative du/dx. This occurs since the heat release rate does not vanish at the sonic plane along this Rayleigh line. Hence the solution based on the equilibrium C-J velocity is singular.

A regular solution can be found by the Generalized Chapman-Jouguet criterion, and corresponds to a steeper Rayleigh line (higher detonation velocity). Along this Rayleigh line the flow goes through a sonic transition when the exothermic and endothermic energy release rates balance each other out. Further integration along the Rayleigh line leads to the weak detonation state on the equilibrium Hugoniot, where the flow is supersonic relative to the shock front. The presence of endothermic processes thus provides a path to the weak detonation branch, otherwise inaccessible for an ideal detonation (monotonic heat release).

The steady-state assumption can be relaxed when carrying out non-steady computations of the transient development of pathological detonations. In that case, no criterion is necessary to obtain the asymptotic steady detonation solution if it exists.

For activation energies of the exothermic reaction below a critical value, asymptotically stable solutions could be obtained. For these stable solutions, a steady reaction zone is matched with the unsteady flow downstream, in agreement with Taylor's criterion for the existence of a stable detonation. By adjusting the back boundary condition (changing the piston velocity), the flow field downstream of the steady zone was found to adjust itself, still in agreement with Taylor's criterion of matching a non-steady flow region to a steady-state boundary. Even though no criterion is used to determine the detonation solution in the case of non-steady computations, the asymptotically stable solutions were found to be in agreement with the steady-state solution based on the Generalized C-J criterion. In the unsteady calculations, the heat release rate was indeed found to vanish when the particle velocity was sonic relative to the shock front.

For activation energies of the exothermic reaction above a critical value, no asymptotically stable solution is found. Oscillatory or even chaotic structures are observed instead. In this case, it is not possible to satisfy Taylor's criterion of matching the steady reaction zone with the unsteady flow downstream. This is why unstable detonations are observed. Nevertheless, the time-averaged properties of these unstable pathological detonations appear to be in agreement with the steady-state analysis based on the Generalized C-J criterion.

Although the steady-state analysis has some limitations (it cannot predict the stability of the detonation wave), it is nevertheless very powerful in determining the pathological detonation solution, at least on the average. The use of the Generalized C-J criterion to determine the steady-state solution of pathological detonations is thus validated in the present study.

Chapter 4

Detonations with Large Momentum Losses

Although the turbulent flow field in very rough-walled or in obstacle-filled tubes is very difficult to describe theoretically, an attempt is made in the present chapter to model the propagation of a detonation in such an environment via a quasi one-dimensional approach. Large momentum losses are thought to be responsible for the velocity deficits of detonation waves (down to sonic velocity) observed experimentally. Heat losses alone could not account for such a large departure from ideal C-J behavior. The exact physical processes in the reaction zone of a detonation in an obstacle field are extremely complex to model theoretically. In the present study, a simple source term is introduced in the momentum equation for the ZND structure of the detonation to account for the frictional losses, to at least investigate the possibility of low velocity detonation solutions as a consequence of friction.

In previous studies of detonation with friction by Zel'dovich [71], Gelfand et al. [30], Zel'dovich et al. [74], and others, the detailed investigation of the existence and stability of detonation solutions was only carried out for shock velocities down to a certain critical value. Recently, Brailovsky and Sivashinsky [6] numerically modeled low-velocity detonation-like phenomena in porous media. Due to the very strong resistance of the porous medium to the gas flow, they assumed that inertial effects can be neglected and used Darcy's law for the momentum equation. Hence, shock waves were not brought up in their study, and they considered the possibility of fast combustion waves driven by the diffusion of pressure only. In this chapter, the possible steady-state detonation solutions based on the Euler equations will be explored more extensively, with friction represented by a source term in the momentum equation. It will be determined whether solutions exist for the entire range of shock velocities ranging from the ideal C-J value down to that of a sonic wave. Similar to pathological detonations, the so-called Generalized C-J criterion has to be applied to seek these steady-state solutions with momentum losses. It will also be verified if steady-state detonations can be realized asymptotically in a transient calculation where a criterion to determine the steady-state detonation solution is not required.

4. 1 – THE EFFECT OF FRICTION ON DETONATION PROPAGATION

The effect of friction on the propagation of a detonation can be analyzed by drawing the analogy to steady one-dimensional compressible fluid flow subjected to heat transfer and friction. Heat addition to the flow and friction both tend to bring the flow towards $M = 1$. In subsonic flow, friction and heat addition tend to accelerate the flow and for supersonic flow, the effect is reversed. A decrease in Mach number causes an increase in pressure, whereas an increase in Mach number causes a decrease in pressure. Thus, heat addition and friction cause the density and pressure to decrease for subsonic flow, and vice-versa for supersonic flow.

In the presence of sufficiently large amounts of heat addition and friction, the flow may become choked ($M = 1$), so that a maximum possible mass flow rate is obtained. When the choking condition is achieved, there are in general only two possible inlet conditions compatible with the choked state: a subsonic solution, and a supersonic one. One must therefore adjust the inlet conditions to match with the choked flow downstream.

A detonation propagating in a rough tube also involves heat addition (through chemical reactions) and friction downstream of the shock front. To compute the detonation state, one must solve for the eigenvalue detonation velocity compatible with the back boundary condition (e.g. sonic plane). This is analogous to the steady compressible 1-D flow problem with heat addition and friction, where only one supersonic inlet condition is found to be compatible with the choked flow downstream.

Since detonations propagate at a constant velocity, the detonation process is a steady one only when viewed in a reference frame attached to the shock front. Although physical processes such as friction and heat release do not depend on the reference frame chosen, it is more convenient to investigate their effect in this moving frame, rather than in the laboratory frame in which the detonation process is an unsteady one. The transformation from the fixed laboratory frame (Fig. 4.1a) to the shock-attached frame (Fig. 4.1b) requires a simple Galilean transformation in which only the particle velocities are affected, through the relation:

$$u_{abs} = D - u_{rel}$$

where u_{abs} is the particle velocity in the fixed laboratory frame, u_{rel} is the particle velocity in the shock–attached frame, and D is the detonation velocity. The chemical heat release takes place within the moving flow, in the shock-attached frame (Fig. 4.1b). Since the flow downstream of the shock front and throughout the reaction zone is subsonic relative to the shock, a positive chemical energy release results in an increase of the particle velocity u_{rel}. The flow pressure is found to decrease due to the chemical reactions (and this is irrespective of the chosen reference frame). On the other hand, the friction acts in the fixed laboratory reference (attached to the tube walls, Fig. 4.1a), so that the friction effect in the laboratory frame must be converted to the shock-attached frame to investigate its effect on the detonation propagation.

For the range of Mach numbers usually involved in detonation calculations, the shocked gas at the V-N state propagates at a supersonic velocity relative to the laboratory frame. Immediately downstream of the shock wave, the friction therefore tends to increase the pressure and reduce the Mach number of the flow in the laboratory frame. In the shock-attached frame, this corresponds to an increase in both the flow Mach number and pressure (the pressure does not depend on the reference frame). Hence, chemical energy release and friction both initially contribute to the increase of the Mach number in the shock-attached frame, but have opposite effects on the pressure.

According to the Generalized C-J criterion, the positive chemical heat release rate must be balanced by a negative rate of frictional loss at the sonic plane (relative to the shock). In order for such a balance to occur, the friction effect must become negative prior to the sonic plane (i.e. the friction must tend to reduce the Mach number in the shock-attached frame). This implies that the transition from supersonic to subsonic flow relative to the walls must occur within the reaction zone of the explosive mixture, prior to the sonic plane. With the flow being then subsonic relative to the walls, the friction tends to accelerate it with respect to the laboratory frame, which translates in a negative effect in the shock-attached frame. The effects of chemical energy release and friction on the flow Mach number thus oppose each other in the later part of the reaction zone.

Keeping in mind the roles played by friction and chemical heat release in one-dimensional compressible fluid flow, the detailed structure of detonations with friction shall now be investigated.

4.2 – STEADY-STATE DETONATIONS WITH FRICTION

The general form of the *du/dx* equation for the detonation structure (derived in Appendix I) is now specialized to describe detonations with friction by equating m and q to zero, i.e.:

$$\frac{du}{dx}=\frac{(\gamma-1)}{c^2-u^2}\left\{\dot{\lambda}Q+fu\left[\frac{\gamma}{\gamma-1}\frac{u}{M}-1\right]\right\} \tag{4.1}$$

where the friction function f is given by Eqn. 2.5:

$$f=-k_f\,\rho(M-u)|M-u| \tag{2.5}$$

Without loss of generality, the friction factor k_f is assumed to be constant for simplicity in the present study. Due to the presence of a source term in the momentum equation, the pressure can no longer be obtained algebraically from the particle velocity. It is now necessary to simultaneously integrate an additional differential equation for the pressure as well. This differential equation is derived from the conservation of momentum equation with a source term, in the shock-attached frame, i.e.:

$$\frac{1}{\gamma}\frac{dp}{dx}+\rho u\frac{du}{dx}=-f$$

Isolating the pressure derivative yields:

$$\frac{dp}{dx}=-\gamma M\frac{du}{dx}-\gamma f \tag{4.2}$$

where $M = \rho u$ from the conservation of mass. For the chemical reactions, a simple irreversible Arrhenius rate law is used, i.e.:

$$\dot{\lambda} = \frac{d\lambda}{dt} = k(1-\lambda)\exp\left(\frac{-E_a M}{\rho u}\right)$$

where the pre-exponential factor k is arbitrarily set to a value of 100 throughout the present study. This set of coupled ordinary differential equations can now be integrated to obtain the detailed structure of the detonation.

The eigenvalue detonation velocity M can be solved for a given value of the friction factor k_f. The function $M\ vs\ k_f$ for high activation energies is found to be multi-valued for some range of the friction factor. In other words, the steady-state analysis provides more than one detonation solution for a given k_f. It is therefore more convenient to iterate for the friction factor that satisfies the Generalized C-J criterion for a given shock velocity. The resulting $M\ vs\ k_f$ curve has a Z-shape (Fig. 4.2a). In the limit of low and high values of k_f, there is a unique detonation solution for a given k_f. However, in between, there is a range of friction factors for which there are three possible steady-state solutions. Stewart and Yao [61], in their study of detonations with curvature (no friction) also observed a Z-shaped curve for $M\ vs\ \kappa$ (where κ is the curvature of the detonation front). They associated the lower branch of the $M\ vs\ \kappa$ curve with a low velocity detonation mode for condensed explosives.

For low values of the activation energy, the $M\ vs\ k_f$ curve is single-valued throughout (Fig. 4.2b). The shock velocity decreases monotonically towards $M = 1$ as the friction factor is increased. A few $M\ vs\ k_f$ curves are shown for various values of the activation energies in Fig. 4.2c. It can be seen that for a given friction factor, higher detonation velocities are obtained for lower activation energies. This is due to the fact that the detonation solution is governed by a competition between the rate of heat release and the rate of frictional losses. Lower values of the activation energy yield higher rates of chemical heat release, due to the minus sign in the Arrhenius rate law equation, i.e. $\dot{\lambda} = k(1-\lambda)\exp(-E_a/RT)$. Hence, for a given detonation velocity, a higher value of the friction factor is necessary for the two rates to balance one another. This is why the M *vs* k_f curves for low activation energies are located above those for higher E_a.

One can define various detonation regimes to clarify the multiplicity of solutions. Four different regimes, labeled with roman numerals, can be identified in Fig. 4.3 for the high activation energy case. Regime I starts from the C-J solution $M = M_{CJ}$, in the limit of $k_f = 0$ and ends at the first turning point, referred to as the first extinction limit ($M = M_{ext1}$). Regime II is defined to start from the first extinction limit, and terminates at a critical value of the shock velocity, referred to as $M = M_{cr}$, which is found to be equal to the sound speed of the burned products. Regime III starts from this critical shock velocity M_{cr} and proceeds down to the second turning point, referred to as the second extinction limit ($M = M_{ext2}$). Regime IV starts from this second turning point and continues until $M = 1$. Detonations propagating according to regimes III and IV are referred to as low-velocity detonations (LVD), since the detonation velocity is significantly below the C-J value.

The critical shock velocity M_{cr} that defines regimes II and III can be determined analytically. Since M_{cr} is equal to the sound speed in the burned products, the state at the sonic plane ($u_{rel} = c_b$) corresponds to the detonation products being completely at rest in the fixed laboratory frame

($u_{abs} = M - u_{rel} = M - c_b = 0$). When the flow is at rest ($u_{rel} = M$), the friction function f goes to zero. Hence for the numerator of the du/dx equation to go to zero (as required by the Generalized C-J criterion), the rate of chemical energy release $\dot{\lambda}$ therefore has to go to zero as well, and this can occur only when $\lambda = 1$. Thus, this is the limiting case where the sonic plane coincides with the end of the reaction zone ($\lambda = 1$) and the shock front velocity is then equal to the sound speed of the burned products. By setting the condition $u_{rel} = M$ and $\lambda = 1$, an analytical expression for M_{cr} can be found (the detailed derivation is shown in Appendix VI), i.e.:

$$M_{cr} = \left[\gamma(\gamma - 1)Q + 1\right]^{1/2}$$

This critical shock velocity is found to be independent of the activation energy. Since the flow is at rest ($u_{rel} = M$), the normalized specific volume becomes equal to unity from the conservation of mass. Moreover, since the state ahead of the shock and the detonation products are both at rest relative to the laboratory, the state at the end of the reaction zone for a shock velocity M_{cr} corresponds to that of a constant volume explosion, i.e.:

$$p_{cr} = \gamma(\gamma - 1)Q + 1$$

$$v_{cr} = 1$$

This implies that the induced motion of the detonation products within the reaction zone is negligible, so that the detonation process for $M = M_{cr}$ can be thought of as a constant volume explosion boundary that propagates steadily through the fresh mixture. Even though globally there is no expansion of the detonation products ($v_{cr} = 1$), the friction-generated pressure peak allows a local expansion of the products that drives the shock front (the detailed pressure profile for a critical detonation $M = M_{cr}$ is discussed in the next section).

Since the flow is at rest (in the laboratory frame) at the end of the reaction zone, the boundary condition at the wall is already satisfied. As a result, a region of uniform state must connect the end of the reaction zone to the wall. The thermodynamic profiles are therefore similar to those for an overdriven detonation supported by a constant velocity piston, where a region of uniform state also connects the reaction zone to the piston surface. However, there is no external momentum input in the present case. Whereas the ideal overdriven detonation solution depends on the piston velocity, the detonation propagating at $M = M_{cr}$ in the present case would not be affected by a reduction in the piston velocity (a backward moving piston) since the sonic plane effectively isolates the reaction zone from the flow downstream.

There exists no such analytical formula to obtain the detonation solutions at the two extinction limits. One must integrate the structure equations. A thorough discussion of the detonation structure for each of the aforementioned regimes shall now be presented.

4.2.1 – Steady-State Results – Regimes I and II

In regimes I and II, the flow must go through a sonic plane, where the rate of chemical energy release is exactly balanced by the rate of frictional loss. This corresponds to the numerator and denominator of the *du/dx* equation simultaneously vanishing (Generalized C-J criterion). It is then possible to integrate Eqns. 4.1 and 4.2 further to get the profiles past the sonic plane, until the end of the reaction zone. This is done by obtaining the indeterminate slope *du/dx* at the sonic plane using l'Hospital's rule (using the method of Appendix III with a source term in the momentum equation). At the end of the reaction zone ($\lambda = 1$), the flow is brought to rest. For an Arrhenius rate law, this is found to happen asymptotically at infinity, even though the sonic plane is located at a finite distance from the shock front.

Steady-state particle velocity profiles are shown for regimes I and II ($M > M_{cr}$) in Fig. 4.4a for a high value of the activation energy ($E_a = 32$). It is more convenient to plot the velocity profiles in the fixed laboratory frame since this allows us to check if the flow is brought to rest. Moreover, this facilitates the comparison with the transient results obtained in the laboratory frame in section 4.3. From this graph, it is clearly seen that as M is reduced (by changing the friction factor), the value of u_{abs} at the sonic plane also goes down, and eventually reaches zero when $M = M_{cr}$, in agreement with the previous discussion of the properties of the flow when $M = M_{cr}$. For $M > M_{cr}$, the thermodynamic variables asymptotically approach the constant volume explosion state beyond the sonic plane.

Steady-state pressure profiles for regimes I and II are shown in Fig. 4.4b, for the high activation energy case. Initially, an increase in pressure above the V-N state value can be observed due to friction, as discussed in section 4.1.1. As the chemical reaction rate becomes more important, the pressure eventually drops. The pressure tends to the constant volume explosion state value ($p = \gamma(\gamma - 1)Q + 1$) asymptotically for all cases.

For a lower activation energy ($E_a = 22$) the M *vs* k_f curve monotonically decreases with increasing friction factor. As a result, there is no regime II observed, since the slope $\partial M/\partial k_f$ is negative throughout. The absolute velocity and pressure profiles for $E_a = 22$ are shown in Fig. 4.5a and 4.5b respectively. The main qualitative difference observed between the particle velocity and pressure profiles for $E_a = 22$ and $E_a = 32$ is the larger reaction zone length for the $E_a = 22$ case, especially for low shock velocities. This is due to the fact that the $E_a = 22$ case involves larger friction factors.

The value of λ (the degree of reaction) at the sonic plane is found to be equal to 1 for an ideal detonation ($k_f = 0$) and also for the critical case $M = M_{cr}$. For regimes I and II ($M_{cr} < M < M_{CJ}$), the value of λ at the sonic plane is slightly below, but very close to unity (Fig. 4.6), indicating that chemical equilibrium has not been attained. The detonation velocity deficits therefore cannot be attributed to incomplete energy release at the sonic plane, but rather to large momentum losses within the reaction zone. Similar results are obtained for the two activation energies ($E_a = 22$ and $E_a = 32$), and the detonation solution corresponding to the minimum value of λ does not have any particular physical meaning (for example, it is not associated with an inflection point or the extinction point on the M *vs* k_f curve).

Therefore, from a steady-state point of view, the only difference between regimes I and II is the sign of the slope in the M *vs* k_f curve (negative in regime I, positive in regime II). The first extinction point, where the slope of the M *vs* k_f curve is infinite, does not have any other characteristics, as far as steady-state analysis is concerned.

The characteristics of the steady-state detonation solutions for regimes III and IV ($M < M_{cr}$) shall now be investigated.

4.2.2 – Steady-State Results – Regimes III and IV

For regimes III and IV, the shock velocities are below the sound speed of the burned products ($M < c_b = \sqrt{p_b v_b}$). Hence, no sonic plane ($u_{rel} = c_b$) can be observed in the flow, unless the particle velocity u_{rel} becomes larger than the shock velocity M (negative velocity relative to the walls). However, this is not possible, since the friction function f would become positive, and the du/dx equation would not vanish. Since the flow downstream of the shock is then subsonic throughout (relative to the shock) for $M < M_{cr}$, the Generalized C-J criterion can no longer be used as a criterion to seek a particular solution of interest.

For $M = M_{cr}$, it is found that the flow is at rest ($u_{rel} = M$) when chemical equilibrium is reached. Since the particle velocity cannot become larger than the shock velocity ($u_{rel} < M$), the above result suggests that one could perhaps continue to seek a steady detonation solution below M_{cr} using this condition as a criterion, i.e. the flow being at rest (in the absolute frame) at the end of the reaction zone ($u_{rel} = M$ and $\lambda = 1$). As the flow is entirely subsonic relative to the shock front, there is no singular point within the reaction zone. This criterion will now be referred to as the LVD criterion. Such a criterion has already been suggested by Ershov [23] as a possible wave structure when studying detonations in porous media. However, Ershov did not investigate the transition from the cases where the Generalized C-J criterion applies to these low velocity detonations.

In the M *vs* k_f graphs shown in Fig. 4.2, the curve is continuous in value and first derivative at $M = M_{cr}$, i.e. at the transition from the solutions based on the Generalized C-J criterion, to the solutions based on the LVD criterion. This suggests that, indeed, this criterion may be a valid one.

Absolute particle velocity profiles for different values of the shock velocity M below M_{cr} are shown in Fig. 4.7a for a high value of the activation energy ($E_a = 32$) yielding the presence of both regimes III and IV. As dictated by the LVD criterion, u_{abs} goes to zero at the end of the reaction zone, for all values of the shock velocity below M_{cr}. The pressure profiles for different values of the shock velocity M below M_{cr} are shown in Fig. 4.7b. The increase in pressure beyond the V-N point due to the friction is very high. Such a large pressure rise brings the mixture to a high enough temperature so that the chemical reaction rate becomes significant (triggering of the chemical reaction), and generates expansion waves which drive the shock. For all shock velocities, the value of the pressure quickly converges to the constant volume explosion value. For shock velocities below some limiting value, the V-N pressure is found to be lower than the constant volume explosion pressure.

For a lower activation energy ($E_a = 22$) the M *vs* k_f curve monotonically decreases with increasing friction factor. As a result, there is no regime III observed, since the slope $\partial M / \partial k_f$ is negative throughout. The absolute velocity and pressure profiles for $M < M_{cr}$ and $E_a = 22$ are shown in Fig. 4.8. Again, the main qualitative difference observed between the particle velocity and pressure profiles for $E_a = 22$ and $E_a = 32$ is the longer reaction zone for the $E_a = 22$ case due to the larger friction factors involved.

The second extinction point, where the slope of the M *vs* k_f curve is infinite, does not have any other particularities, as far as steady-state analysis is concerned. Therefore, from a steady-state point of view, the only difference between regimes III and IV is the sign of the slope in the M *vs* k_f curve (negative in regime III, positive in regime IV).

Similar to the case $M = M_{cr}$, the flow is at rest at the end of the reaction zone for regimes III and IV. Therefore, a region of uniform state must connect the end of the reaction zone to the wall. However, for $M < M_{cr}$, the detonation state would now be affected by a backward-moving piston, since there is no longer a sonic plane relative to the shock front embedded in the flow to isolate the reaction zone. As a result, a backward-moving piston or even an open-ended tube would probably not permit the existence of a detonation moving with velocity $M < M_{cr}$. This is due to the fact that with a negative velocity ($u_{abs} < 0$) satisfying the above boundary conditions, the numerator of the du/dx equation cannot vanish, due to a change of sign in the friction and heat loss source terms.

4.2.3 – Summary of Steady-State Results

The absolute particle velocity and pressure profiles for some values of the shock velocity ranging from $M = M_{CJ}$ down to $M = 1$ are shown in Fig. 4.9, for a high value of the activation energy ($E_a = 32$). A smooth transition is observed as the value of the shock velocity is varied from one regime to the other.

It is also convenient to show the detonation process on a $p - v$ diagram. Due to the presence of a source term in the momentum equation, the integral curves are no longer straight lines (Rayleigh lines) on the $p - v$ plane. Integral curves for various detonation solutions are shown in Fig. 4.10 for shock velocities ranging from M_{CJ} down to a value of M below M_{cr}. In all cases, the final state is the constant volume explosion state on the equilibrium Hugoniot. Here again, a smooth transition is observed as the shock velocity is varied from one regime to the other. This suggests that the LVD criterion is probably a valid criterion to solve for the steady-state detonation solution for shock velocities below the sound speed of the burned products ($M < M_{cr}$).

As pointed out in section 4.1, friction tends to increase the pressure downstream of the detonation shock front. This pressure increase becomes larger as the shock velocity is reduced (larger friction factors). When the chemical heat release rate becomes dominant, the pressure then drops, and the subsequent expansion of the products drives the shock front. The flow is then matched to the rear boundary condition, i.e. choking condition for regimes I and II, and flow at rest ($u_{rel} = M$) at the end of the reaction zone for regimes III and IV.

On the basis of the steady-state analysis, the four propagation regimes correspond to mathematically acceptable solutions (provided the detonation tube has a fixed end in the case of regimes III and IV). However, the existence of a steady-state solution does not guarantee that it may be realized asymptotically from arbitrary initial conditions. A transient analysis will now be carried out to verify the validity of the steady-state criterion based on the flow being completely stopped at the end of the reaction zone (LVD criterion). Also, in the cases where the steady-state analysis predicts more than one solution for a given value of the friction factor, the transient analysis will determine which of these steady-state solutions may be asymptotically achieved.

4.3 – TRANSIENT DEVELOPMENT OF DETONATIONS WITH FRICTION

4.3.1 – The Numerical Method

The present transient study of the development of detonations with friction is investigated through the use of an Eulerian detonation code based on the piecewise parabolic method (PPM) [13], a high order extension of Godunov's method, and a simple conservative shock front tracking algorithm [11]. The Rankine-Hugoniot equations are used to compute the state across the cell containing the shock front. An adaptative mesh refinement [3] is also used for a more effective and economical representation of the small length scales near the shock front. A coarse grid is used throughout the entire domain, with a fine mesh refinement superimposed in the vicinity of the shock. The coarse grid of 20 numerical cells with a refinement ratio of 5 provides 100 cells in the half reaction zone. The code has been successfully validated against the ideal detonation results of Fickett and Wood [28] by setting the friction factor k_f equal to zero.

4.3.2 – Low Activation Energy (Single-Valued M *vs* k_f)

The simpler low activation energy case shall first be considered, when the M *vs* k_f curve is not multi-valued. A very low value of the activation energy ($E_a = 10$) is selected, to ensure that asymptotically stable solutions are obtained at all friction levels. In the low E_a range, only regimes I and IV are possible, according to the steady-state analysis.

For a low value of the friction factor corresponding to regime I ($k_f = 0.9299$), an asymptotically stable solution is obtained (Fig. 4.11). The resulting shock pressure is found to be in agreement with the predictions from the steady-state analysis using the Generalized C-J criterion. The local Mach number of the flow is indeed found to be very close to unity ($M = 1.0076$) when the chemical energy release rate just balances the rate of heat loss to friction. This result confirms the existence of asymptotically stable detonations in regime I, and validates the use of the Generalized C-J criterion for this regime.

The value of the friction factor corresponding to $M = M_{cr}$ in the steady-state analysis is now selected ($k_f = 4.578$). After the initial blast, the shock pressure asymptotically decays towards a stable value corresponding to the steady-state predictions (Fig. 4.13). The particle velocity profile (in the fixed reference frame) indicates that the flow comes to rest at the end of the reaction zone (Fig. 4.14a), and the sound speed of the burned products is indeed equal to the shock front velocity. The pressure peak in the reaction zone (Fig. 4.14b) permits the expansion of the detonation products towards the constant volume explosion pressure. This result confirms the validity of the Generalized C-J criterion down to the critical shock velocity M_{cr}.

A low velocity detonation (LVD) is now investigated (regime IV) by selecting a larger value of the friction factor ($k_f = 16.51$). Once again, an asymptotically stable solution is obtained (Fig. 4.15). The shock pressure is found to be in agreement with the steady-state analysis based on the LVD criterion (flow at rest in the absolute frame at the end of the reaction zone). The particle velocity profile confirms that the flow comes to rest at the end of the reaction zone, where the flow is still subsonic relative to the shock front (Fig. 4.16a). The pressure profile indicates that the final state is again the constant volume explosion state (Fig. 4.16b) This result confirms the existence of asymptotically stable low velocity detonations, and the validity of the LVD criterion to predict the detonation state in regime IV.

A larger value of the activation energy for which the M *vs* k_f curve is also single-valued ($E_a = 22$) is now considered. For a low value of the friction factor ($k_f = 0.1230$), the shock pressure is found to oscillate around a mean value after the initial transient, rather than reaching an asymptotically stable value (Fig. 4.17). This mean value is found to be in agreement with the steady state prediction based on the Generalized C-J criterion.

For a larger value of the friction factor corresponding to a LVD ($k_f = 0.3973$), large amplitude oscillations are observed (Fig. 4.18). Although the shock pressure oscillates around the steady-state prediction based on the LVD criterion, the time-averaged shock pressure is found to be 16% above the steady-state value. Nevertheless, the absolute velocity profile indicates that the particle velocity at the end of the reaction zone fluctuates around zero (Fig. 4.19) in agreement with steady-state considerations.

The pulsating detonations obtained for $E_a = 22$ indicate that the friction effectively increases the activation energy level (Fig. 4.17 and Fig. 4.18), since the ideal case $k_f = 0$ yields a stable detonation for this value of the activation energy. This may be due to the fact that friction causes a reduction in detonation velocity, hence a reduction in the post-shock temperature. This increases the value of the (E_a/T) term at the V-N point in the chemical rate law equation. For a given value of the activation energy, the instability level is thus increased by increasing the value of k_f, as can be seen by comparing Figs. 4.17 and 4.18.

In the present section, the existence of asymptotically stable detonations corresponding to regimes I and IV has been confirmed. The use of the Generalized C-J and the LVD criteria to determine the asymptotically stable solutions has been validated. However, when the detonation becomes unstable, and the shock front oscillates, the average shock pressure may deviate from the steady-state predictions.

4.3.3 – High Activation Energy (Multi-Valued M *vs* k_f)

The cases where the M *vs* k_f curve is multi-valued shall now be investigated, to determine which of the possible solutions will be asymptotically achieved for given initial condition. This also permits the stability of the solutions in regimes II and III to be investigated.

A value of the activation energy close to the minimum case of multi-valued M *vs* k_f curves is selected ($E_a = 27$). A friction factor for which three steady-state solutions are possible is chosen ($k_f = 0.07065$). The shock pressure profile is shown in Fig. 4.20. Extremely large and irregular oscillations with chaotic periods are obtained, so that no steady-state solution is reached. Thus, it is not possible to compare the unsteady solution with the steady-state predictions. This is not a surprising result, since even the frictionless ideal case ($k_f = 0$) leads to large oscillations for $E_a = 27$.

Unfortunately, it is therefore not possible to investigate the multiple solution case with the present model, since the values of the activation energies for which multi-valued M *vs* k_f curves are obtained are above the stability limit and no steady-state solutions can be achieved.

A rate-law that would not depend so strongly on the temperature could perhaps yield more stable solutions and yet, still provide a multi-valued M vs k_f curve. Zel'dovich et al. [73] suggested a rate law which accounts for the ignition of the mixture at the wall, and the subsequent spreading of the reaction towards the tube axis. This rate law does not depend strongly on the temperature. However, it is based on the distance from the shock front, which is not convenient for a transient unsteady computation. Instead, a source term will be included in the equation for the conservation of energy, to account for the heat transfer to the walls and obstacles. An Arrhenius rate law coupled with source terms in the momentum and energy equations is found to yield multi-valued M vs k_f curves in a range of activation energy values giving stable solutions.

4.4 – DETONATIONS WITH FRICTION AND HEAT TRANSFER

Momentum losses are always accompanied by heat transfer. Therefore, the present model can be refined by including the effect of heat transfer in the previous investigations with friction. Zel'dovich et al. [73] already performed a steady-state analysis of detonation with heat transfer and friction and found that the introduction of heat losses yields to a more efficient cooling and deceleration of the gas and an increase in fuel combustion inefficiency ($\lambda < 1$) in the system. However, they only considered the detonation solutions based on the Generalized C-J criterion (they did not investigate the complete spectrum of possible solutions). In the present section, the combined effect of friction and heat transfer on low velocity detonations shall be investigated.

4.4.1 – Steady-State Results for Detonations with Friction and Heat Transfer

In smooth tubes, a relation between the momentum and heat losses can be obtained through the Reynolds analogy, as discussed in Chapter 2, i.e.:

$$\frac{h_c}{\rho u_{rel} C_p} = \frac{f}{2}$$

Through this relation, the coefficient of heat transfer is expressed in terms of the friction function f. A single parameter (here k_f) can thus be used to model the effect of both friction and heat transfer. Even though this relation is only applicable to smooth tubes, it can still be used here, since only a qualitative behavior is sought. A more realistic model, such as that used by Zel'dovich et al. [73], would require an additional parameter in the heat transfer function. A source term q, derived from the Reynolds analogy, is thus introduced in the conservation equations, i.e.:

$$q = \frac{\gamma}{\gamma - 1} \frac{f}{u_{rel}} (T - T_w)$$

As a result, the du/dx equation now becomes:

$$\frac{du}{dx} = \frac{(\gamma - 1)\left[\dot{\lambda} Q + q/\rho\right] + f/\rho\left[\gamma u - D(\gamma - 1)\right]}{\left(c^2 - u^2\right)}$$

This can be integrated within the reaction zone to get the profiles of the thermodynamic variables. The differential equation for the pressure is not affected by the introduction of a source term in the energy equation.

As for the case of detonations with friction alone, a critical detonation velocity M_{cr} is found below which the Generalized C-J criterion no longer applies. However, due to the presence of a source term in the energy equation, it is no longer possible to obtain an analytical expression for M_{cr}. Steady-state detonation solutions are nevertheless found using the Generalized C-J criterion for $M > M_{cr}$, and the LVD criterion for $M < M_{cr}$. The LVD criterion is again found to be applicable, since the source term q also goes to zero when the flow is brought to rest (q is directly related to f, through Reynolds analogy).

For a low activation energy ($E_a = 8$), the $M\ vs\ k_f$ curve decreases monotonically as the friction term is increased, so that the function is single-valued (Fig. 4.21a). The transition to activation energies where multiple solutions are possible occurs at much lower values than for the case with friction only. For $E_a = 12$, the $M\ vs\ k_f$ curve is multi-valued with a Z shape (Fig. 4.21b), similar to the $E_a = 32$ case with friction only (Fig. 4.2a), so that all four regimes are possible. For higher values of the activation energy, the shape of the $M\ vs\ k_f$ curve changes. For $E_a = 22$, the second extinction limit occurs in the vicinity of $M = 1$ for very low friction factor (Fig. 4.21c). As a result, regime IV is practically non-existent and the maximum value of k_f corresponds to the value at the first extinction limit. Regime III occurs for a very limited range of small friction factors. Various $M\ vs\ k_f$ curves are shown in Fig. 4.21d. As in the case with friction alone, higher detonation velocities are obtained with lower values of the activation energy for a given friction factor.

The absolute velocity and pressure profiles for $E_a = 12$ are shown in Fig. 4.22. These steady-state profiles are qualitatively similar to those obtained with friction only, except that the final uniform state no longer corresponds to the constant volume explosion state. This is due to the fact that the equilibrium Hugoniot (including the constant volume explosion state) cannot be reached when the energy is not conserved (presence of heat losses). This is better illustrated on a $p - v$ diagram (Fig. 4.23). The integral curves are not straight lines due to the presence of a source term in the momentum equation and a large increase in pressure is also observed after the V-N point, similar to the case with friction only. However, the integral curves no longer all converge to a common point (constant volume explosion state) as in the case with friction only, due to the external heat losses.

The transient development of a low velocity detonation with both friction and heat transfer shall now be investigated. This computation will determine which solution is preferred, in the case when the steady-state analysis provides more than one solution.

4.4.2 – Transient Results for Low Activation Energy

For a low activation energy of $E_a = 8$, the $M\ vs\ k_f$ curve monotonically decreases and it is single valued, such that only regimes I and IV are possible. For a low value of the friction factor corresponding to regime I ($k_f = 0.2017$), the asymptotically stable detonation is in agreement with the steady-state predictions based on the Generalized C-J criterion (Fig. 4.24). The pressure profile is also in excellent agreement with the steady-state predictions (Fig. 4.25). The thermodynamic variables at the plane where the effective heat release rate vanishes are within 1% of the steady-state sonic plane values. This result confirms the validity of the Generalized C-J criterion when source terms are included in both the momentum and energy equations.

A stable LVD case (regime IV) is now investigated, by selecting a larger value of the friction factor ($k_f = 1.762$). The asymptotically stable solution is in agreement with the steady-state predictions based on the LVD criterion of flow at rest at the end of the reaction zone (Fig. 4.26). The particle velocity profile indicates that indeed, the flow is completely at rest at the end of the reaction zone (Fig. 4.27), in agreement with the LVD criterion.

4.4.3 – Transient Results for High Activation Energy

A higher activation energy ($E_a = 12$) is now considered to study the case where there exists more than one steady-state solution for a given friction factor. A value of the friction factor for which three steady-state solutions are possible is investigated ($k_f = 0.2$). From a blast wave initiation, only the solution on the upper branch of the M *vs* k_f curve could be obtained (Fig. 4.28a).

In order to achieve the two other steady-state solutions in the transient analysis, the computations are initialized with the corresponding steady-state ZND profiles. For the intermediate solution (regime II), the shock front propagates at the prescribed velocity for a limited time, but suddenly exhibits a large overshoot. The shock pressure decay is seen to be similar to that of a blast wave. The regime I solution is then asymptotically reached (Fig. 4.28b). The regime II solution is thus unstable.

The low velocity detonation (regime IV) is now investigated by initiating the computations with the appropriate ZND profile. Once again, the shock front propagates at the prescribed velocity for a limited time, but suddenly exhibits a large overshoot. The shock pressure decay is then similar to that of a blast wave, and the regime I solution is asymptotically reached (Fig. 4.28c). Regime IV cannot be approached from a blast wave in the case of multiple solutions.

To verify the existence of stable detonations in regime III, a different value of the friction factor has to be selected ($k_f = 0.16$). By initiating the detonation with the appropriate steady-state profiles, once again the shock front accelerates and the regime I solution is asymptotically reached (Fig. 4.28d).

A higher activation energy ($E_a = 22$) is now considered to study the case where the regime IV is practically non-existent. Only the solutions on the upper branch of the M *vs* k_f curve (regime I) could be reached from a blast wave initiation (Fig. 4.29a), irrespective of the strength of the blast wave. When the computations are initiated with the ZND profile corresponding to the steady-state solution on the lower branch of the M *vs* k_f curve (regime II), the shock front accelerates to the regime I solution after some initial transient decay (Fig. 4.29b). By selecting a value of the friction factor above the extinction limit, the detonation is found to fail (Fig. 4.30) no matter how strong the blast wave is.

The present unsteady analysis therefore shows that the only stable regimes are regimes I and IV, but regime IV can only be realized when the M *vs* k_f curve is single-valued for the given friction factor.

4.5 – CONCLUSION

4.5.1 – Propagation Mechanism

For an ideal detonation, the chemical heat release rate drives the pressure down from the V-N state to the sonic plane. For detonations with friction, a pressure rise is observed after the V-N state, instead of a drop, due to friction effects. When the chemical reaction rate becomes dominant over the rate of frictional loss, the pressure eventually decays (Fig. 4.31a). This pressure drop associated with the expansion of the products provides the momentum necessary to drive the detonation shock front.

In the first part of the reaction zone, where the pressure increases above the V-N value, the rate of chemical heat release is almost negligible, since the shock temperature is very low. The role of friction is thus to slowly increase the temperature within the reaction zone up to a level where the chemical reaction rate accelerates. As compared to ideal detonations, the induction time is thus longer. Once the peak in pressure is achieved, the remaining section of the reaction zone is then very similar to that of an ideal detonation, where the momentum required to drive the shock comes from the pressure drop from the peak value down to the end of the reaction zone. The pressure and chemical heat release rate profiles for an ideal detonation are shown in Fig. 4.31b to compare with Fig. 4.31a. The propagation of such low velocity detonations thus occurs on account of the friction that initially increases the pressure and temperature to a high enough level to generate a rapid energy release accompanied with a large increase in pressure, which then causes an expansion of the detonation products. The propagation mechanism of LVD is thus characterized by an "induction zone" where the role of friction is essential. Without this pressure rise due to friction, the propagation of a steady detonation would not be possible since the pressure at the end of the reaction zone is above that at the V-N spike.

4.5.2 – The Steady-State Criteria

Due to the losses within the reaction zone (friction and heat losses), the classical criteria of Chapman and Jouguet fail to predict the detonation state for a given friction factor. Regular solutions are obtained by integrating along an integral curve where the flow goes through a sonic transition when the effective heat release rate vanishes (numerator of $du/dx \rightarrow 0$). Such solutions are thus governed by the Generalized C-J criterion, similar to the pathological detonations in Chapter 3. For pathological detonations, the Generalized C-J criterion was used to generate all possible detonation solutions for different mixture parameters. However, for detonations with friction, the Generalized C-J criterion fails to predict the steady-state detonation solution for shock velocities below some critical value M_{cr}. This is due to the fact that the flow within the reaction zone becomes entirely subsonic relative to the shock, so that no sonic plane can be embedded within the flow. An alternative criterion, referred to as the LVD criterion, was proposed to obtain steady-state solutions below M_{cr}, down to sonic values of the shock front. This criterion is based on the flow being at rest (in the fixed laboratory frame) when equilibrium is reached. The slope of all variables become zero there, so that a uniform quiescent state extends back to the end wall, thus satisfying the boundary conditions. The curve of the dependence of the shock velocity on the friction factor k_f is found to be continuous in value and in slope at M_{cr}. A smooth transition between the solutions based on the Generalized C-J criterion and those based on the LVD criterion is thus observed. This suggests (but does not confirm) that this criterion may be a valid one.

To confirm the existence of these low velocity detonations ($M < M_{cr}$) and the validity of the LVD criterion, the steady-state assumption is relaxed and the transient development of a detonation with friction is considered. In unsteady computations, no criterion is necessary for the back boundary conditions, and the steady reaction zone has to be matched with the unsteady flow downstream (Taylor's criterion). For sufficiently low values of the activation energy of the chemical reactions, asymptotically stable detonation solutions are reached. These asymptotically stable detonations are indeed found to be in agreement with the steady-state predictions based on the Generalized C-J criterion for $M \geq M_{cr}$, and based on the LVD criterion for $M \leq M_{cr}$. The transient analysis thus confirms the validity of the two steady-state criteria to determine the solution of stable detonations with friction, and with friction and heat transfer (using the Reynolds analogy). In Chapter 5, an investigation will be carried out to determine how all the steady-state criteria could be merged into a single universal one.

4.5.3 – The Existence of Stable Solutions

The existence of a steady-state solution (based on one of the two criteria) does not guarantee that such a solution is stable or can be asymptotically achieved from arbitrary initial conditions. For high values of the activation energy of the chemical reactions, oscillatory solutions, rather than stable ones, are obtained, similar to the pathological and ideal detonation case. This indicates that for some mixture parameters, the steady reaction zone cannot be matched to the unsteady flow downstream (Taylor's criterion not satisfied).

For ideal and pathological detonations, the limiting activation energy above which oscillatory solutions are obtained is around 25. However, in the case of detonations with friction, the stability limit is reduced. For instance, an oscillatory solution is obtained for $E_a = 22$ with a relatively low value of the friction factor (Fig. 4.17). This is due to the fact that the velocity deficit due to friction causes a reduction in the post-shock temperature, and hence an effectively higher value of the ratio (E_a/T) is obtained. Moreover, when the friction factor is increased further, an even larger velocity deficit is obtained (low-velocity detonation), yielding much larger oscillations for the same value of the activation energy (Fig. 4.18).

Irrespective of the activation energies, there exist some steady-state solutions that cannot be reached asymptotically, even as the average of an oscillatory solution. This happens when the M vs k_f curve is multi-valued (2 or 3 possible shock velocities for a given friction factor). The present transient analysis demonstrates that when there exist multiple steady-state solutions for a given friction factor, only the regime I solution can be achieved asymptotically. Hence, the steady-state solutions lying on the portion of the M vs k_f curve where the slope is positive ($dM/dk_f > 0$, regimes II and III) are unstable solutions, in agreement with the work of Stewart and Yao [61] on detonation with curvature. Based on their Shock Dynamics model of the propagation of the detonation, stable propagation of the shock is only possible for $dM/d\kappa < 0$ (κ is the curvature). For high values of the activation energy ($E_a = 22$ in the case of detonation with friction and heat transfer), there is a maximum value of k_f above which no steady-state solution is possible. This result has been confirmed by the transient calculations (Fig. 4.30).

Carrying out transient calculations is therefore essential in determining the stability of steady-state solutions. Hence, the present study clearly demonstrates that the existence of a steady-state solution does not guarantee that it can be observed in nature.

4.5.4 – Comparison with Experimental Observations

In the present chapter, source terms in the momentum and energy conservation equations have been added to account for the non-ideal propagation of detonations in obstacle-filled tubes and in porous medium. Through the use of simple and arbitrary source terms, the 1-D detonation computations (steady-state and transient) have exhibited the same qualitative behavior as that observed experimentally. For instance, a continuous spectrum of detonation solutions ranging from the ideal C-J detonation down to very low velocity detonations with Mach number close to unity is obtained numerically. A continuous spectrum of detonation velocities was also observed in the experiments of Makris [50] and Lyamin et al. [48] in porous media. For some range of activation energies and friction factors, the M *vs* k_f curve has been found to be multi-valued, the different solutions corresponding to different detonation propagation modes. Such a behavior has also been observed experimentally for gaseous detonations propagating in obstacle-filled tubes (Lee et al. [43], Peraldi et al. [55]). In particular, the so-called choking regime observed by Peraldi et al., where the detonation velocity is close to the sound speed in the burned products seems to correspond to the low-velocity detonation solutions (LVD) obtained in the present numerical study. For high values of the activation energy, a maximum value of the friction factor above which no steady-state solution exists has been found. This is in qualitative agreement with the experiments in obstacle-filled tubes, where the detonation is found to fail for some mixture properties and obstacle arrangement.

Thus, the present study indicates that it is indeed possible to model at least qualitatively the complex 3-D propagation of detonations in obstacle-filled tubes and in porous media within the framework of a 1-D numerical model with simple and arbitrary source terms. The use of more realistic chemical rate laws and source terms could possibly permit a direct comparison between the numerical results and the experimental ones. However, such a comparison is beyond the scope of the present qualitative study.

Chapter 5

Conclusions

In this thesis, a detailed investigation of the propagation of non-ideal detonations, i.e. detonations that are not governed by the classical C-J criterion, was carried out. Whereas the solution to ideal C-J detonations can be found from the global conservation laws and equilibrium thermodynamics, without consideration of the rate processes, the solution for non-ideal detonations requires the consideration of the structure of the detonation wave. In the present study, the general method for predicting the non-ideal detonation solution has been examined and the existence of these steady solutions has been verified via a numerical study of the transient process of detonation development.

Non-ideal behavior is accounted for by including source terms in the conservation equations (in differential form) for a quasi 1-D detonation. To get a steady-state solution for non-ideal detonations, the structure of the detonation in the non-equilibrium reaction zone must be considered, rather than simply using the global conservation laws and equilibrium thermodynamics. To seek that steady-state solution, a criterion to determine the detonation solution is needed in general, since there exists a whole spectrum of possible solutions to the differential equations for the structure. A physically meaningful solution must be regular, so when a singularity is encountered along the integral curve, a particular solution that is regular at the singularity must be selected. The singularity usually arises when the denominator of the differential equation for the particle velocity (du/dx) vanishes, corresponding to the detonation products flowing at a sonic velocity relative to the shock front. To avoid this singularity, a particular solution must be selected in which the numerator of the du/dx equation simultaneously vanishes. In the case of non-ideal detonations, the source terms accounting for the non-ideal behavior appear in the numerator of the du/dx equation, thus affecting the regular solution.

Even though the steady-state ideal C-J solution can be found from the global conservation equations, the detonation structure equations can alternatively be used to determine the solution also. Using the detonation structure equations, the steady-state solution must be a singularity-free solution. For instance, solutions with detonation velocities below the C-J value are not regular, since the sonic plane is achieved prior to complete chemical equilibration. As a result, the denominator vanishes while the numerator remains finite, yielding an infinite value of the derivative du/dx. For detonation velocities above the C-J value, there are two possible solutions, i.e. the strong and the weak detonation solutions on the equilibrium Hugoniot curve. The weak solution is ruled out since an expansion shock would be required to connect the strong and the weak detonation states. The strong solution is a regular one, since the particle velocity always remains subsonic relative to the shock front. However, a strong detonation must be supported by a moving piston. It is therefore not sufficient to seek a regular solution. One must also consider the back boundary conditions.

When source terms are present in the conservation equations, a regular solution can be found for which the numerator (including the non-ideal effects) is also found to vanish when the denominator goes to zero. This occurs when the flow velocity is sonic relative to the shock front. Since the flow is not yet at equilibrium at that point, chemical reactions and relaxation processes are occurring in the flow downstream. However, these effects should not influence the propagation of the detonation front, since the sonic plane acts as a barrier effectively isolating the steady reaction zone from the unsteady flow downstream. It is therefore important, once again, to consider the complete flow field. It is not sufficient to have a singularity-free solution.

The steady-state analysis based on the detailed detonation structure does not permit us to determine whether a solution will be stable to perturbations or not. A solution that exists in nature must be a stable solution. Therefore, the steady-state analysis alone is not sufficient to determine which steady solutions can be realized in nature. A linear stability analysis can be carried out by investigating the response of the steady-state solution to small perturbations. Alternatively, the stability of a steady-state solution can be studied through an unsteady calculation, where the transient development of the detonation is considered. In this case, no criterion is needed to seek a particular solution, and no a priori assumption regarding the steady-state solution has to be imposed. The main conclusions from the steady-state and transient calculations are shown in the following sections.

5.1 – PATHOLOGICAL DETONATIONS

The experimental data gathered in the present study has confirmed the existence of pathological detonations in H_2-Cl_2 mixtures, i.e. detonation velocities in excess of the equilibrium C-J predictions. Numerical detonation structure calculations with the detailed chemical kinetics of H_2-Cl_2 have shown the presence of an overshoot in the energy release function responsible for the excess in detonation velocity, in agreement with the work of Guénoche et al. [33].

However, the steady-state analysis does not provide any indication regarding the stability of the detonation solutions. An unsteady calculation for the transient development of the detonation can be carried out to determine whether the steady-state pathological solutions can be approached asymptotically. A simple model (first suggested by Fickett and Davis [29]) involving two consecutive irreversible reactions has been considered in the present transient study to model pathological detonations. The transient analysis reveals that for exothermic activation energies E_{a_1} below a critical value, the whole spectrum of steady-state pathological solutions based on the Generalized C-J criterion can be obtained asymptotically from a strong blast initiation. For values of E_{a_1} above the critical value (around 25), oscillatory and even chaotic behaviors are observed. Nevertheless, the time-averaged properties of these unstable pathological detonations are found to correspond to the steady-state predictions.

By adjusting the velocity of a piston moving behind the detonation wave, various back boundary conditions have been simulated. The resulting asymptotically stable solutions were always found to satisfy both the regular solution requirement, and the back boundary condition dictated by the piston velocity. Hence, the present transient analysis validates the use of the Generalized C-J criterion to determine the detonation state for pathological detonations.

5.2 – DETONATIONS WITH FRICTION AND HEAT TRANSFER

When source terms are included in the conservation equations for momentum and energy, a velocity deficit with respect to the ideal C-J predictions is observed, due to frictional and heat losses. Regular solutions are found when the numerator of the *du/dx* equation vanishes as the rates of chemical heat release and frictional and heat losses balance each other out at the sonic plane.

For detonation velocities below the sound speed of the burned products ($M < c_b$), singularities can no longer be observed, since the flow remains subsonic throughout relative to the shock front (the denominator never reaches zero). The back boundary condition of zero particle velocity at the end of the reaction zone can be considered to determine the steady-state detonation solution, as suggested by Ershov [23]. Rather than seeking a regular solution, the steady-state solution is thus found by directly matching the steady reaction zone with the back boundary condition at the wall.

A whole spectrum of steady-state solutions for detonations with friction and heat transfer can be found for detonation velocities ranging from the ideal C-J value down to the velocity of a sonic wave. For sufficiently high values of the activation energy of the chemical reactions and within some range of the friction factor, there is more than one possible steady-state solution for a given mixture and tube roughness, and the M *vs* k_f curve has a Z-shape. The present transient analysis shows that when the M *vs* k_f curve is multi-valued, only one solution can be approached asymptotically for a given value of the friction factor. The regime I solution, when it exists for a given value of the friction factor, is the only one that can be achieved. The solutions for the regimes II and III must be ruled out, as they never occur in a transient analysis. This result has already been pointed out by Stewart and Yao [61] for detonations with curvature. According to their Detonation Shock Dynamics model, a stable propagation of the shock is only possible on the portion of the M *vs* κ curve (where κ is the curvature of the shock) where the slope $dM/d\kappa$ is negative.

The stability limit of E_a is found to be significantly below that for ideal detonations. This indicates that friction and heat transfer increase the level of instability. This can be explained by the fact that lower detonation velocities are obtained and hence lower post-shock temperatures. A lower post-shock temperature implies a higher value of the ratio E_a/T in the Arrhenius rate law, thus a higher effective activation energy. When the activation energy is below the stability limit, the asymptotically stable solutions are found to be in agreement with the steady-state predictions based on the Generalized C-J criterion (regime I) and the LVD criterion (regime IV). In Regime IV, the detonation can steadily propagate despite the fact that there is no global expansion of the detonation products (in the case with friction only), since the thermodynamic variables at the end of the reaction zone correspond to those for the constant volume explosion. A local expansion of the products occurs within the reaction zone due to the friction-induced pressure peak. This local expansion is responsible for driving the detonation front.

The existence of low-velocity detonations (regime IV) increases the range of known stable steady-state solutions from the earlier works of Zel'dovich et al. [73] and others. This wider range of possible solutions allows us to draw parallels between the present theoretical results and experimental observations. For instance, Makris [50] and Lyamin et al. [48] measured a continuous range of detonation velocities (as low as 30% of the ideal C-J value) in porous media. Their results can be associated with the single-valued M *vs* k_f curves obtained in the present theoretical study, corresponding to a continuous spectrum of stable solutions for all values of the friction factor.

In the obstacle-filled tube experiments of Lee et al. [43], Peraldi et al. [55] and Teodorczyk et al. [63], two distinct high-speed propagation regimes are observed, i.e. the quasi-detonation and the choking regimes. These two propagation modes can be associated with regimes I and IV when the M *vs* k_f curves are found to be multi-valued in the present theoretical study. The sudden transition of one propagating mode to the other observed experimentally when changing the initial conditions corresponds to the case when the friction factor is increased above its value at the first extinction limit. An abrupt transition from regime I to regime IV is then observed.

The activation energies used in Chapter 4 may seem unrealistic (very low). However, one has to keep in mind that the Arrhenius rate law is probably not suitable in the case of low velocity detonations (LVD) where the bulk temperature immediately downstream of the shock front would not be high enough to initiate chemical reactions in a real experiment. In the case of LVD, the triggering of chemical reactions most likely occurs near the walls due to the reflected shocks, and the reactions then spread towards the tube axis, as suggested by Zel'dovich et al. [74]. Moreover, the models used to account for the interaction with the obstacles in the present study are very crude and simple, since their purpose is only to illustrate the qualitative behavior of non-ideal detonations subjected to high levels of friction and heat transfer. More realistic chemical rate laws and source terms would certainly bring the theoretical results in a closer agreement with the experimental results, but this is beyond the scope of this work.

Nevertheless, the present study demonstrates that it is possible to simulate qualitatively the behavior of non-ideal detonations within the framework of a one-dimensional model where the 3-D effects are averaged out across the cross-section of the explosive and appropriate source terms are included in the momentum and energy equations.

5.3 – CRITERIA FOR STEADY-STATE DETONATIONS

Throughout the present study, different criteria have been discussed for determining the steady-state detonation properties of ideal and non-ideal detonations due to different mechanisms. None of these steady-state criteria have been found to be universally applicable. However, the detailed examination of the integral curves corresponding to the steady-state solutions has revealed similar features in all cases of ideal and non-ideal detonations considered in this work. For instance, the detonation solution was always found at the transition between two distinct behaviors along the integral curves. In one case, the numerator of the du/dx equation vanishes prior to the denominator, and the opposite situation is observed in the second case. Moreover, the detonation solution is always found to correspond to the vanishing numerator case, whereas the denominator was not always equal to zero, such as for ideal detonations with reversible chemistry. The detonation solution therefore lies on a limiting integral curve where $NUM = 0$ occurs prior to $DEN = 0$, at the transition to the family of integral curves where $DEN = 0$ occurs prior to $NUM = 0$. Defining a regular solution as one where no singularity ($DEN = 0$ while $NUM \neq 0$) occurs in the flow field, a universal criterion can be defined to determine the steady-state detonation solutions based on the detonation structure. This criterion can be expressed as:

The detonation solution corresponds to the minimum (local)
detonation velocity yielding a regular solution.

A local minimum, rather than a global one, is sought, to take the multiple solution case into account. The solutions for regimes II and III (chapter 4), known to be unstable from the transient analysis, are ruled out using the universal criterion. This is due to the fact that the solutions for these regimes correspond to local maxima in detonation velocities instead of minima. This is only a consequence of the present formulation of this universal criterion.

This universal criterion is similar to the original criterion of Chapman, since it also seeks a minimum detonation velocity solution compatible with the conservation equations. This steady-state criterion even applies for detonations with curvature. All the steady-state criteria used in the present work are found to be special cases of this universal criterion.

Contributions to Knowledge

For non-ideal detonations, no systematic general discussion of the criterion to determine a unique solution to the conservation laws had yet been carried out. This unique solution must be found from the detailed consideration of the detonation structure where the non-ideal mechanisms manifest themselves. The contribution of this study is a thorough analysis of the criterion to obtain steady-state solutions for non-ideal detonations arising from friction, heat transfer and pathological effects of chemical reactions. The transient development of these non-ideal detonations and the determination of the asymptotic approach to the steady-state was also investigated through a numerical study.

List of References

1. Akyurtlu, A., *An investigation of the structure and detonability limits of hydrogen-chlorine detonations*, Ph.D. thesis, University of Wisconsin-Madison, 1975
2. Bdzil, J.B., Steady-state two-dimensional detonation, *J. Fluid Mech.* 108:195-226, 1981
3. Berger, M.J. and Colella, P., Local adaptive mesh refinement for shock hydrodynamics, *J. Comput. Phys.* 82:64-84, 1989
4. Berthelot, M., Vieille, P., On the velocity of propagation of explosive processes in gases. *Compt. Rend. Hebd. Séances Acad. Sci.* 93:18-21, 1881
5. Boris, J.P., Book, D.L., Flux-corrected transport I, SHASTA, a fluid transport algorithm that works, *Journal of Computational physics* 11:38-69, 1973
6. Brailovsky, I. and Sivashinsky, G.I., On deflagration to detonation transition, *Combust. Sci. Tech.* 130:201-231, 1997
7. Braithwaite, M., Farran, T., Gladwell, I., Lynch, P.M., Minchinton, A., Parker I.B., Thomas, M.R., A detonation problem posed as a differential/algebraic boundary value problem, *Math.Engng Ind.* (3) 1:45-57, 1990
8. Campbell, A.W., Malin, M.E., Holland, T.E., Detonation in homogeneous explosives, *2nd ONR Symp. On Detonation*, p. 454-477, 1955
9. Chan, S.K., A theory to predict the velocity-diameter relation of explosives, *7th Symposium (International) on Detonation*, pp. 589-601, 1981
10. Chapman, D.L., On the rate of explosion in gases. *Philos. Mag.* 47:90-104, 1899

11. Chern, I.L. and Colella, P., “A conservative front tracking method for hyperbolic conservation laws,” *Lawrence Livermore National Laboratories Report No. UCRL-97200*, 1987

12. Chue, R.S. , *High speed deflagration and its transition to detonation*, PhD Thesis, McGill University, Montréal, Canada, 1993

13. Colella, P. and Woodward, P.R., The piecewise parabolic method (PPM) for gas-dynamical simulations, *J. Comput. Phys.* 54:174-201, 1984

14. Courant, R., Friedrichs, K.O., *Supersonic flow and shock waves*, Interscience Publishers, Inc., New-York, 1948

15. Dabora, E.K., *The influence of a compressible boundary on the propagation of gaseous detonations*. University of Michigan Technical Report 05170-1-T (Ph.D. Thesis), Ann Arbor, Michigan, 1963

16. Devonshire, A.F.,Theoretical Research Report No. 3/43

17 Dionne, J.-P., Lee, J.H.S., Modeling the detonation properties of heterogeneous explosives, *Shock Compression of Condensed Matter* 317-320, AIP, 1997

18. Dionne, J.-P., Duquette, R., Yoshinaka, A., Lee, J.H.S., Pathological detonations in H_2-Cl_2. *Proceedings of the 17th International Colloquium on the Dynamics of Explosions and Reactive Systems*, Universität Heidelberg, Germany, (submitted to Combustion Science and Technology, in Print), 1999

19. Döring, W., Über den Detonationsvorgang in Gasen, *Ann. Phys.* 43:421-436, 1943

20. Duff, R.E., Calculation of reaction profiles behind steady-state shock waves. I. Application to detonation waves. *J. Chem. Phys.* 28:1193-1197, 1958

21. Dupré, G., *Etude des mécanismes de propagation des déflagrations et des détonations dans les azotures gazeux d'hydrogène , de chlore et de brome*, PhD. Thesis, Université d'Orléans, France, 1978

22. Erpenbeck, J.J., Stability of steady-state equilibrium detonations, *Physics of Fluids* 5:604-614, 1962

23. Ershov, A.P., A convective detonation wave in a porous structure, *Combustion, Explosion, and Shock Waves* 33(1):81-88, 1997

24. Eyring, H., Powell, R.E., Duffey, G.H., Parlin, R.B., The stability of detonation, *Chem. Rev.* 45:69-181, 1949

25. Fay, J.A., Opel, G., Two-dimensional effects in gaseous detonation waves. *J. Chem. Phys.* 29:955-956, 1958

26. Fay, J.A., Two-dimensional detonations: velocity deficit. *Phys. Fluids* 2:283-289, 1959

27. Fedorov, A.V., Khmel, T.A., Types and stability of detonation flows of aluminum particles in oxygen, *Combustion, Explosion, and Shock Waves*, (32) 2:181-190, 1996

28. Fickett, W., Wood, W.W., Flow calculations for one-dimensional pulsating detonations, *Physics of Fluids* (9) 5:903-916, 1966

29. Fickett, W., Davis, W.C., *Detonation*, University of California Press, 1979

30. Gelfand, B.E., Frolov, S.M., Polenov, A.N., Specific features of detonation in systems with losses of an arbitrary type, *Archivum Combustionis* (7) 1-2:197-214, 1987

31. Gelfand, B.E., Frolov, S.M., Nettleton, M.A., Gaseous detonations – A selective review, *Prog. Energy Combust. Sci.* 17:327-371, 1991

32. Guénoche, H., Manson, N., Influence des conditions aux limites transversales sur la propagation des ondes de choc et de combustion, *Revue de l'Institut Français du Pétrole* 2:50-69, 1949

33. Guénoche, H., Le Diuzet, P., Sèdes, C., Influence of the heat-release function on the detonation states. *Progress in Astronautics and Aeronautics: Dynamics of Explosions* 75: 387-407, AIAA, New-York, 1981

34. Huerta, M.A., Steady detonation waves with losses, *Phys. Fluids* 28:2735-2743, 1985

35 Johnson, J.N., Tang, P.K., Forest, C.A., Shock-wave initiation of heterogeneous reactive solids, J. Appl. Phys. 57(9):4323-4334, 1985

36. Jones, H., A theory of the dependence of the rate of detonation of solid explosives on the diameter of the charge, *Proc. R. Soc. London Ser.A* 189:415-427, 1947

37. Jouguet, E., On the propagation of chemical reactions in gases. *J. de Mathématiques Pures et Appliquées* 1:347-425, 1905, 2:5-85, 1906

38. Kistiakowsky, G.B., Knight, H.T., Malin, M.E., *J. Chem. Phys.* 20:884, 1952

39. Knystautas, R., Lee, J.H., Detonation parameters for the hydrogen-chlorine system, *Progress in Astronautics and Aeronautics: Dynamics of Explosions* 114: 32-44, AIAA, New-York, 1988

40. Lee, J.H., Knystautas, R., Bach, G.G., Formation and propagation mechanism of diverging gaseous detonation waves, *McGill University Report* #6905, 1969

41. Lee, J.H., Knystautas, R., Guirao, C., Bekesy, A., Sabbagh, S., On the instability of H_2-Cl_2 gaseous detonations, *Combustion and Flame* 18:321-325, 1972

42. Lee, J.H., Knystautas, R., Guirao, C.M., C-J Detonation studies on H_2-Cl_2, CS_2-O_2 and CO-H_2-O_2-N_2 mixtures, *MERL Report 72-6*, McGill University, Montréal, 1972

43. Lee, J.H.S., Knystautas, R., Freiman, A., High speed turbulent deflagrations and transition to detonation in H_2-air mixtures, *Comb. Flame* 56:227-239, 1984

44. Lee, J.H.S., Zhang, F., Friction-induced oscillatory behaviour of one-dimensional detonations, *Proc. R. Soc. Lond. A* 446:87-105, 1994

45. Lee, J.H.S., Zhang, F., Chue, R.S., Some fundamental problems of detonation instabilities and its relation to engine operation. In *Buckmaster, L. Jackson, T.L. & Kumar, A. (eds) Combustion in high-speed flows*, pp. 541-574. The Netherlands: Kluwer Academic Publishers, 1994

46. Lee, J.J. , *Detonation mechanisms in a condensed phase porous explosive*, PhD Thesis, Université de Sherbrooke, Sherbrooke, Canada, 1997

47. Liu, J.J., A thermodynamic analysis of quasi-one dimensional self-sustaining gaseous detonation waves, *Proc. R. Soc. Lond. A* 455:2757-2780, 1999

48. Lyamin, G.A., Mitrofanov, V.V., Pinaev, and A.V., Subbotin, V.A., A.A. Borissov (ed.), *Dynamic structure of detonation in gaseous and dispersed Media*, p. 51-75, 1991

49. MacCormack, R.W., The effect of viscosity in hypervelocity impact cratering, *AIAA paper* 69:354, 1969

50. Makris, A. , *The propagation of gaseous detonations in porous media*, PhD Thesis, McGill University, Montréal, Canada, 1993

51. Mallard, E., Le Chatelier, H.L., On the propagation velocity of burning in gaseous explosive mixtures, *Compt. Rend. Hebd. Séances Acad. Sci.* 93:145-148, 1881

52. Mamontov G.M., Mitrofanov, V.V., and Subbotin, V.A., *Detonatsiya I udarnye volny*, Chernogolovka, 52-56, 1980

53. Manson, N., Guénoche, H., Effect of the charge diameter on the velocity of detonation waves in gas mixtures, , *6th Symposium (Int) Combust.*, 6:631-639, The Combustion Institute, Pittsburgh, PA, 1956

54. Nahmani, G., Manheimer, Y., Detonation of nitromethane., *J. Chem. Phys.* 24:1074-1077, 1956

55. Peraldi, O., Knystautas, R., Lee, J.H., Criteria for transition to detonation in tubes, *21st Symposium (Int) Combust.*, 21:1629-1637, The Combustion Institute, Pittsburgh, PA, 1986

56. Rybanin, S.S., Effect of inhomogeneities in an explosive on the critical detonation diameter, *Zhurnal Prikladnoi Mekhaniki I Tekhnicheskoi Fiziki*, 10(4):141-144, 1969

57. Sharpe, G.J., Linear stability of pathological detonations, submitted to *J. Fluid Mech.*, 1999

58. Sharpe, G.J., Falle, S.A.E.G., One-dimensional nonlinear stability of pathological detonations, submitted to *J. Fluid Mech.*, 1999

59. Shchelkin, K.I., Effect of tube surface roughness on origin and propagation of detonation in gases, *Sov. J. Exp. Theor. Phys.* 10:823-827, 1940

60. Son, S.F., Asay, B.W., Bdzil, J.B., Kober, E.M., Reaction rate modeling in the deflagration to detonation transition of granular energetic materials, *Mat. Res. Soc. Symp. Proc.* 418:313-323, 1996

61. Stewart, D.S., Yao, J., The normal detonation shock velocity-curvature relationship for materials with nonideal equation of state and multiple turning points, *Comb. Flame* 113:224-235, 1998

62. Taylor, G.I., The dynamics of the combustion products behind plane and spherical detonation fronts in explosives, *Proc. Roy. Soc. Ser. A* 200:235-247, 1950

63. Teodorczyk, A., Lee, J.H.S., Knystautas, R., *22nd Symposium (Int.) Combust.*, 22: 1723-1731, The Combustion Institute, Pittsburgh, PA, 1988

64. Von Neumann, J., Theory of detonation waves, *Off. Sci. Res. Dev. Rep. 549*, Balist. Res. Lab. File No. X-122, Aberdeen Proving Ground, Md, 1942

65. Wood, W.W., Kirkwood, J.G., Structure of a steady-state plane detonation wave with finite reaction rate, *J. Chem. Phys.* 22:1915-1919, 1954

66. Wood, W.W., Kirkwood, J.G., Diameter effect in condensed explosives. The relation between velocity and radius of curvature of the detonation wave, *J. Chem. Phys.* (22) 11:1920-1924, 1954

67. Wood, W.W., Kirkwood, J.G., On the existence of steady-state detonations supported by a single chemical reaction, *J. Chem. Phys.* 25:1276-1277, 1956

68. Wood, W.W., Kirkwood, J.G., Hydrodynamics of a reacting and relaxing fluid, *J. Appl. Phys.* 28:395-398, 1957

69. Wood, W.W., Parker, F.R., Structure of a centered rarefaction wave in a relaxing gas. *Phys. Fluids* 1:230-241, 1958

70. Wood, W.W., Salzburg, Z.W., Analysis of steady-state supported one-dimensional detonations and shocks. *Phys. Fluids* 3:549-566, 1960

71. Zel'dovich, Ya.B., On the theory of the propagation of detonation in gaseous systems. *Zh. Eksp. Teor. Fiz.* 10:542-568, 1940

72. Zeldovich, Ya.B., Ratner, S.B., *ZhETF* 11:170, 1941

73. Zel'dovich, Ya.B, Gelfand, B.E., Borisov, A.A., Frolov, S.M., Polenov, A.N., Reaction zone in low-velocity detonation of gases in tubes with rough walls, *Sov. J. Chem. Phys.* (4) 2:447:464, 1986

74. Zel'dovich, Y.B., Borisov, A.A., Gelfand, B.E., Frolov, and S.M., Mailkov, A.E., *Prog. Astro. Aero. 114:211-231*, 1988

Appendix I

Steady ZND Equations with Source Terms

The steady ZND equations with source terms can be derived from the time-dependent conservation equations (mass, momentum and energy) in differential form (Euler equations) and the equation of state (EOS), where the source terms ($m, f,$ and q) account for the non-ideal effects. The following equations are called the unsteady Euler equations with source terms:

$$\frac{\partial \rho}{\partial t'} + \frac{\partial(\rho u')}{\partial x'} = m$$

$$\frac{\partial(\rho u')}{\partial t'} + \frac{\partial}{\partial x'}\left(\rho u'^2 + p\right) = f$$

$$\frac{\partial(\rho e')}{\partial t'} + \frac{\partial}{\partial x'}\left[u'(\rho e' + p)\right] = q$$

$$e' = \frac{p}{\rho(\gamma - 1)} - \lambda Q + \frac{1}{2}u'^2$$

where ρ, u, p, x, t, Q, γ, and e are the density, particle velocity, pressure, distance, time, chemical heat release, ratio of specific heats, and the sum of the internal and kinetic energies respectively. The primes indicate values relative to the fixed reference frame. A polytropic equation of state (EOS) is assumed for simplicity, where λ denotes the degree of reaction ($\lambda = 0$ corresponds to unreacted explosive, $\lambda = 1$ corresponds to fully reacted explosive). The above equations are first rewritten in terms of a reference frame attached to the shock. The following transformations are made:

$$x = x_s(t') - x' \qquad \frac{\partial}{\partial t'} = \frac{\partial}{\partial t} + D\frac{\partial}{\partial x}$$

$$t = t'$$

$$\frac{\partial}{\partial x'} = -\frac{\partial}{\partial x}$$

$$u = D - u'$$

where D is the shock velocity and x_s refers to the position of the shock. Applying these transformations, the conservation equations become:

$$\frac{\partial \rho}{\partial t} + \frac{\partial(\rho u)}{\partial x} = m$$

$$\frac{\partial}{\partial x}\left[p + \rho u^2\right] + \frac{\partial}{\partial t}\left[\rho u\right] = Dm - f + \rho\frac{dD}{dt}$$

$$\frac{\partial(\rho e)}{\partial t} + \frac{\partial}{\partial x}\left[u(\rho e + p)\right] = \frac{1}{2}D^2 m - Df + q + \rho u\frac{dD}{dt}$$

To obtain a steady-state solution, all the time derivatives are set equal to zero. One is then left with a much simpler system:

$$\frac{d(\rho u)}{dx} = m \tag{1}$$

$$\frac{d}{dx}\left(\rho u^2 + p\right) = Dm - f \tag{2}$$

$$\frac{d}{dx}\left[u(\rho e + p)\right] = \frac{1}{2}D^2 m - Df + q \tag{3}$$

$$e = \frac{p}{\rho(\gamma - 1)} - \lambda Q + \frac{1}{2}u^2$$

This system of equations can be reduced, by eliminating e from the above equations. The equation for e shall first be differentiated:

$$\frac{de}{dx} = \frac{1}{\gamma - 1}\left[\frac{1}{\rho}\frac{dp}{dx} - \frac{p}{\rho^2}\frac{d\rho}{dx}\right] + u\frac{du}{dx} - Q\frac{d\lambda}{dx}$$

Substituting the expression for e and its derivative in the energy equation (Eqn. 3), one obtains:

$$\frac{du}{dx}\left(\rho e + p + \rho u^2\right) + u\frac{d\rho}{dx}\left[e - \frac{p}{\rho(\gamma - 1)}\right] + u\frac{dp}{dx}\left[\frac{\gamma}{\gamma - 1}\right] - \rho\dot{\lambda}Q = \frac{1}{2}D^2 m - Df + q$$

Substituting the momentum equation (Eqn. 2) in the above yields:

$$\frac{du}{dx}\left(\rho e + p + \rho u^2\left(1 - \frac{2\gamma}{\gamma - 1}\right)\right) + u\frac{d\rho}{dx}\left[e - \frac{p}{\rho(\gamma - 1)} - \frac{u^2\gamma}{\gamma - 1}\right] + \frac{u\gamma}{\gamma - 1}[Dm - f] - \rho\dot{\lambda}Q = \frac{1}{2}D^2 m - Df + q$$

Substituting now the mass equation (Eqn. 1) yields:

$$\frac{du}{dx}\left(\rho e + p - \rho u^2\left(\frac{\gamma + 1}{\gamma - 1}\right) - \rho\left[e - \frac{p}{\rho(\gamma - 1)} - \frac{u^2\gamma}{\gamma - 1}\right]\right) + m\left[e - \frac{p}{\rho(\gamma - 1)} - \frac{u^2\gamma}{\gamma - 1}\right] - \rho\dot{\lambda}Q = \frac{1}{2}D^2 m - Df + q - \frac{u\gamma}{\gamma - 1}[Dm - f]$$

It is now possible to obtain an ordinary differential equation for the particle velocity. Isolating *du*/*dx* and simplifying the expression yields:

$$\frac{du}{dx} = \frac{(\gamma - 1)\left[\rho\dot{\lambda}Q + q\right] + m\left[-\gamma u(D - u) + c^2\right] + f\left[\gamma u - D(\gamma - 1)\right]}{\rho c^2 \eta} \tag{4}$$

where $\eta = 1 - u^2/c^2$ is the gasdynamic parameter. The above is the differential equation for the particle velocity u to be integrated across the reaction zone to get the detonation structure when all three source terms are present. For the ideal detonation case, the source terms m, f, and q are set equal to zero, so that Eqn. 4 reduces to:

$$\frac{du}{dx} = \frac{(\gamma - 1)\dot{\lambda}Q}{c^2 \eta}$$

In this thesis, Eqn. 4 is also specialized to detonation with friction only ($m = 0, q = 0$) and detonation with friction and heat transfer ($m = 0$). The source term m, generally corresponding to area divergence, has already received considerable attention and is not considered in this work.

Appendix II

Normalization of the ZND Structure Equations

In Appendix I, a general differential equation for the particle velocity within the reaction zone was derived. In this Appendix, this expression will be rewritten in terms of normalized variables, better suited for the study of both steady-state and transient detonations. The differential equation was given as:

$$\frac{du}{dx} = \frac{(\gamma - 1)\left[\rho \dot{\lambda} Q + q\right] + m\left[-\gamma u(D-u) + c^2\right] + f\left[\gamma u - D(\gamma - 1)\right]}{\rho c^2 \eta}$$

where $\eta = 1 - u^2/c^2$ is the gasdynamic parameter. Rewriting the gasdynamic parameter in terms of the particle velocity, and writing the sound speed as $c = \sqrt{\gamma p/\rho}$, the above equation becomes:

$$\frac{du}{dx} = \frac{(\gamma - 1)\left[\rho \dot{\lambda} Q + q\right] + m\left[-\gamma u(D-u) + \gamma p/\rho\right] + f\left[\gamma u - D(\gamma - 1)\right]}{\gamma p - \rho u^2}$$

As the source term m is not considered in this work ($m = 0$), the above equation reduces to::

$$\frac{du}{dx} = \frac{(\gamma - 1)\left[\rho \dot{\lambda} Q + q\right] + f\left[\gamma u - D(\gamma - 1)\right]}{\gamma p - \rho u^2}$$

The above variables will now be normalized according to the following:

$$u' = \left(\frac{u}{c_o}\right),\ \rho' = \left(\frac{\rho}{\rho_o}\right),\ Q' = \left(\frac{Q}{c_o^2}\right),\ q' = \left(\frac{q}{\gamma p_o c_o / x_{1/2}}\right),\ f' = \left(\frac{f}{\gamma p_o / x_{1/2}}\right),$$

$$M=\left(\frac{D}{c_o}\right),\ x'=\left(\frac{x}{x_{1/2}}\right),\ p'=\left(\frac{p}{p_o}\right),\ t'=\left(\frac{t}{x_{1/2}/c_o}\right)$$

The differential equation for the particle velocity, in normalized form, becomes:

$$\frac{du'}{dx'}=\frac{\left[\dot{\lambda}'Q'+\frac{q'}{\rho'}\right]+\frac{f'M}{\rho'}\left[\frac{\gamma}{(\gamma-1)}\frac{u'}{M}-1\right]}{\frac{1}{(\gamma-1)}\left(\frac{p'}{\rho'}-u'^2\right)}$$

The denominator can be written in terms of the sound speed. Using normalized variables, the sound speed is expressed as $c'=\sqrt{p'/\rho'}$:

$$\frac{du'}{dx'}=\frac{\left[\dot{\lambda}'Q'+\frac{q'}{\rho'}\right]+f'u'\left[\frac{\gamma}{(\gamma-1)}\frac{u'}{M}-1\right]}{\frac{1}{(\gamma-1)}\left(c'^2-u'^2\right)}$$

The normalized expression for the momentum source term f' is:

$$f'=-\rho' k_f(M-u')|M-u'|$$

where k_f is an arbitrary dimensionless friction factor, and the velocity u' is defined with respect to the moving shock. The expression for the energy source term q' is based on the Reynolds analogy, relating the heat losses to the corresponding momentum losses in a tube with friction:

$$q'=\frac{1}{\gamma-1}\frac{f'}{u'}\left[\frac{p'}{\rho'}-T'_w\right]$$

where the normalized adiabatic wall temperature T'_w is set equal to one in the present work. The value of q' is thus dependent on the value of the friction source term f'.

In this thesis, the primes, indicating the normalized variables, are dropped, since only normalized quantities are considered (except in section 3.1 dealing with detailed kinetics). Dropping the primes, the normalized equations can thus be summarized as:

$$\frac{du}{dx} = \frac{\left[\dot{\lambda}Q + \frac{q}{\rho}\right] + fu\left[\frac{\gamma}{(\gamma-1)}\frac{u}{M} - 1\right]}{\frac{1}{(\gamma-1)}\left(c^2 - u^2\right)}$$

$$f = -\rho k_f (M-u)|M-u|$$

$$q = \frac{1}{\gamma - 1}\frac{f}{u}\left[\frac{p}{\rho} - 1\right]$$

Appendix III

The Saddle Point Condition

The differential equation for the particle velocity, when integrated within the reaction zone, may lead to a singular point when the denominator vanishes. This happens when the flow becomes sonic relative to the shock front. To avoid this singularity, the Generalized C-J criterion states that the numerator of *du/dx* must go to zero simultaneously, leading to an indeterminate value of the derivative at the sonic plane. This Appendix provides a method to obtain the value of the derivative *du/dx* at the sonic point, using l'Hospital's rule. The *du/dx* equation for a two-rate law system shall first be obtained by setting the source terms m, f, and q to zero in the result from Appendix II. It is then possible to split the chemical heat release rate into two expressions:

$$\frac{du}{dx}=\frac{\dot{\lambda}_1 Q_1+\dot{\lambda}_2 Q_2}{\frac{1}{(\gamma-1)}\left(c^2-u^2\right)}=\frac{\mu}{\psi}\rightarrow\frac{0}{0}=\frac{\frac{d\mu}{dx}}{\frac{d\psi}{dx}}=\frac{\mu_x}{\psi_x}$$

One therefore has to derive expressions for μ_x and ψ_x, where:

$$\mu=\dot{\lambda}_1 Q_1+\dot{\lambda}_2 Q$$

$$\psi=\frac{pv-u^2}{(\gamma-1)}$$

The density and the specific volume are related through $v=1/\rho$. The chemical rate laws are expressed as:

$$\dot{\lambda}_1=k_1(1-\lambda_1)\exp\left(\frac{-E_{a_1}}{pv}\right)\quad\text{and}\quad\dot{\lambda}_2=k_2(\lambda_1-\lambda_2)\exp\left(\frac{-E_{a_2}}{pv}\right)$$

An expression for μ_x is first obtained:

$$\mu_x = \frac{\partial \mu}{\partial x} = \frac{\partial \mu}{\partial t}\frac{\partial t}{\partial x} = \frac{1}{u}\frac{\partial \mu}{\partial t} = \frac{1}{u}\left(\frac{\partial \dot{\lambda}_1}{\partial t}Q_1 + \frac{\partial \dot{\lambda}_2}{\partial t}Q_2\right)$$

where:

$$\frac{\partial \dot{\lambda}_1}{\partial t} = -\frac{\dot{\lambda}_1^2}{(1-\lambda_1)} + \dot{\lambda}_1\left(\frac{E_{a_1}}{pv}\right)\left[\frac{1}{Mv} - \frac{\gamma M}{p}\right]u\frac{\partial u}{\partial x}$$

and:

$$\frac{\partial \dot{\lambda}_2}{\partial t} = \frac{\dot{\lambda}_2\dot{\lambda}_1 - \dot{\lambda}_2^2}{\lambda_1 - \lambda_2} + \dot{\lambda}_2\left(\frac{E_{a_2}}{pv}\right)\left[\frac{1}{Mv} - \frac{\gamma M}{p}\right]u\frac{\partial u}{\partial x}$$

Substituting these derivatives back into μ_x gives:

$$\mu_x = \frac{1}{u}\left\{\frac{\dot{\lambda}_1^2}{(1-\lambda_1)}Q_1' + \left(\frac{\dot{\lambda}_2^2 - \dot{\lambda}_2\dot{\lambda}_1}{\lambda_1 - \lambda_2}\right)Q_2\right\} - \frac{\partial u}{\partial x}\left(\frac{1}{pv}\right)\left[\frac{1}{Mv} - \frac{\gamma M}{p}\right]\left\{\dot{\lambda}_1 E_{a_1} Q_1 + \dot{\lambda}_2 E_{a_2} Q_2\right\}$$

This expression can be simplified using the conservation of mass equation $M = u/v$ and the sonic condition $u^2 = pv$ (satisfied at the saddle point):

$$\mu_x = \frac{1}{u}\left\{\frac{\dot{\lambda}_2(\dot{\lambda}_2 - \dot{\lambda}_1)}{(\lambda_1 - \lambda_2)}Q_2 + \frac{\dot{\lambda}_1^2}{(1-\lambda_1)}Q_1\right\} + \frac{\partial u}{\partial x}\left(\frac{\gamma - 1}{u^3}\right)\left[\dot{\lambda}_1 E_{a_1} Q_1 + \dot{\lambda}_2 E_{a_2} Q_2\right]$$

For convenience, this is rewritten as:

$$\mu_x = L + K\left(\frac{\partial u}{\partial x}\right)$$

where:

$$L = \frac{1}{u}\left\{\frac{\dot{\lambda}_2(\dot{\lambda}_2 - \dot{\lambda}_1)}{(\lambda_1 - \lambda_2)}Q_2 + \frac{\dot{\lambda}_1^2}{(1-\lambda_1)}Q_1\right\}$$

$$K = \left(\frac{\gamma - 1}{u^3}\right)\left[\dot{\lambda}_1 E_{a_1} Q_1 + \dot{\lambda}_2 E_{a_2} Q_2\right]$$

An expression for ψ_x shall now be obtained:

$$\psi_x = \frac{1}{(\gamma - 1)}\left[p\frac{\partial v}{\partial x} + v\frac{\partial p}{\partial x} - 2u\frac{\partial u}{\partial x}\right]$$

The derivatives $\partial v/\partial x$ and $\partial p/\partial x$ can be expressed in terms of $\partial u/\partial x$ using the mass and momentum conservation equations respectively:

$$\frac{\partial v}{\partial x}=\frac{v}{u}\frac{\partial u}{\partial x}=\frac{1}{M}\frac{\partial u}{\partial x} \qquad \frac{\partial p}{\partial x}=-\gamma M\frac{\partial u}{\partial x}$$

Substituting these in the expression for ψ_x and rearranging yields:

$$\psi_x=-u\frac{(\gamma+1)}{(\gamma-1)}$$

For convenience, this is rewritten as:

$$\psi_x=R\left(\frac{\partial u}{\partial x}\right)+S$$

where:

$$R=-u\left(\frac{\gamma+1}{\gamma-1}\right) \quad \text{and} \quad S=0$$

It is now possible to obtain an expression for $\partial u/\partial x$ by combining μ_x and ψ_x:

$$\frac{\partial u}{\partial x}=\frac{\mu_x}{\psi_x}=\frac{K(\partial u/\partial x)+L}{R(\partial u/\partial x)}$$

A quadratic in $\partial u/\partial x$ is thus obtained:

$$R\left(\frac{\partial u}{\partial x}\right)^2-K\left(\frac{\partial u}{\partial x}\right)-L=0$$

Solving this using the standard quadratic equation solution yields:

$$\frac{\partial u}{\partial x}=\frac{K\pm\sqrt{K^2+4RL}}{2R}$$

There are two possible solutions. The positive sign yields a positive $\partial u/\partial x$, corresponding to a continuous slope at the sonic plane leading to the weak detonation state. The negative sign yields a negative $\partial u/\partial x$ (discontinuity in slope). Integration of the conservation equations using this value of $\partial u/\partial x$ leads to the strong detonation state.

Appendix IV

ZND Equations with Detailed Chemistry

In this Appendix, the ZND detonation structure equations for the case of an ideal gas with detailed chemistry will be derived. The derivation starts from the steady-state conservation equations from Appendix I:

$$\frac{d(\rho u)}{dx} = m$$

$$\frac{d}{dx}\left(\rho u^2 + p\right) = Dm - f$$

$$\frac{d}{dx}\left[u(\rho e + p)\right] = \frac{1}{2}D^2 m - Df + q$$

Note that the above equations are all dimensional. The source terms m, f, and q shall now be omitted, leading to this simpler form:

$$\frac{d(\rho u)}{dx} = 0$$

$$\frac{d}{dx}\left(\rho u^2 + p\right) = 0$$

$$\frac{d}{dx}\left[u(\rho e + p)\right] = 0$$

Now, instead of using the polytropic gas equation of state with a constant ratio of specific heats γ, the ideal gas equation of state shall be used, coupled with a caloric equation of state:

$$p = \rho R_s T$$

$$h = h(T)$$

The energy conservation equation is currently written in terms of e, the sum of the internal and kinetic energies. Since the enthalpy h is tabulated, it is more convenient to express e in terms of h:

$$e = h - \frac{p}{\rho} + \frac{u^2}{2}$$

Here, h is the enthalpy per unit mass of the mixture. It is more convenient to express it in terms of the tabulated molar enthalpies for each chemical species, and express the result per mass of the mixture. The term λQ disappears, since it is included in $\tilde{h}_i$ (enthalpy of formation). Also, the ideal gas EOS can be used to equate p/ρ to $R_s T$:

$$e = \frac{\sum n_i \tilde{h}_i}{m_t} - R_s T + \frac{u^2}{2}$$

where m_t is the total mass of the mixture (constant) and n_i represents the number of moles of the chemical specie i. The $\tilde{h}_i$ are tabulated in terms of the temperature. To obtain the ZND equations, the derivative de/dx is first obtained:

$$\frac{de}{dx} = \frac{1}{m_t}\frac{d}{dx}\left(\sum_i n_i \tilde{h}_i\right) - R_s \frac{dT}{dx} - T\frac{dR_s}{dx} + u\frac{du}{dx}$$

Expanding the derivatives using the chain rule, and rearranging yields:

$$\frac{de}{dx} = \frac{dT}{dx}\left\{\frac{1}{m_t}\sum_i n_i \frac{d\tilde{h}_i}{dT} - R_s\right\} + \sum_i \frac{dn_i}{dt}\left\{\frac{\tilde{h}_i}{m_t u} - \frac{T}{u}\frac{\partial R_s}{\partial n_i}\right\} + u\frac{du}{dx}$$

The derivative dT/dx can readily be obtained by differentiating the equation of state $T = p/\rho R_s$:

$$\frac{dT}{dx} = \frac{\partial T}{\partial p}\frac{dp}{dx} + \frac{\partial T}{\partial \rho}\frac{d\rho}{dx} + \frac{\partial T}{\partial R_s}\frac{dR_s}{dx}$$

Expanding the derivatives using the chain rule, and rearranging yields:

$$\frac{dT}{dx} = \frac{1}{\rho R_s}\frac{dp}{dx} - \frac{p}{\rho^2 R_s}\frac{d\rho}{dx} - \frac{p}{\rho u R_s^2}\sum_i \frac{\partial R_s}{\partial n_i}\frac{dn_i}{dt}$$

The three conservation equations shall now be combined with the expressions for de/dx and dT/dx. Upon performing a series of algebraic and simplifying steps, an expression involving only du/dx is obtained:

$$\frac{du}{dx}=\frac{1}{u}\frac{\sum_i \frac{dn_i}{dt}\left\{\frac{R_s\bar{h}_i}{\sum_j n_j\, d\bar{h}_j/dT}-T\frac{\partial R_s}{\partial n_i}\right\}}{u-\frac{R_sT}{u}-\frac{m_t u R_s}{\sum_j n_j\, d\bar{h}_j/dT}}$$

This du/dx equation can readily be integrated, along with the kinetics equations, within prescribed boundary conditions. The other thermodynamic variables can be computed algebraically for any value of the independent variables u and n_i through the use of the integrated conservation equations and the equation of state. One then obtains:

$$\rho=\frac{\rho_o D}{u}$$

$$p=p_o+\rho_o D^2-(\rho_o D)u$$

$$T=p/\rho R_s$$

where R_s is obtained from:

$$\mathrm{R_s}=\frac{\sum_\mathrm{i}\mathrm{n_iM_i}}{\sum_\mathrm{i}\mathrm{n_i}}$$

This form of the du/dx equation is very convenient for computational purposes, but does not show clearly the main physical features of the flow. This equation can be simplified by introducing the expressions below:

$$C_{p_f}=\frac{1}{m_t}\frac{dH}{dt}=\frac{1}{m_t}\sum_j n_j\frac{d\bar{h}_j}{dt}$$

$$C_{p_f}-C_{v_f}=R_s$$

$$\gamma = \frac{C_{p_f}}{C_{v_f}}$$

$$c_f = \sqrt{\gamma P/\rho} = \sqrt{R_s T}$$

where C_{p_f} is the heat capacity at constant pressure and fixed composition, C_{v_f} is the heat capacity at constant volume and fixed composition, γ is the ratio of the heat capacities at constant composition, and c_f is the frozen sound speed (sound speed assuming a fixed composition). Substituting these expressions in the du/dx equation gives:

$$\frac{du}{dx} = \frac{\sum_i \frac{dn_i}{dt}\left\{\frac{\tilde{h}_i}{m} - \frac{\gamma T}{\gamma - 1}\frac{\partial R_s}{\partial n_i}\right\}}{\frac{1}{\gamma - 1}\left(c_f^2 - u^2\right)}$$

This differential equation is now in the same form as that given in Appendix I for the polytropic gas case with source terms. The numerator is thus equivalent to the chemical energy release rate.

Appendix V

The Secondary Shock Velocity M_{sec}

In this appendix, an expression is derived for the value of the secondary shock velocity M_{sec} obtained for supported pathological detonations with the piston velocity u_p above the weak value u_w, but below the strong one u_s ($u_w < u_p < u_s$). The secondary shock wave connects the weak detonation state with a region of constant state extending to the piston surface. To satisfy the conservation equations, the velocity of that shock wave has to be below the detonation front value M. This secondary shock wave thus recedes back from the reaction zone. The shock and particle velocities can be illustrated for the detonation shock and the secondary shock both with respect to the laboratory frame, and their respective shock-attached frames, i.e.:

Detonation shock front

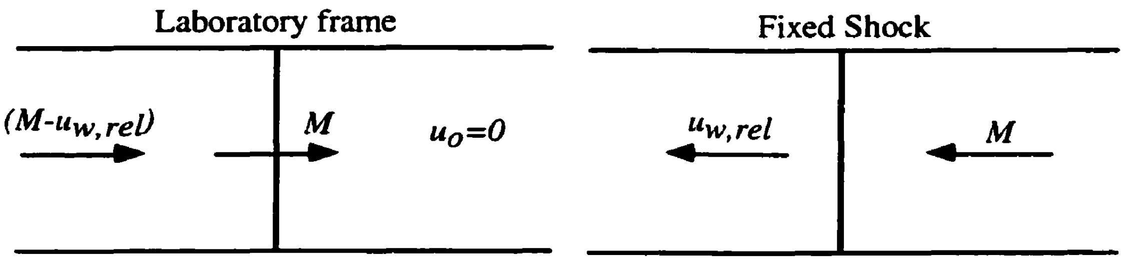

Receding shock

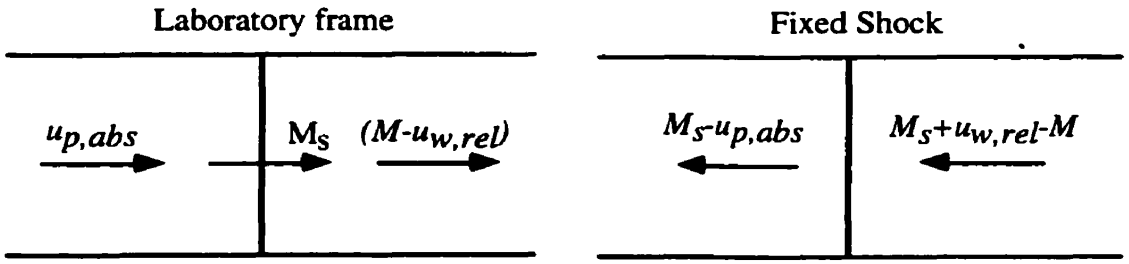

In the above diagrams, the subscript *abs* refers to properties measured with respect to the fixed laboratory frame, and the subscript *rel* refers to properties measured with respect to the shock-attached frame. Based on these diagrams, the conservation equations across the secondary shock (respectively mass, momentum and energy) can be written as:

$$\frac{1}{v_w}\left[M_{sec} + u_{w,rel} - M\right] = \frac{1}{v}\left[M_{sec} - u_{p,abs}\right]$$

$$p_w + \frac{\gamma}{v_w}\left[M_{sec} + u_{w,rel} - M\right]^2 = p + \frac{\gamma}{v}\left[M_{sec} - u_{p,abs}\right]^2$$

$$\frac{p_w v_w}{\gamma - 1} + \frac{\left[M_{sec} + u_{w,rel} - M\right]^2}{2} = \frac{pv}{\gamma - 1} + \frac{\left[M_{sec} - u_{p,abs}\right]^2}{2}$$

Isolating v in the mass equation and substituting it in the momentum and energy equations yields:

$$p_w + \frac{\gamma}{v_w}\left[M_{sec} + u_{w,rel} - M\right]^2 = p + \frac{\gamma}{v_w}\left[M_{sec} - u_{p,abs}\right]\left[M_{sec} + u_{w,rel} - M\right]$$

$$\frac{p_w v_w}{\gamma - 1} + \frac{\left[M_{sec} + u_{w,rel} - M\right]^2}{2} - \frac{\left[M_{sec} - u_{p,abs}\right]^2}{2} = \frac{p v_w}{\gamma - 1}\frac{\left[M_{sec} - u_{p,abs}\right]}{\left[M_{sec} + u_{w,rel} - M\right]}$$

The pressure p in the momentum equation can be isolated and substituted into the energy equation, i.e.:

$$\frac{p_w v_w}{\gamma - 1} + \frac{\left[M_{sec} + u_{w,rel} - M\right]^2 - \left[M_{sec} - u_{p,abs}\right]^2}{2} -$$

$$\frac{v_w\left[M_{sec} - u_{p,abs}\right]}{(\gamma - 1)\left[M_{sec} + u_{w,rel} - M\right]}\left[p_w + \frac{\gamma}{v_w}\left(M_{sec} + u_{w,rel} - M\right)\left(u_{w,rel} + u_{p,abs} - M\right)\right] = 0$$

This equation can be solved numerically for the value of M_{sec}. The remaining variables are found using:

$$p = p_w + \frac{\gamma}{v_w}\left(M_{sec} + u_{w,rel} - M\right)\left[\left(M_{sec} + u_{w,rel} - M\right) - \left(M_{sec} - u_{p,abs}\right)\right]$$

$$v = v_w \frac{\left(M_{sec} - u_{p,abs}\right)}{\left(M_{sec} + u_{w,rel} - M\right)}$$

Appendix VI

The Critical Shock Velocity M_{cr}

In this appendix, an analytical expression is derived for the value of the shock velocity M_{cr} below which the Generalized C-J criterion no longer applies, due to the fact that the flow becomes entirely subsonic relative to the shock front. For this limiting value of the shock velocity, the detonation products are in chemical equilibrium, and completely at rest in the laboratory frame at the sonic plane, i.e.:

$$u_{abs} = 0 \text{ (or } u_{cr} = M_{cr}\text{)}$$

$$\lambda_{cr} = 1$$

$$u_{cr} = c$$

Moreover, as a consequence of $u_{cr} = M_{cr}$, the normalized specific volume at the sonic plane is unity, from the conservation of mass, i.e.:

$$v_{cr} = 1$$

Due to the presence of a source term in the equation for the conservation of momentum, it is not possible to integrate the momentum equation analytically to obtain an algebraic equation. However, it is possible to combine the momentum and energy equations in a differential form to eliminate the source term f. These normalized equations are written as:

$$\frac{\partial(\rho u^2 + p/\gamma)}{\partial x} = -f$$

$$\frac{\partial[u(\rho e + p/\gamma)]}{\partial x} = -Mf$$

Multiplying the momentum equation by M and subtracting the energy equation yields:

$$\frac{\partial\left(M\rho u^2 + Mp/\gamma\right)}{\partial x} = \frac{\partial\left[u(\rho e + p/\gamma)\right]}{\partial x}$$

Rewriting everything in a single derivative yields:

$$\frac{\partial}{\partial x}\left[u(\rho e + p/\gamma) - \left(M\rho u^2 + Mp/\gamma\right)\right] = 0$$

The above can be simplified, i.e.:

$$\frac{\partial}{\partial x}\left[\frac{p}{\gamma}(u - M) + M(e - Mu)\right] = 0$$

Integrating the above yields:

$$\frac{p}{\gamma}(u - M) + M(e - Mu) = const.$$

For the case $M = M_{cr}$, $u = M$ at the sonic plane. Substituting this gives:

$$M\left(e - M^2\right) = const.$$

The value of the constant can be found by evaluating the above equation ahead of the shock front:

$$M\left(e - M^2\right) = M\left(e_o - M^2\right)$$

Replacing e by its definition, and applying the above result for the critical case, one obtains:

$$M\left(\frac{p_{cr}v_{cr}}{\gamma(\gamma-1)} - \lambda Q + \frac{u_{cr}{}^2}{2} - M^2\right) = M\left(\frac{p_o v_o}{\gamma(\gamma-1)} - \lambda_o Q + \frac{M^2}{2} - M^2\right)$$

where p_o and v_o are equal to 1 by definition, $v_{cr} = 1$, $\lambda_{cr} = 1$, $u_{cr} = M_{cr}$, and λ_o is equal to zero, since no reaction has taken place ahead of the shock. The above equation can thus be simplified as follows:

$$\frac{p_{cr}}{\gamma(\gamma-1)} - Q - \frac{1}{\gamma(\gamma-1)} = 0$$

Isolating p_{cr} in the above yields:

$$p_{cr} = \gamma(\gamma - 1)Q + 1$$

The critical shock velocity M_{cr} can be related to the critical pressure p_{cr} through the expression for the sound speed, since the particle velocity is equal to the sound speed:

$$M_{cr} = u_{cr} = c = \sqrt{p_{cr} v_{cr}} = \sqrt{p_{cr}}$$

In summary, one obtains the following critical properties:

$$M_{cr} = \sqrt{\gamma(\gamma - 1)Q + 1}$$

$$p_{cr} = \gamma(\gamma - 1)Q + 1$$

$$u_{cr} = M_{cr}$$

$$v_{cr} = 1$$

$$\lambda_{cr} = 1$$

Figures

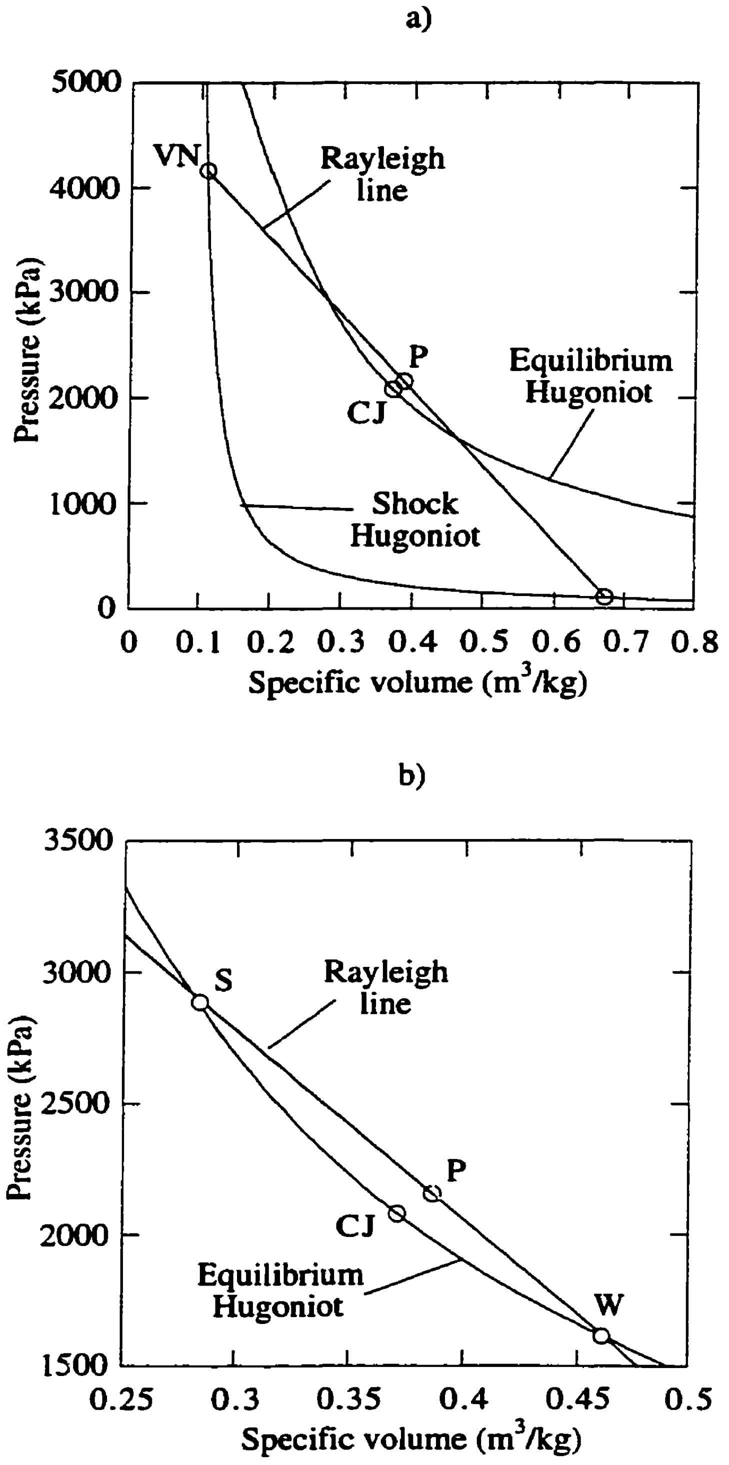

Figure 3.1: $p-v$ diagram for a pathological detonation in H_2-Cl_2 $\phi=1$, $p_o=101.3\,kPa$ (a) Entire diagram, (b) Zoom

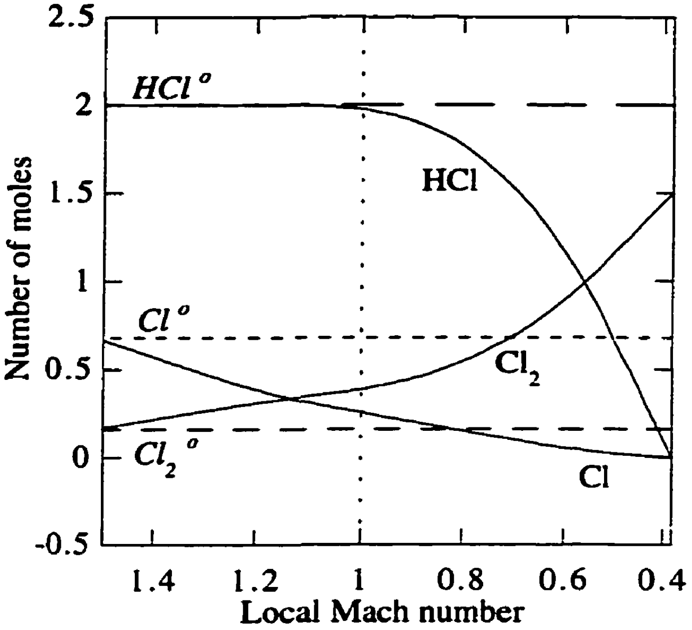

Figure 3.2: Concentration of HCl, Cl and Cl_2 with respect to the local Mach number within the reaction zone for the mixture $H_2 - Cl_2$ $\phi = 0.667$, $p_o = 2\ kPa$. The dotted lines represent the weak equilibrium state values

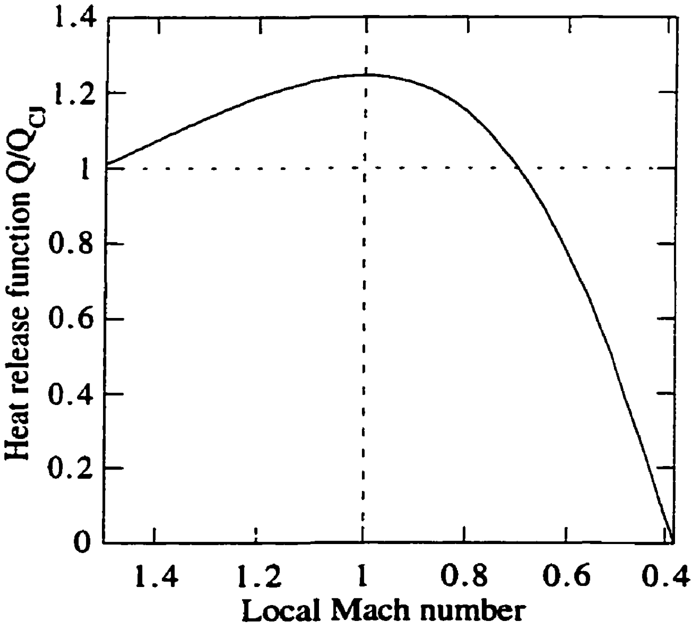

Figure 3.3: Heat release function with respect to the local Mach number within the reaction zone for the mixture $H_2 - Cl_2$ $\phi = 0.667$, $p_o = 2\ kPa$

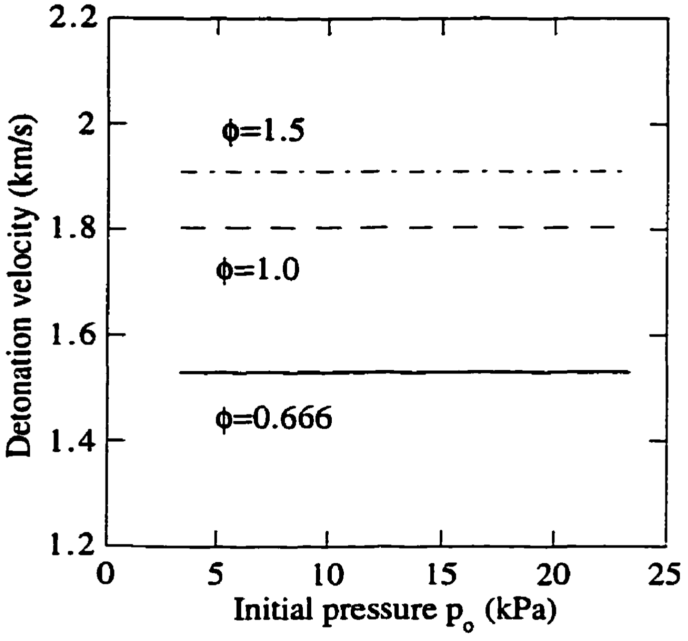

Figure 3.4: Theoretical detonation velocities for the three $H_2 - Cl_2$ mixtures

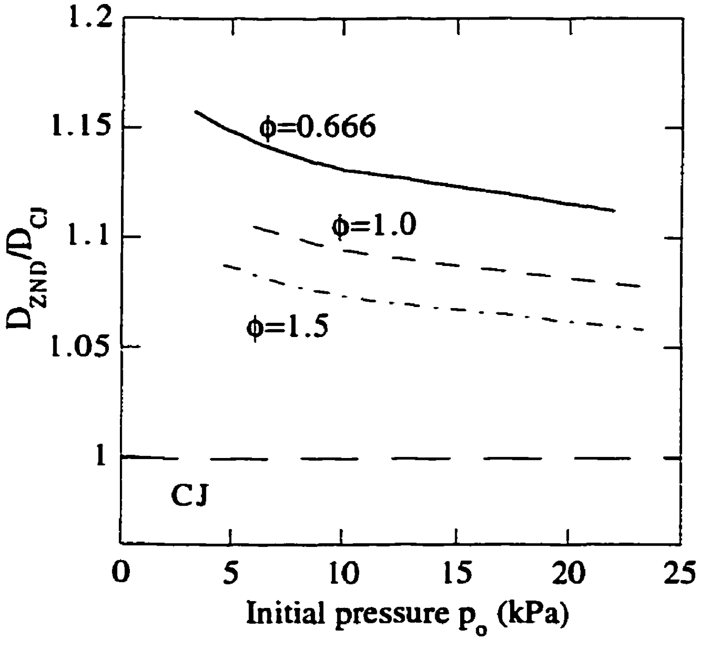

Figure 3.5: Normalized theoretical detonation velocities for the three $H_2 - Cl_2$ mixtures

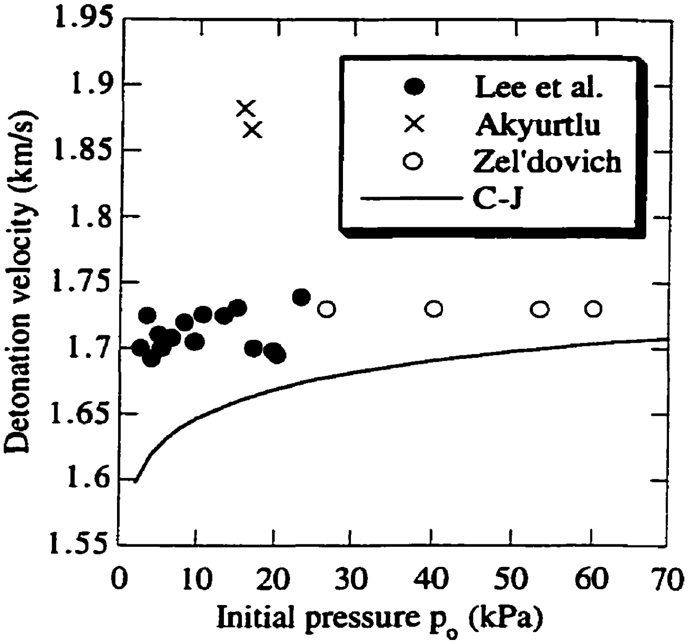

Figure 3.6: Experimental detonation velocity vs. initial pressure for the stoichiometric $H_2 - Cl_2$ mixture. Results from previous works. The C-J predictions are also shown

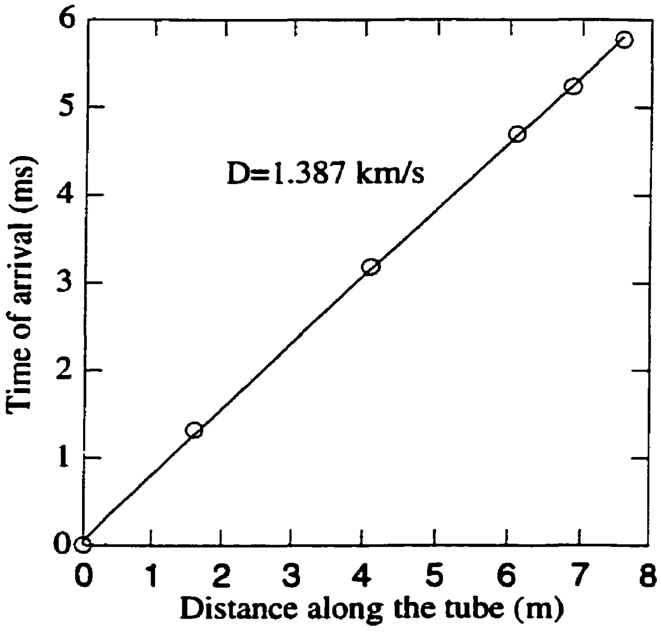

Figure 3.7: Distance-time diagram ($x-t$) for $H_2 - Cl_2$, $\phi = 0.667$, $p_o = 25 kPa$, $D_{exp} = 1.387 km/s$, $D_{CJ} = 1.352 km/s$

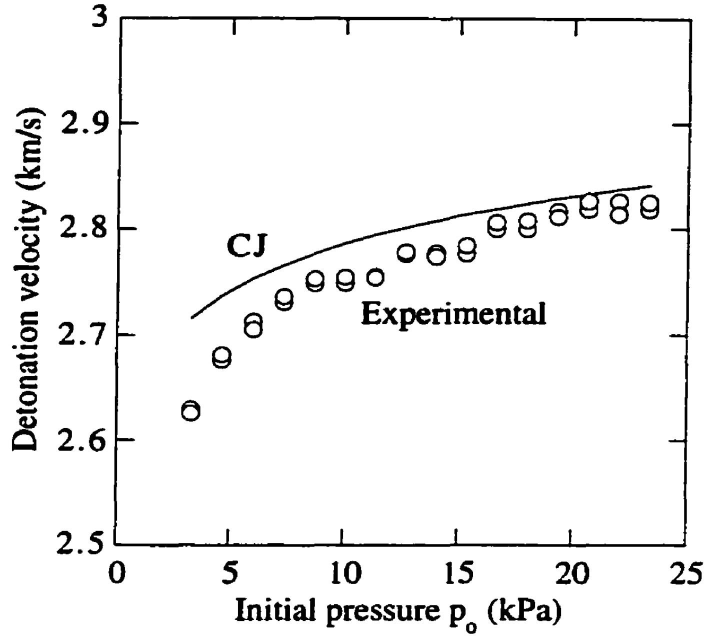

Figure 3.8: Experimental detonation velocities vs. initial pressure for the stoichiometric $C_2H_2 - O_2$ mixture. The C-J predictions are also shown

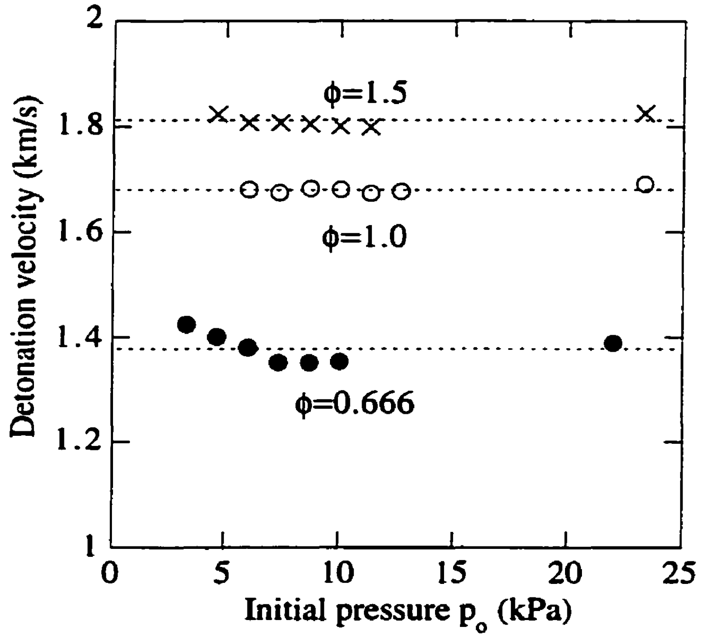

Figure 3.9: Experimental detonation velocities vs. initial pressure for the $H_2 - Cl_2$ mixture (Present work)

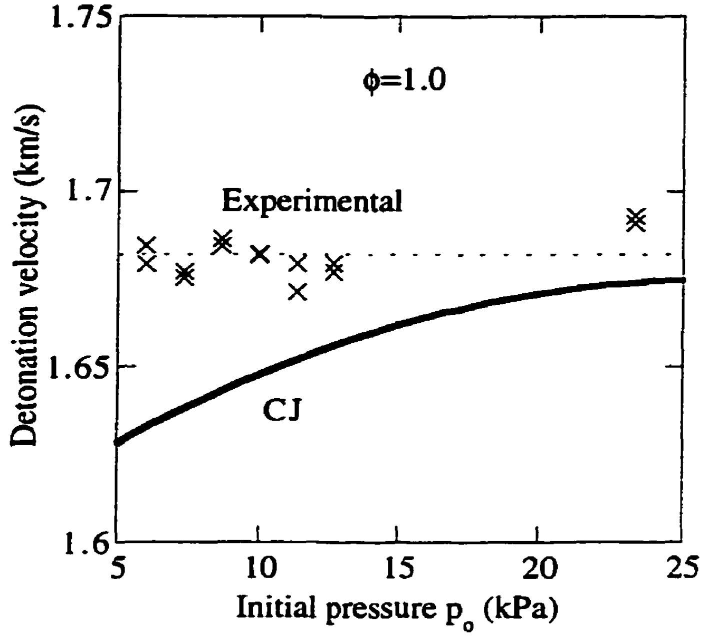

Figure 3.10: Experimental and C-J detonation velocities vs. initial pressure for the stoichiometric $H_2 - Cl_2$ mixture

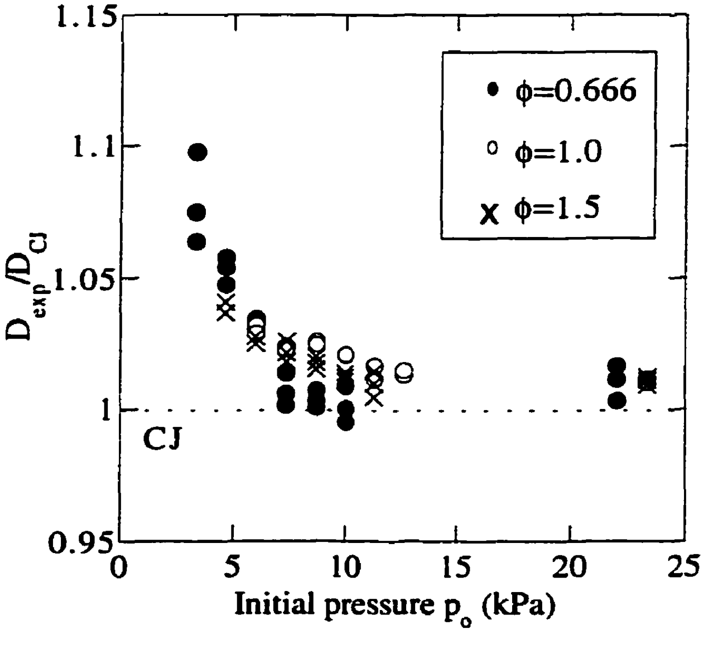

Figure 3.11: Experimental detonation velocities normalized with respect to the C-J predictions vs. initial pressure for the three $H_2 - Cl_2$ mixtures

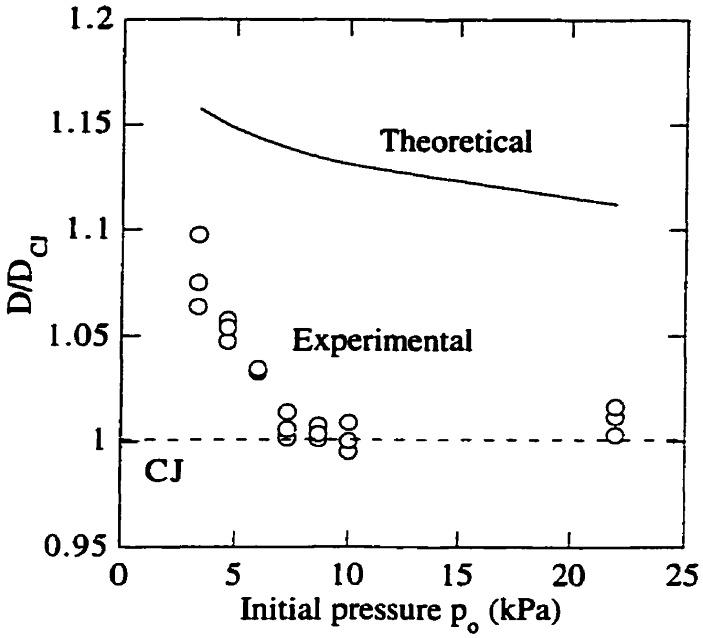

Figure 3.12: Experimental and theoretical normalized detonation velocities for the $\phi = 0.667$ $H_2 - Cl_2$ mixture

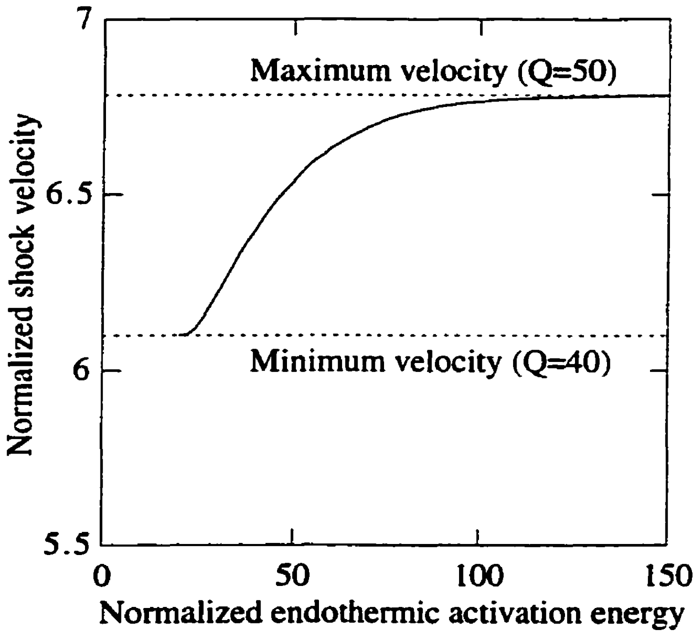

Figure 3.13: The normalized pathological detonation velocity as a function of the endothermic activation energy E_{a_2} ($Q_1 = 50$, $Q_2 = -10$, $\gamma = 1.2$, $E_{a_1} = 22$ and $k_1 = k_2 = 100$)

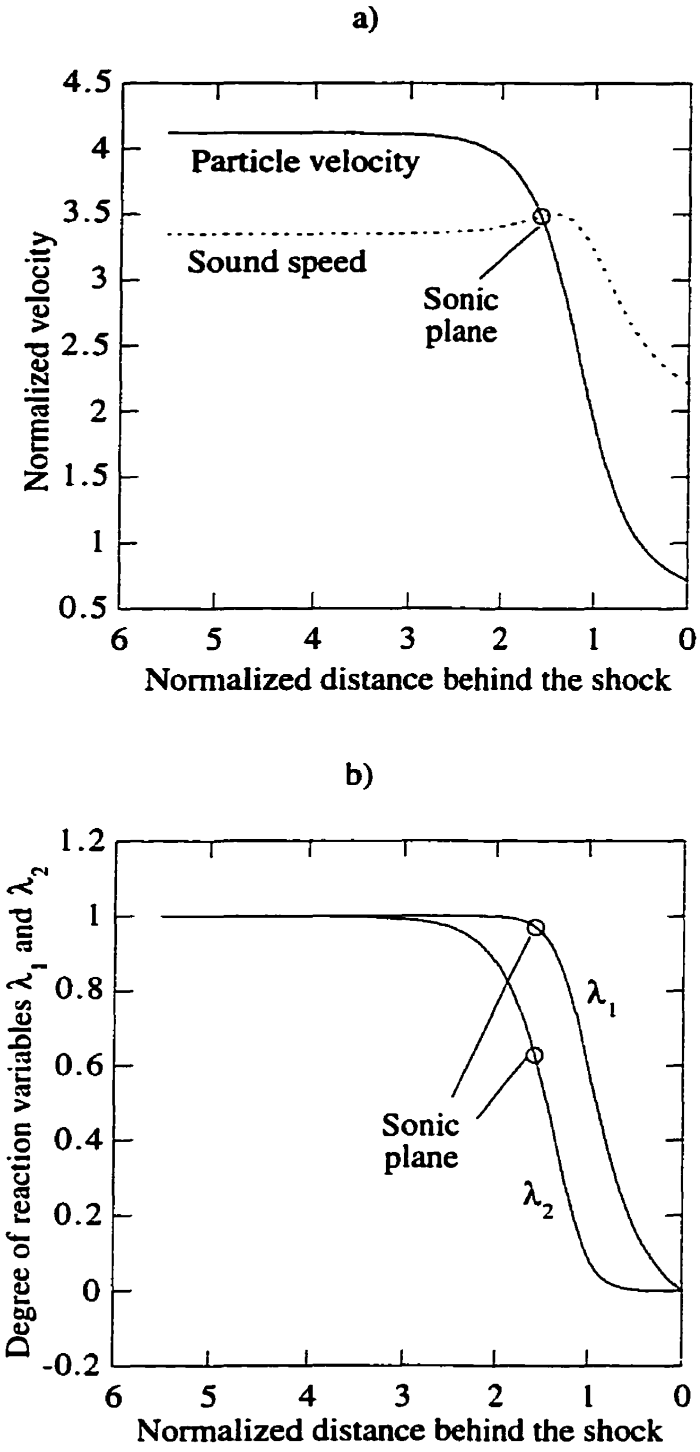

Figure 3.14: Particle velocity (a) and degree of reaction variables (b) within the reaction zone. ($Q_1 = 50$, $Q_2 = -10$, $\gamma = 1.2$, $E_{a_1} = 22$, $E_{a_2} = 32$ and $k_1 = k_2 = 100$)

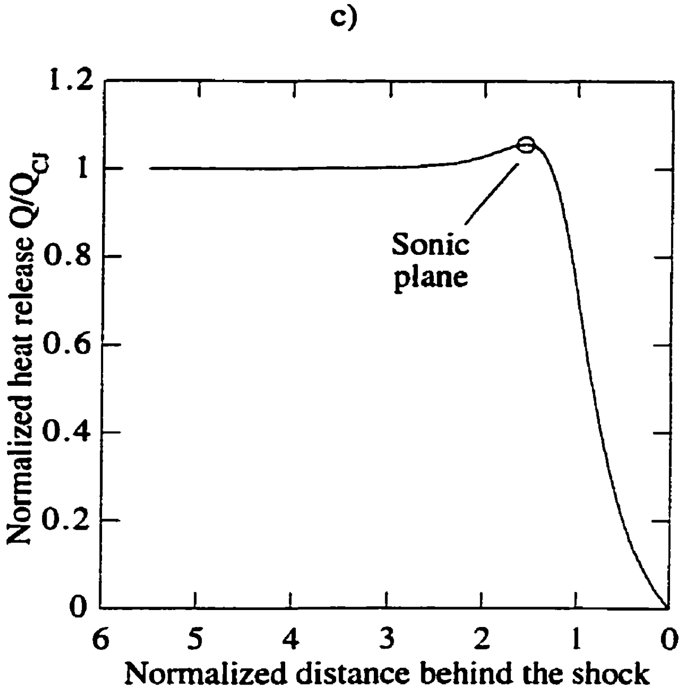

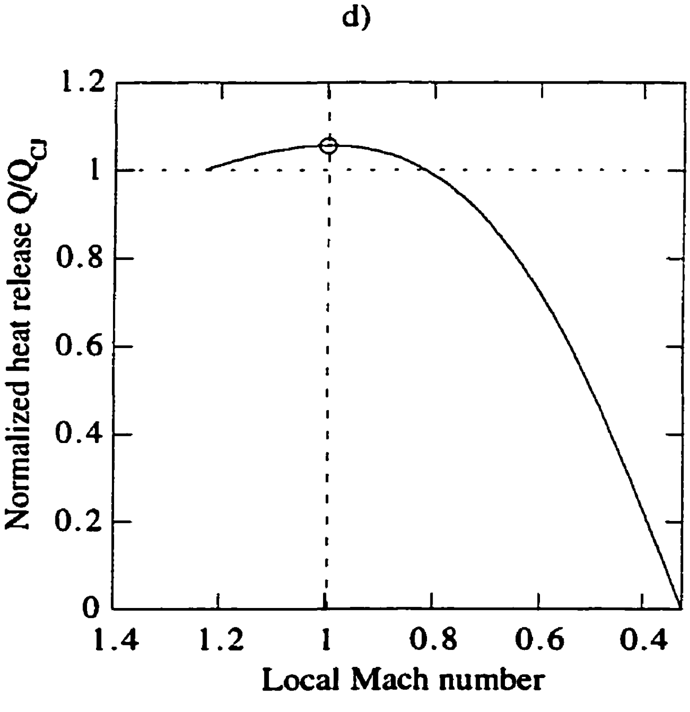

Figure 3.14: Heat release function Q/Q_{CJ} within the reaction zone with respect to the distance (c) and with respect to the local Mach number (d). ($Q_1 = 50$, $Q_2 = -10$, $\gamma = 1.2$, $E_{a_1} = 22$, $E_{a_2} = 32$ and $k_1 = k_2 = 100$)

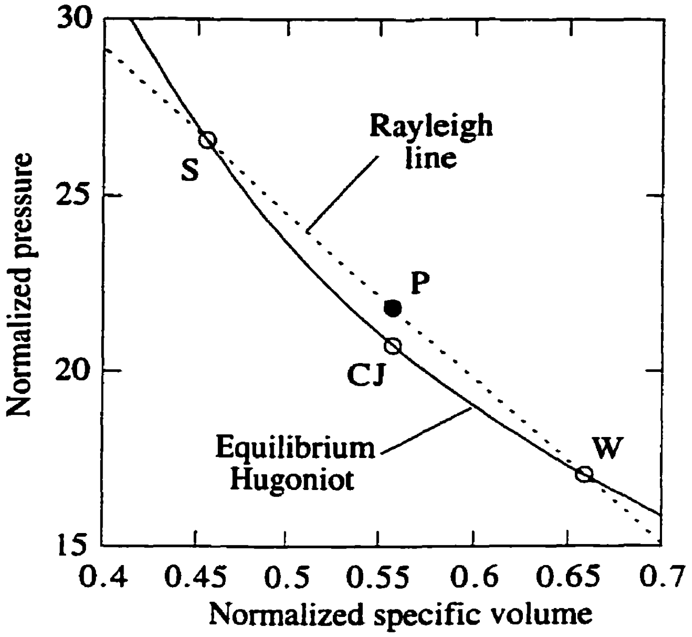

Figure 3.14e: $p-v$ diagram for a pathological detonation ($Q_1=50$, $Q_2=-10$, $\gamma=1.2$, $E_{a_1}=22$, $E_{a_2}=32$ and $k_1=k_2$)

a)

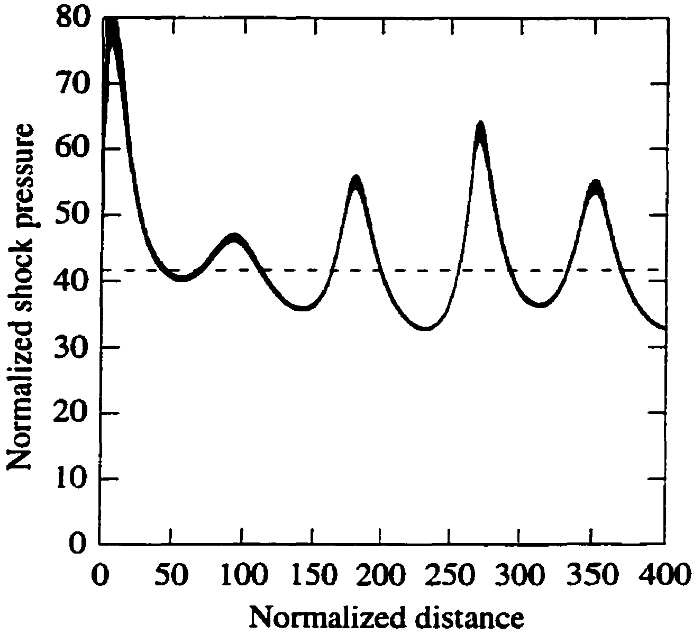

b)

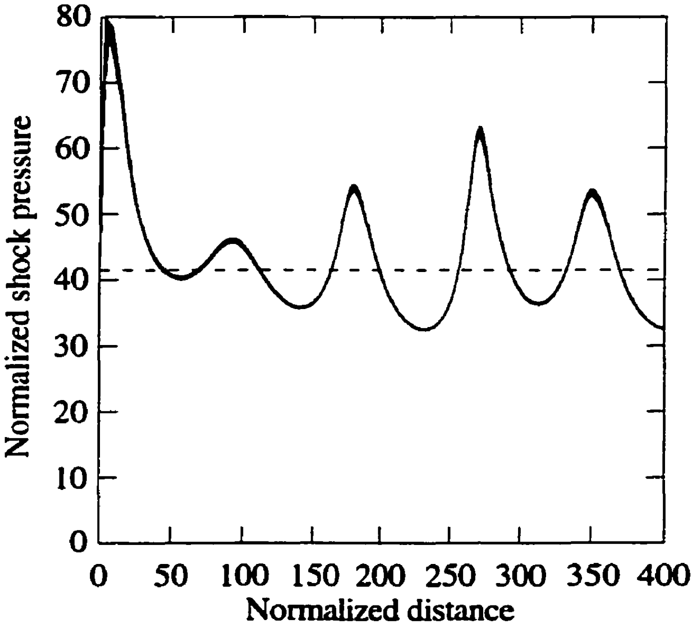

Figure 3.15: The shock pressure profile for an oscillatory pathological detonation ($Q_1 = 50$, $Q_2 = -10$, $\gamma = 1.2$, $E_{a_1} = 22$, $E_{a_2} = 32$ and $k_1 = k_2$). Computations with 50 numerical cells (a) and 100 numerical cells (b) in the half-reaction zone length

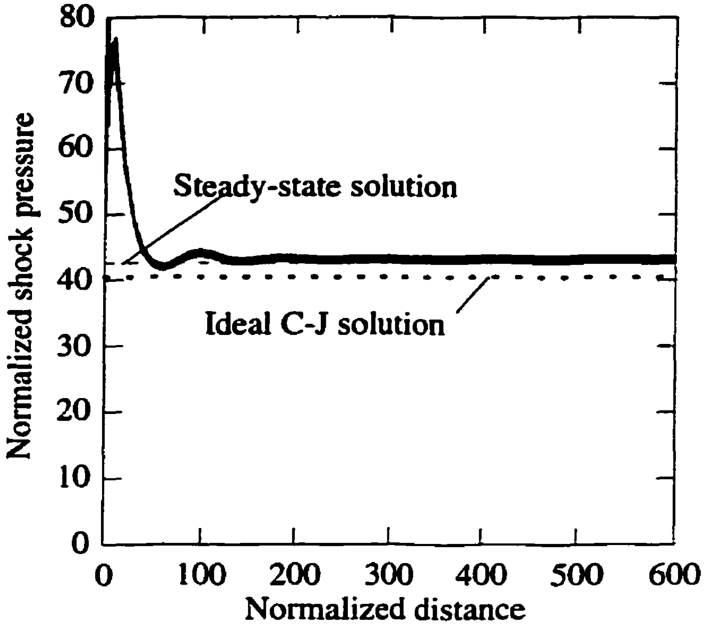

Figure 3.16: The shock pressure profile for a supercritical transient pathological detonation ($Q_1 = 50$, $Q_2 = -10$, $\gamma = 1.2$, $E_{a_1} = 22$, $E_{a_2} = 32$ and $k_1 = k_2$)

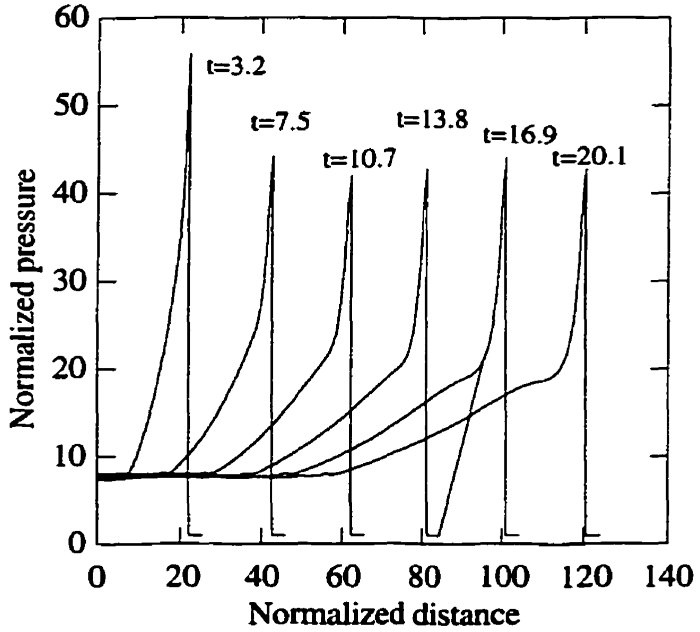

Figure 3.17: The pressure profiles for a supercritical transient pathological detonation ($Q_1 = 50$, $Q_2 = -10$, $\gamma = 1.2$, $E_{a_1} = 22$, $E_{a_2} = 32$ and $k_1 = k_2$)

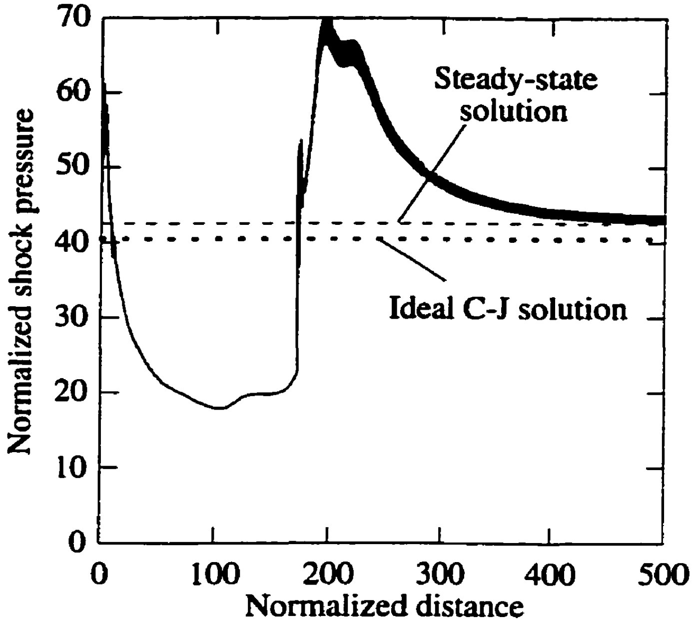

Figure 3.18: The shock pressure profile for a critical transient pathological detonation ($Q_1 = 50$, $Q_2 = -10$, $\gamma = 1.2$, $E_{a_1} = 22$, $E_{a_2} = 32$ and $k_1 = k_2$)

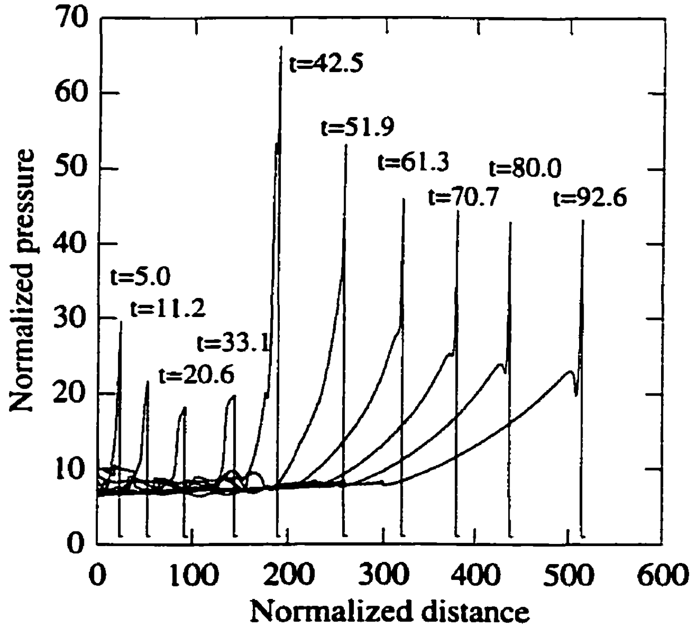

Figure 3.19: The pressure profiles for a critical transient pathological detonation ($Q_1 = 50$, $Q_2 = -10$, $\gamma = 1.2$, $E_{a_1} = 22$, $E_{a_2} = 32$ and $k_1 = k_2$)

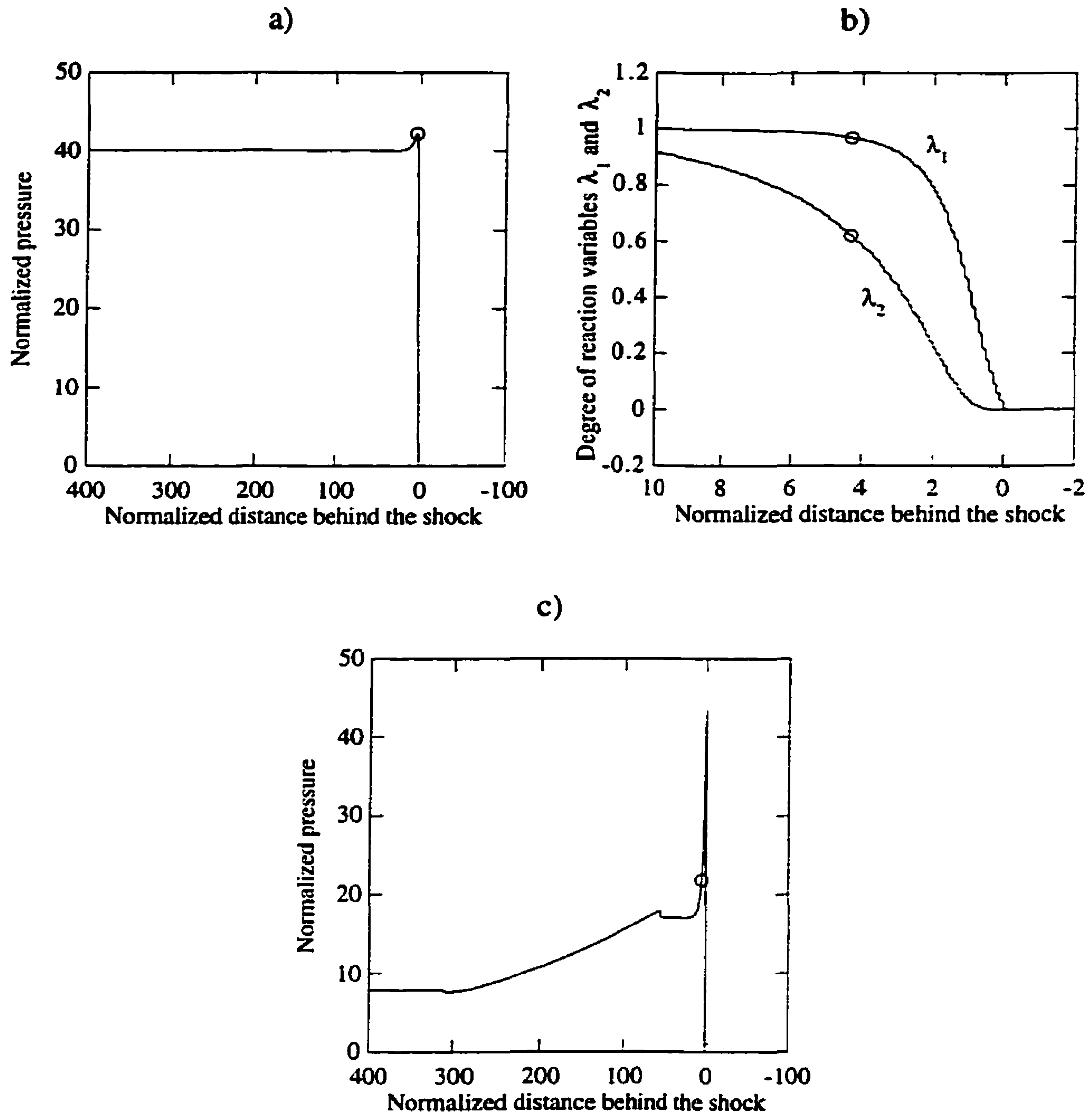

Figure 3.20: Heat release (a), degree of reaction (b) and pressure (c) profiles for a transient pathological detonation ($t = 90$, $Q_1 = 50$, $Q_2 = -10$, $\gamma = 1.2$, $E_{a_1} = 22$, $E_{a_2} = 32$ and $k_1 = k_2$) The hollow circles indicate the point where the heat release rate vanishes

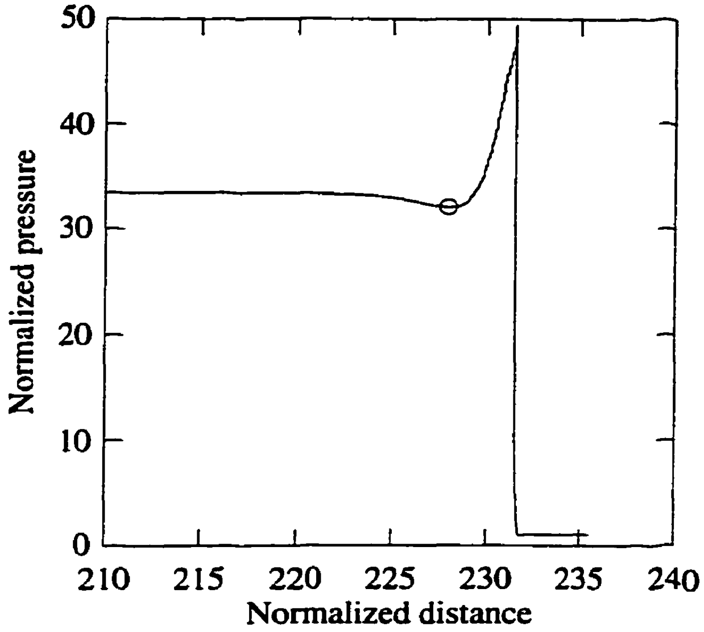

Figure 3.21: Pressure profile for an overdriven detonation. $u_p = 1.2 u_s$ ($Q_1 = 50$, $Q_2 = -10$, $\gamma = 1.2$, $E_{a_1} = 22$, $E_{a_1} = 32$ and $k_1 = k_2$) The hollow circle indicates the point where the heat release rate vanishes

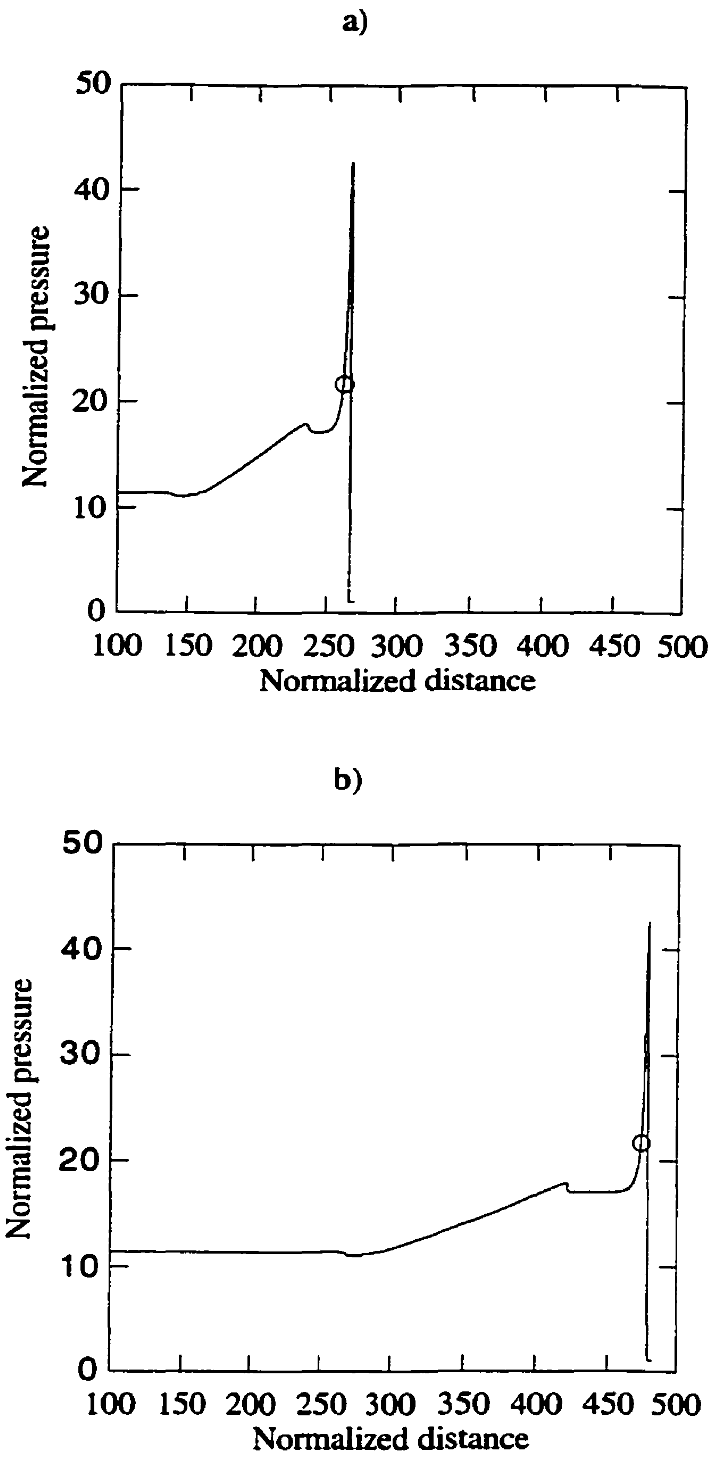

Figure 3.22: Pressure profiles for a piston-supported pathological detonation $u_p < u_w$ ($u_p = 1.0$, $Q_1 = 50$, $Q_2 = -10$, $\gamma = 1.2$, $E_{a_1} = 22$, $E_{a_2} = 32$ and $k_1 = k_2$) at time $t = 61.6$ (a) and time $t = 110$ (b). The hollow circles indicate the point where the heat release rate vanishes

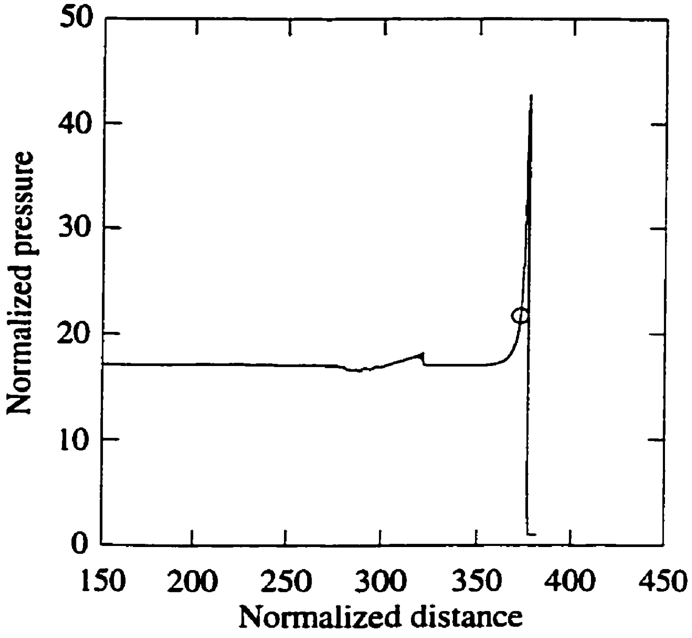

Figure 3.23: Pressure profile for a piston-supported pathological detonation. $u_p = u_w$ ($Q_1 = 50$, $Q_2 = -10$, $\gamma = 1.2$, $E_{a_1} = 22$, $E_{a_2} = 32$ and $k_1 = k_2$) The hollow circle indicates the point where the heat release rate vanishes

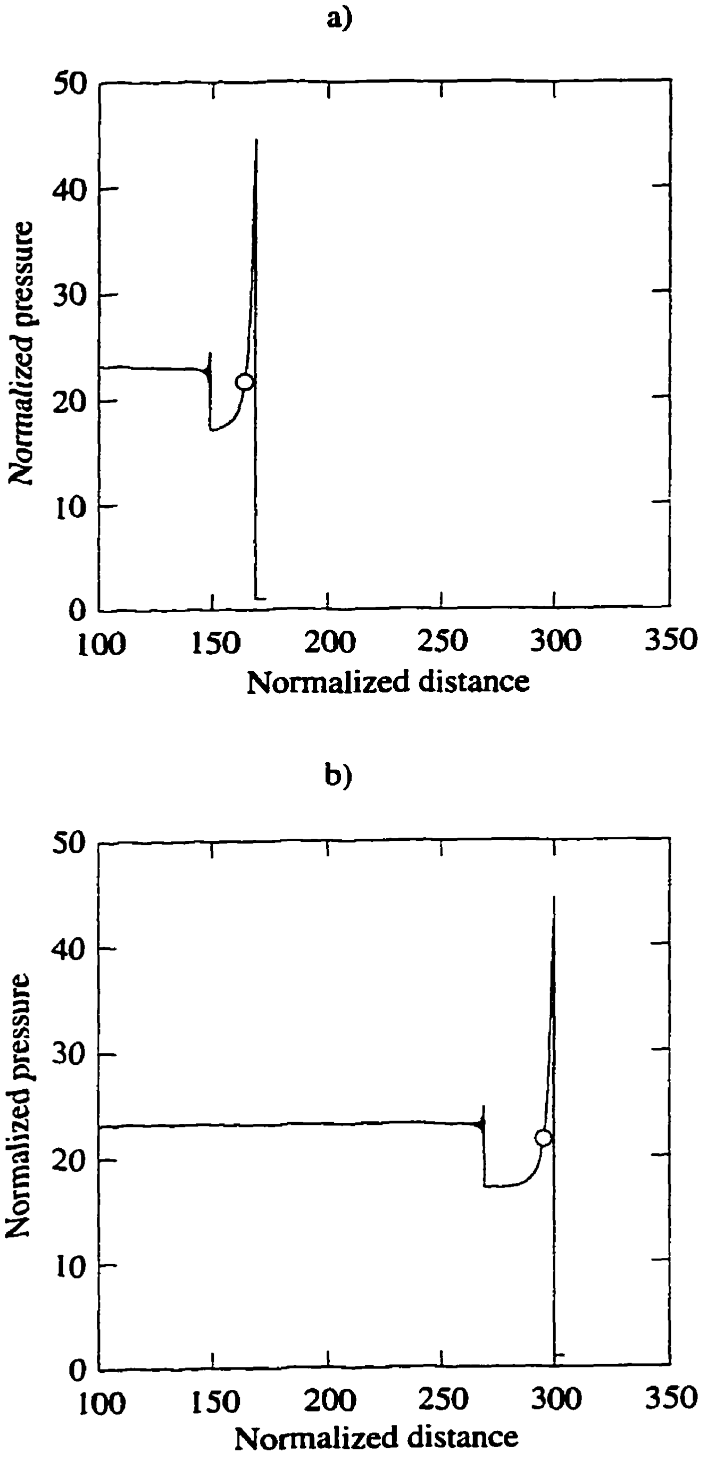

Figure 3.24: Pressure profile for a piston-supported pathological detonation. $u_w < u_p < u_s$ ($u_p = 3.0$, $Q_1 = 50$, $Q_2 = -10$, $\gamma = 1.2$, $E_{a_1} = 22$, $E_{a_2} = 32$ and $k_1 = k_2$) for (a) $t = 51.3$ and (b) $t = 92.0$. The hollow circles indicate the point where the heat release rate vanishes

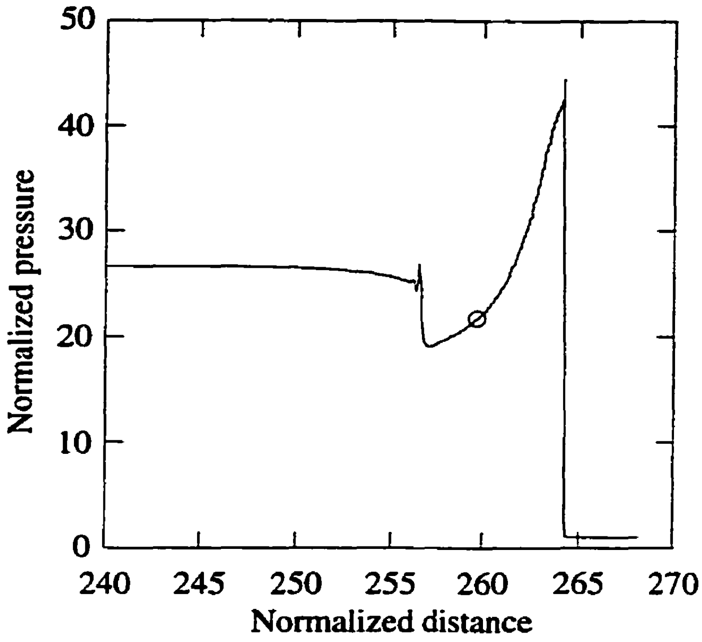

Figure 3.25: Pressure profile for a piston-supported pathological detonation. $u_p = u_s$ ($Q_1 = 50$, $Q_2 = -10$, $\gamma = 1.2$, $E_{a_1} = 22$, $E_{a_2} = 32$ and $k_1 = k_2$) The hollow circle indicates the point where the heat release rate vanishes

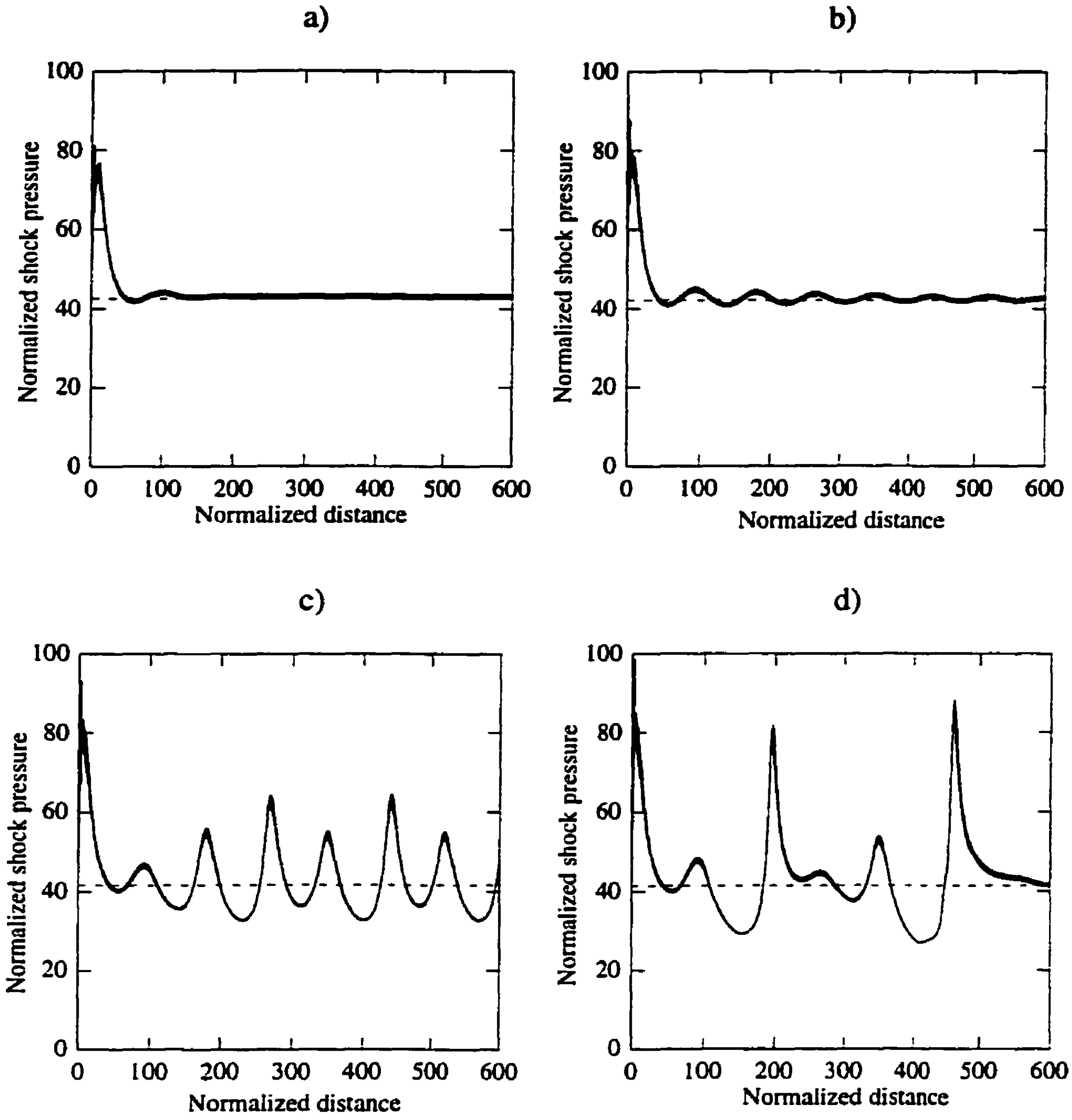

Figure 3.26: The shock pressure profiles for a transient pathological detonation ($Q_1 = 50$, $Q_2 = -10$, $\gamma = 1.2$, $E_{a_2} = 32$ and $k_1 = k_2$) with (a) $E_{a_1} = 22$, (b) $E_{a_1} = 24$, (c) $E_{a_1} = 26$ and (d) $E_{a_1} = 27$

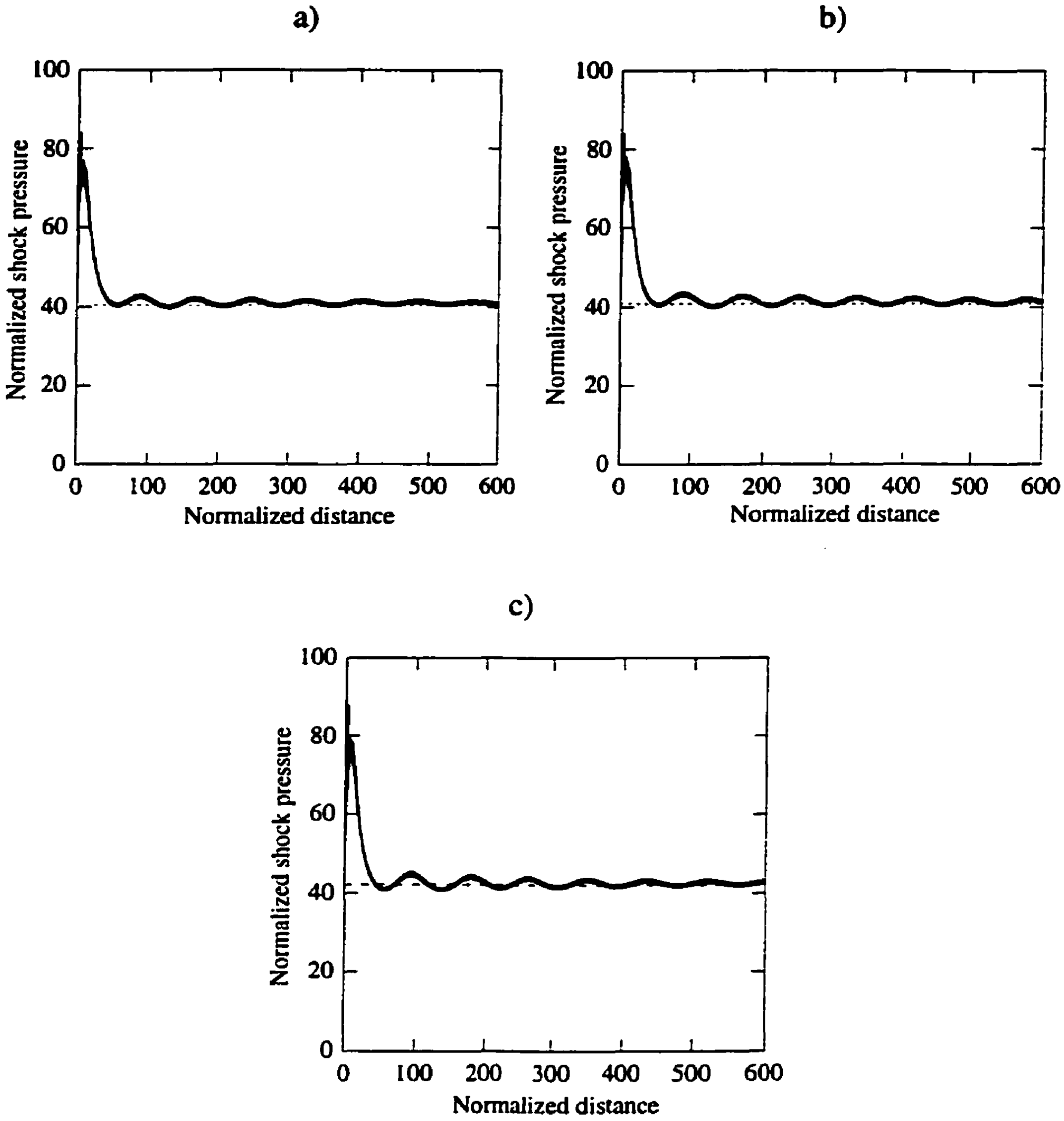

Figure 3.27: The shock pressure profiles for a transient pathological detonation ($Q_1 = 50$, $Q_2 = -10$, $\gamma = 1.2$, $E_{a_1} = 24$, and $k_1 = k_2$) with (a) $E_{a_2} = 24$, (b) $E_{a_2} = 27$ and (c) $E_{a_2} = 32$

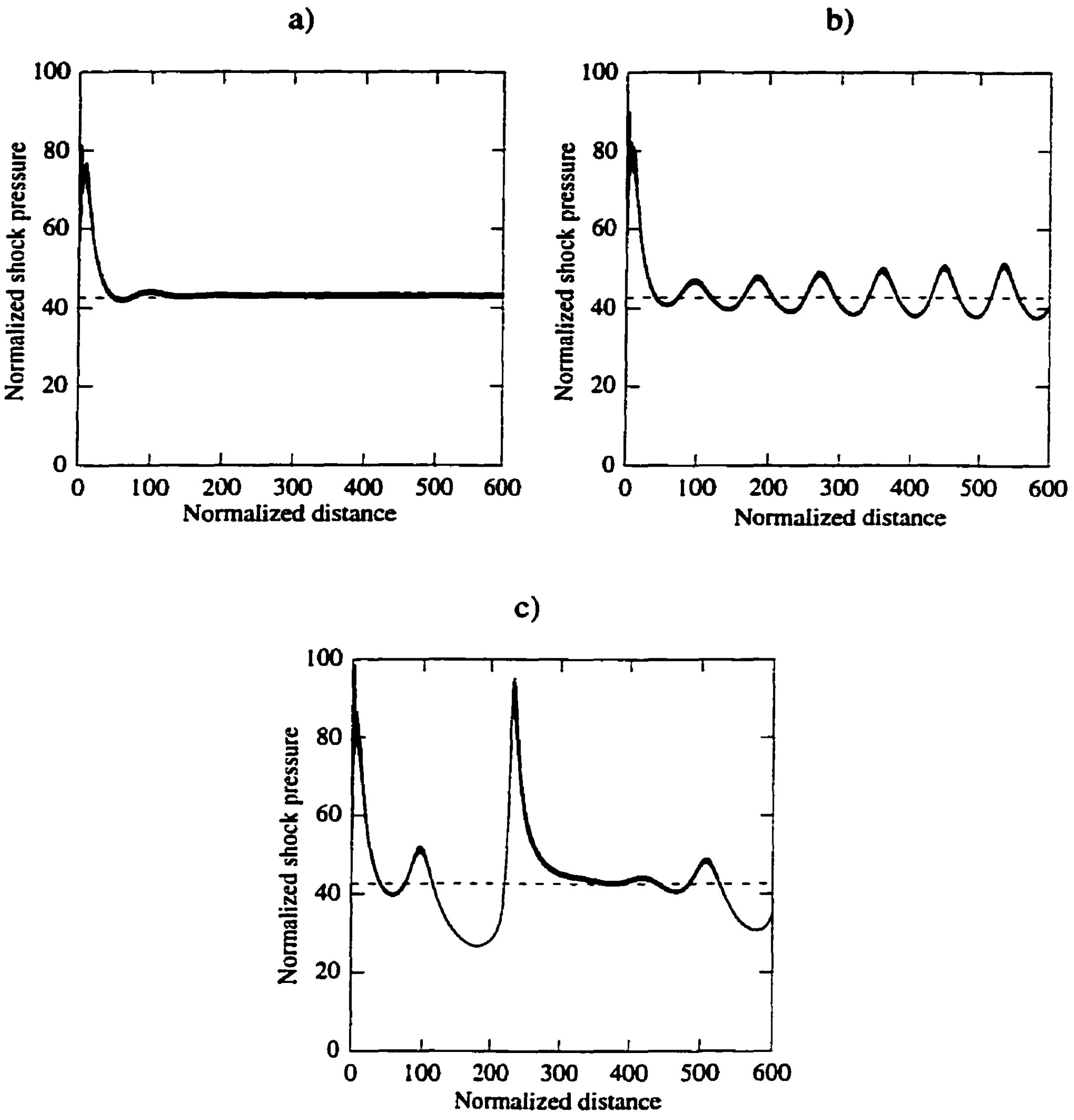

Figure 3.28: The shock pressure profiles for a transient pathological detonation ($Q_1 = 50$, $Q_2 = -10$, $\gamma = 1.2$, and $k_1 = k_2$), with (a) $E_{a_1} = 22$ and $E_{a_2} = 32$, (b) $E_{a_1} = 25$ and $E_{a_2} = 35$, and (c) $E_{a_1} = 27$ and $E_{a_2} = 37$

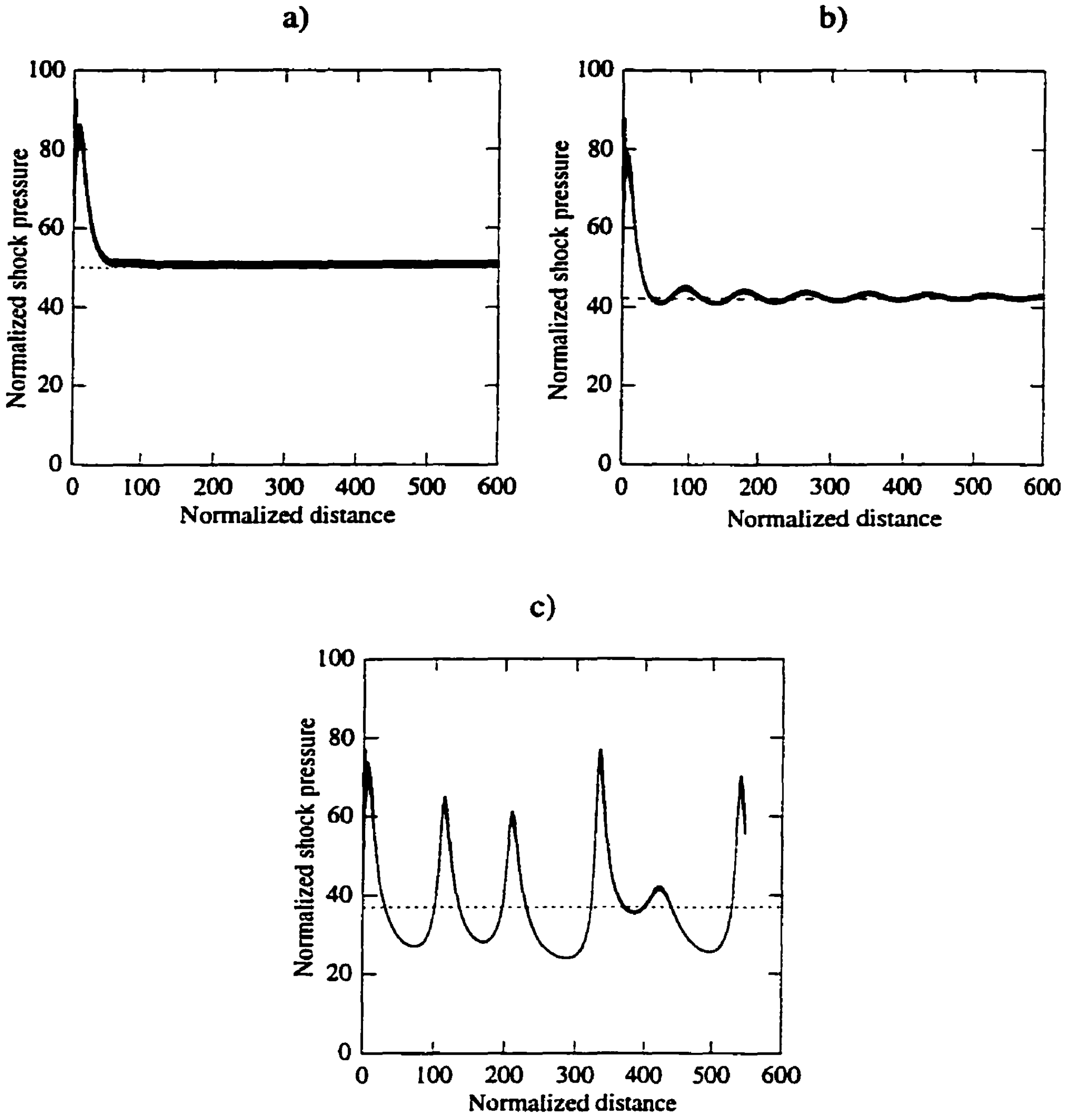

Figure 3.29: The shock pressure profiles for a transient pathological detonation ($Q_1 = 50$, $\gamma = 1.2$, $E_{a_1} = 24$, $E_{a_2} = 32$ and $k_1 = k_2$) with (a) $Q_2 = 0$, (b) $Q_2 = -10$ and (c) $Q_2 = -20$

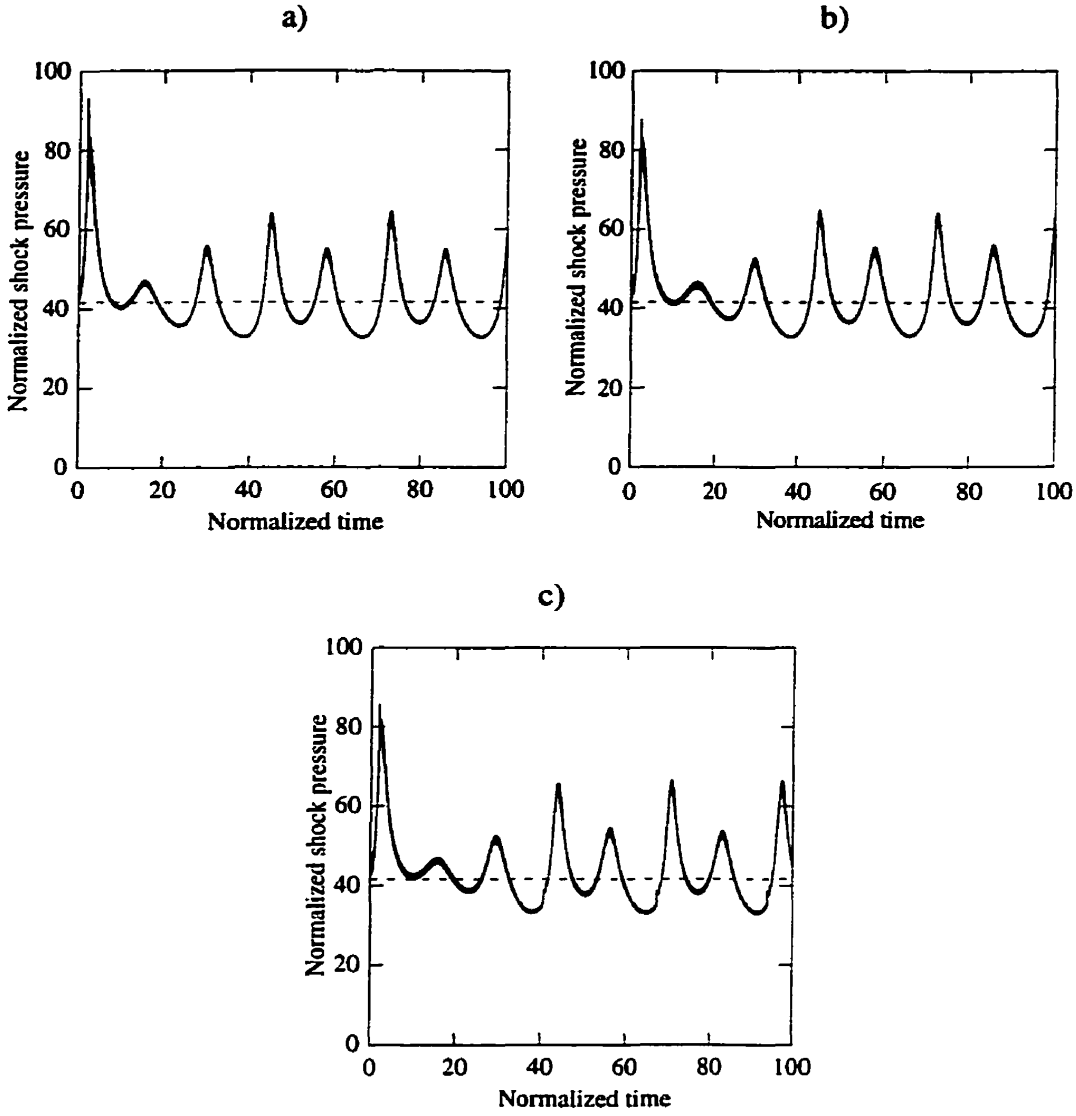

Figure 3.30: The shock pressure profiles for a transient pathological detonation ($Q_1 = 50$, $Q_2 = -10$, $\gamma = 1.2$, $E_{a_1} = 26$, $E_{a_2} = 32$ and $k_1 = k_2$) with (a) $u_p = 0$, (b) $u_p = u_w$ and (c) $u_p = u_s$

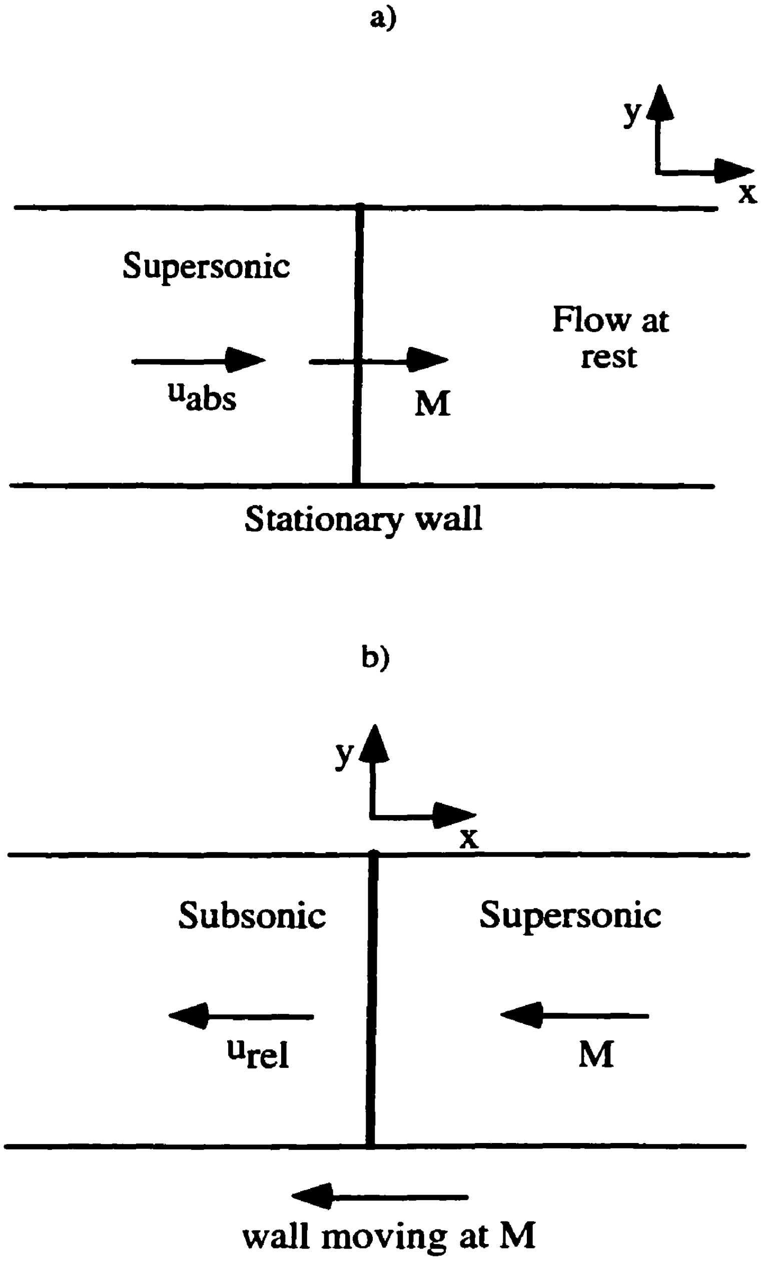

Figure 4.1: The laboratory fixed (a) and the shock-attached (b) reference frames

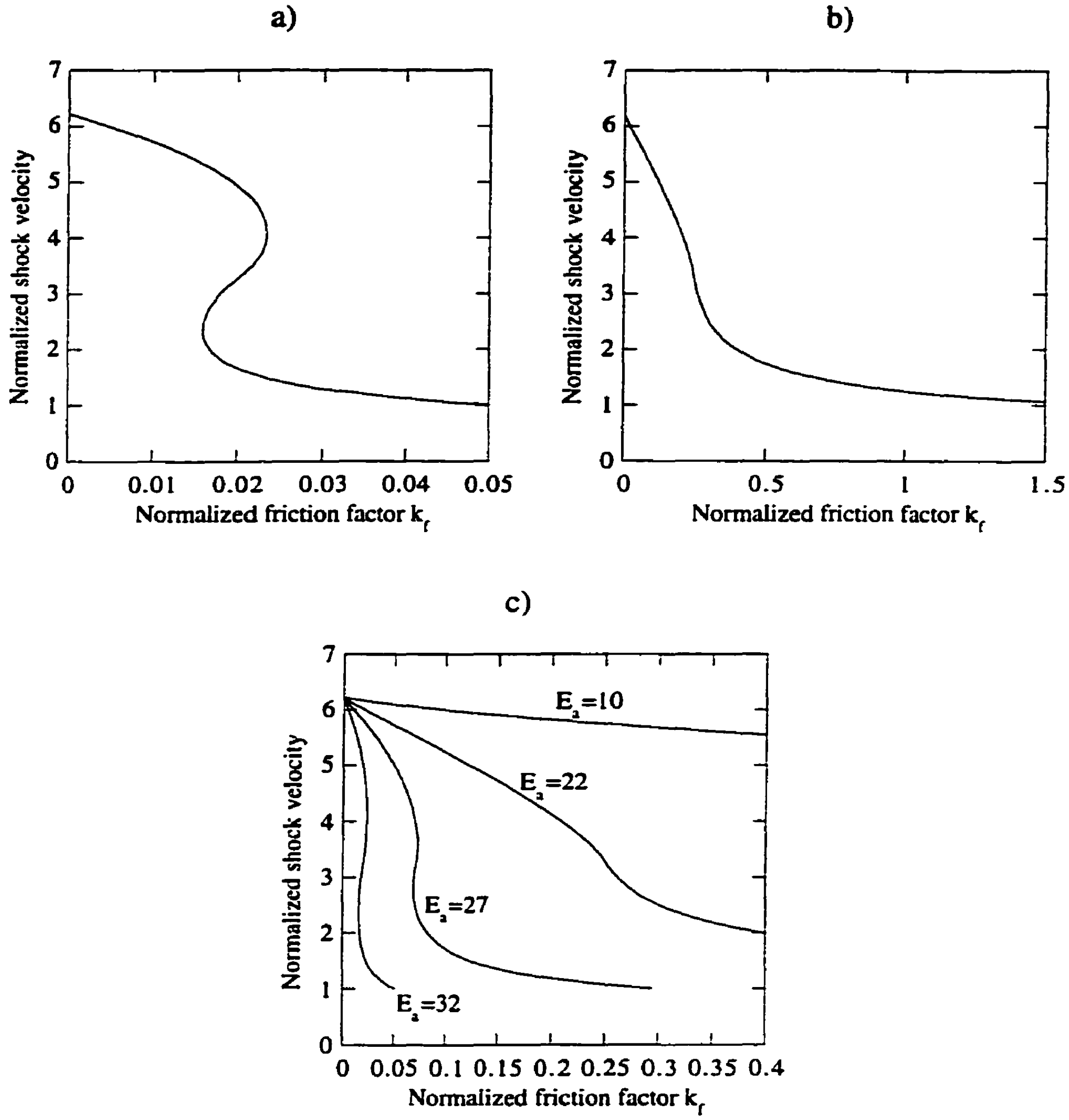

Figure 4.2: The M vs k_f curve for ($Q = 41.667$, $\gamma = 1.2$) with (a) $E_a = 32$, (b) $E_a = 22$ and (c) various activation energies

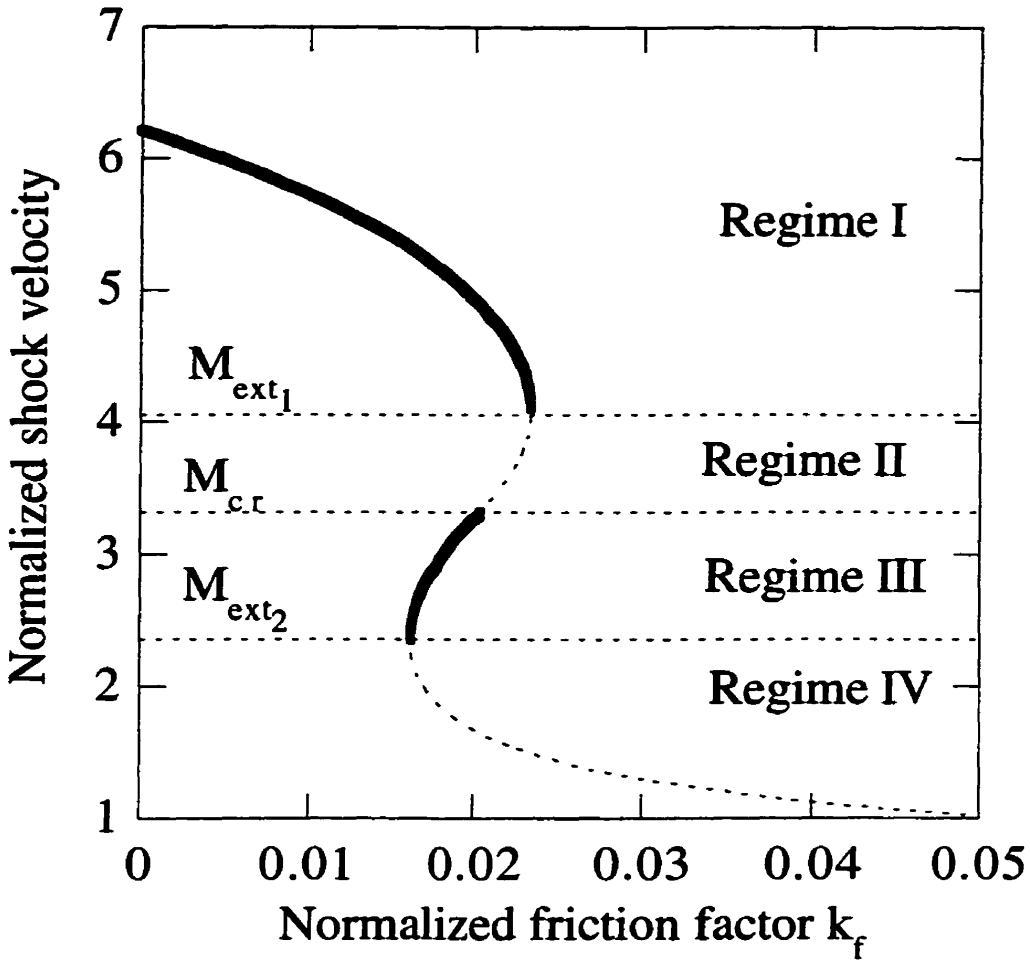

Figure 4.3: The different detonation regimes and critical points ($E_a = 32$, $Q = 41.667$, $\gamma = 1.2$)

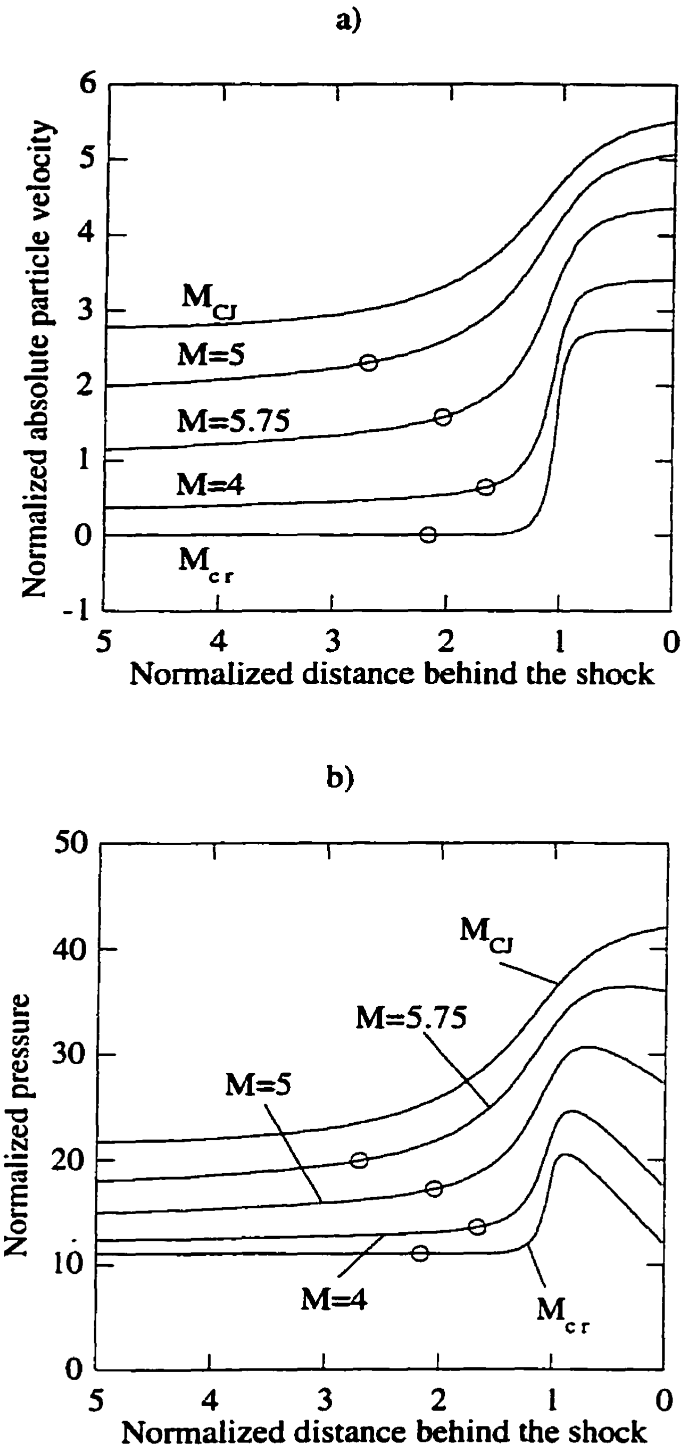

Figure 4.4: The absolute velocity (a) and pressure (b) profiles for different values of $M \geq M_{cr}$ ($E_a = 32$, $Q = 41.667$, $\gamma = 1.2$). The hollow circles indicate the location of the sonic plane (off the graph in the C-J case)

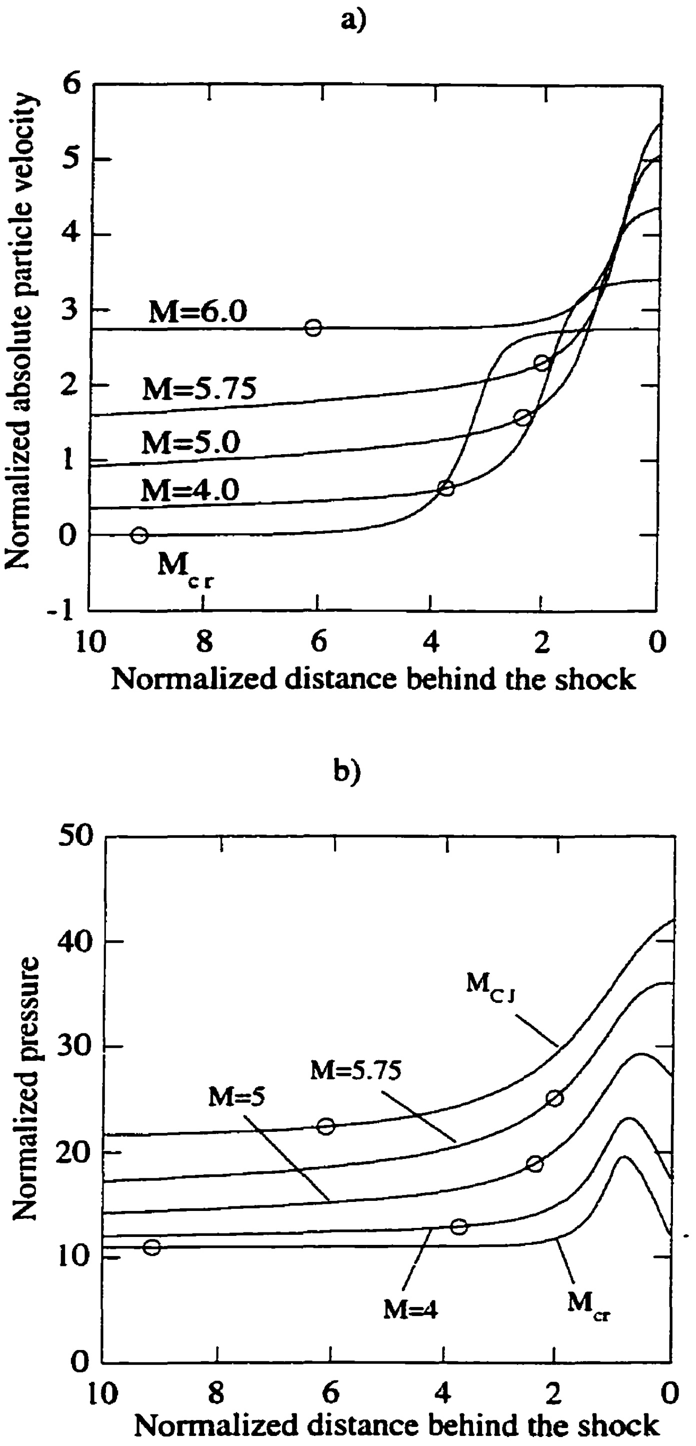

Figure 4.5: The absolute velocity (a) and pressure (b) profiles for different values of $M \geq M_{cr}$ ($E_a = 22$, $Q = 41.667$, $\gamma = 1.2$). The hollow circles indicate the location of the sonic plane

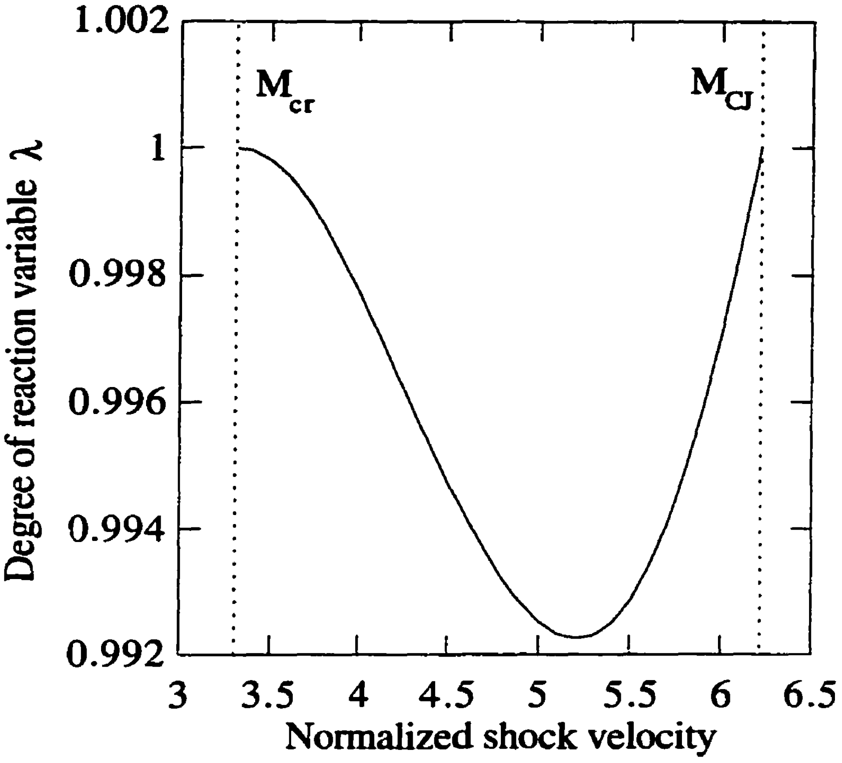

Figure 4.6: The value of the degree of reaction variable λ at the sonic plane vs. the normalized shock velocity M ($E_a = 22$, $Q = 41.667$, $\gamma = 1.2$)

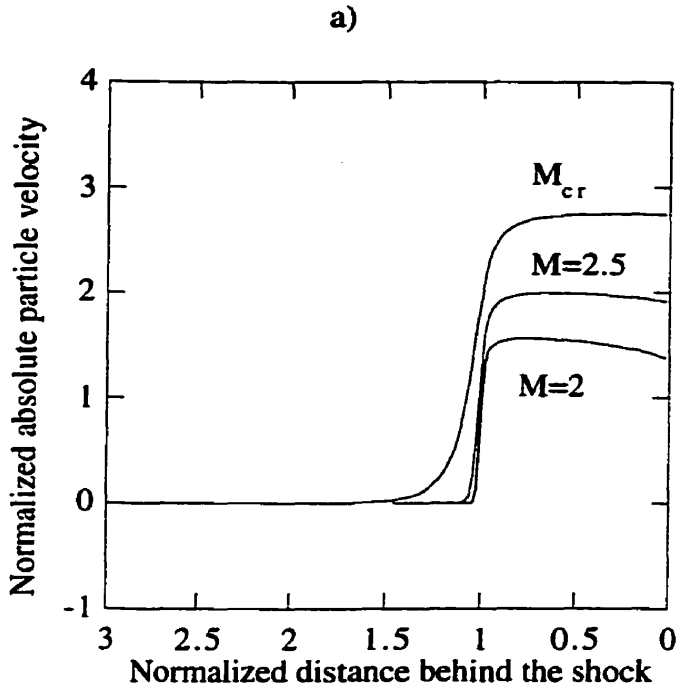

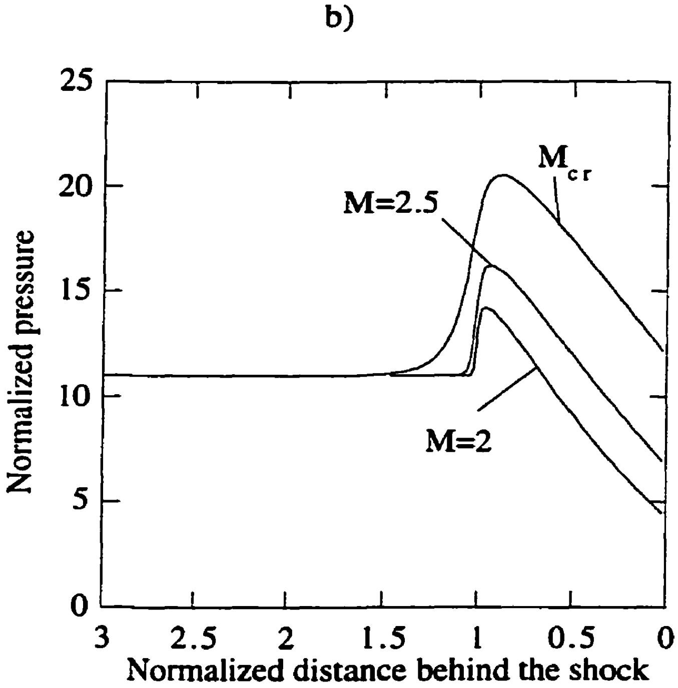

Figure 4.7: The absolute velocity (a) and pressure (b) profiles for different values of $M < M_{cr}$ ($E_a = 32$, $Q = 41.667$, $\gamma = 1.2$)

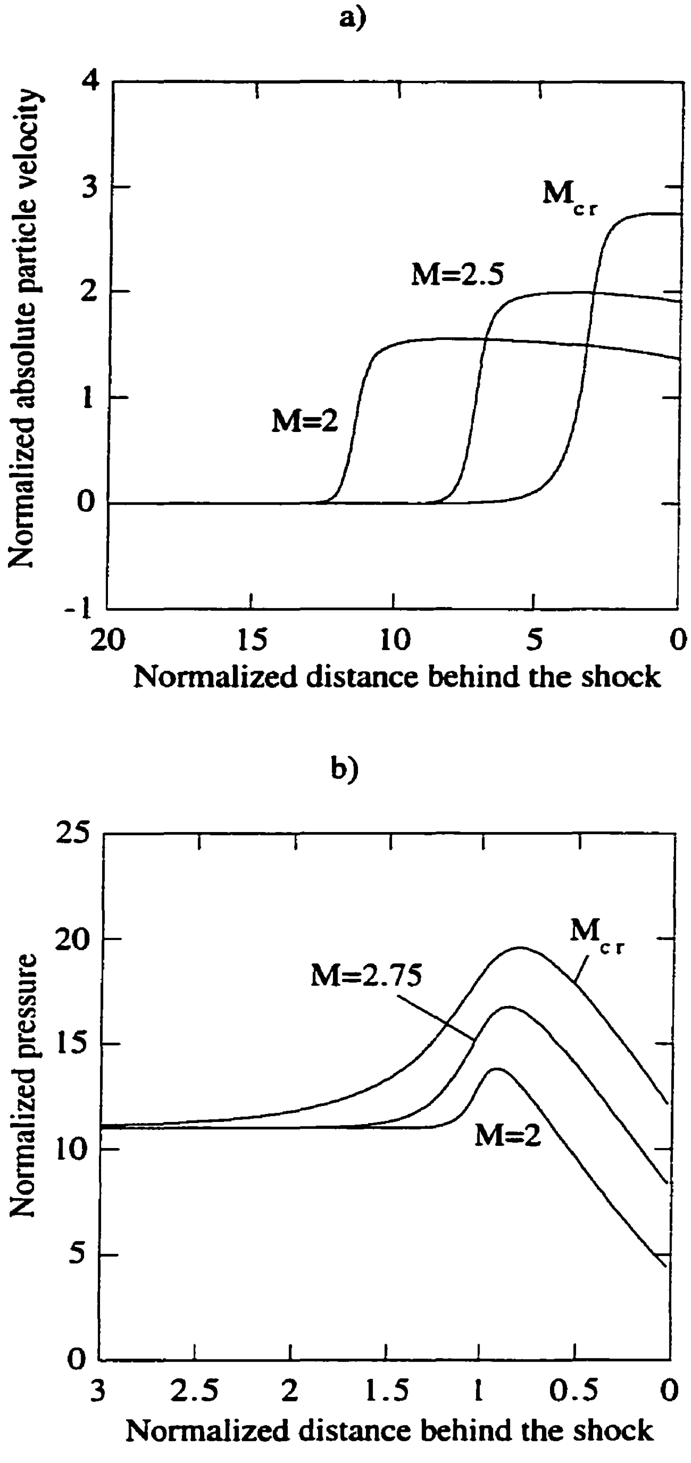

Figure 4.8: The absolute velocity (a) and pressure (b) profiles for different values of $M < M_{cr}$ ($E_a = 22$, $Q = 41.667$, $\gamma = 1.2$)

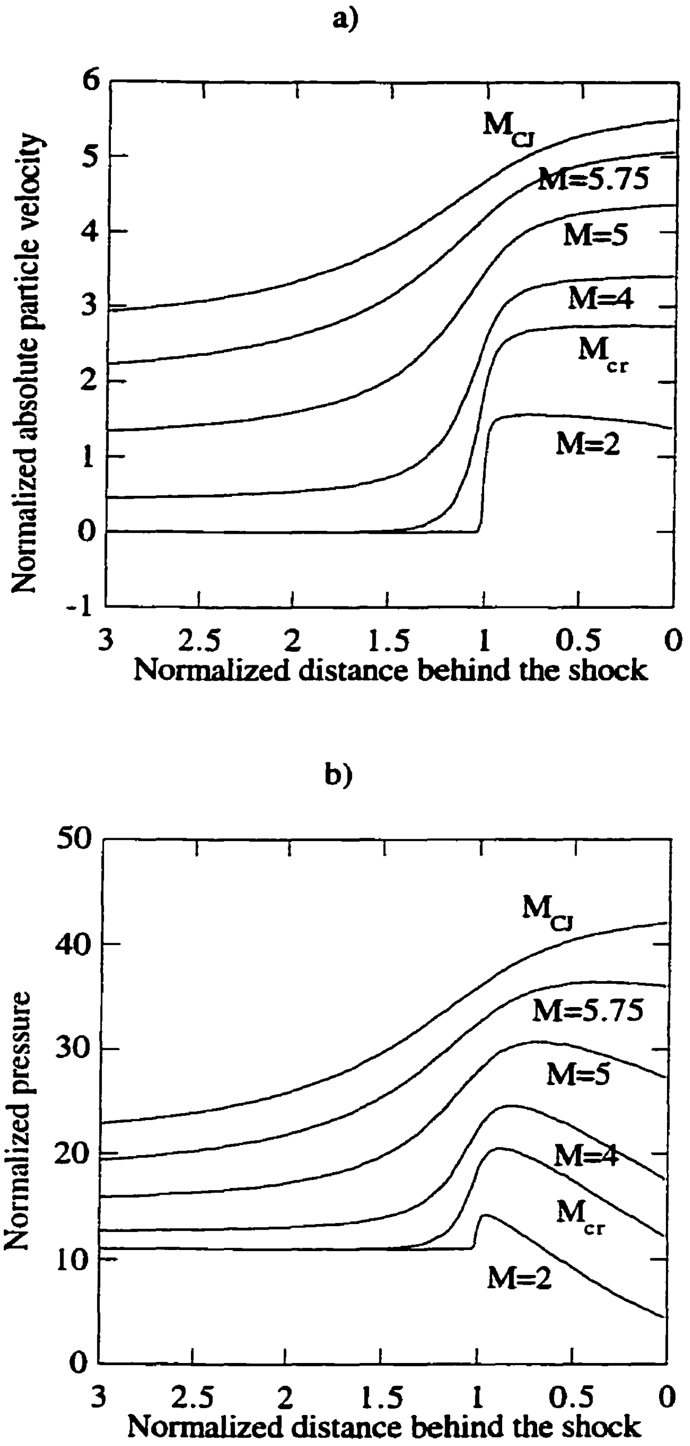

Figure 4.9: The absolute velocity (a) and pressure (b) profiles for different values of $1 < M < M_{cr}$ ($E_a = 32$, $Q = 41.667$, $\gamma = 1.2$)

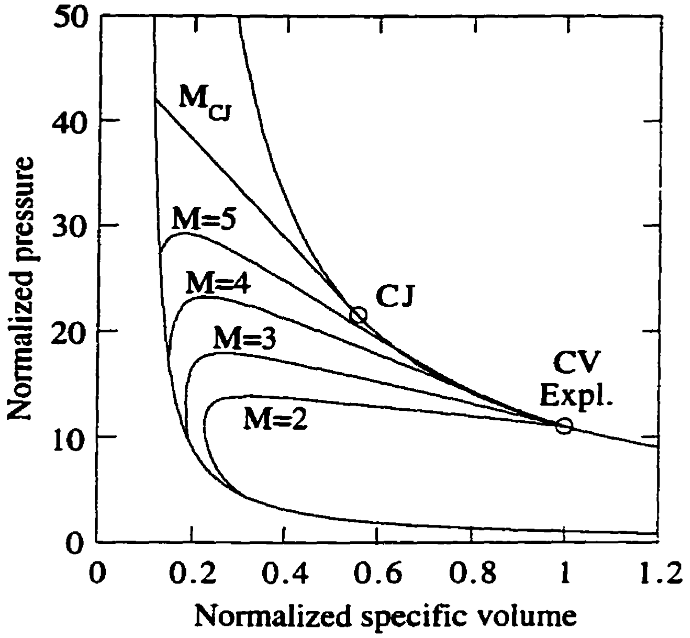

Figure 4.10: Pressure-volume ($p-v$) diagrams for different values of $1 < M < M_{cr}$ ($E_a = 22$, $Q = 41.667$, $\gamma = 1.2$) The hollow circles indicate the C-J and the constant volume explosion states

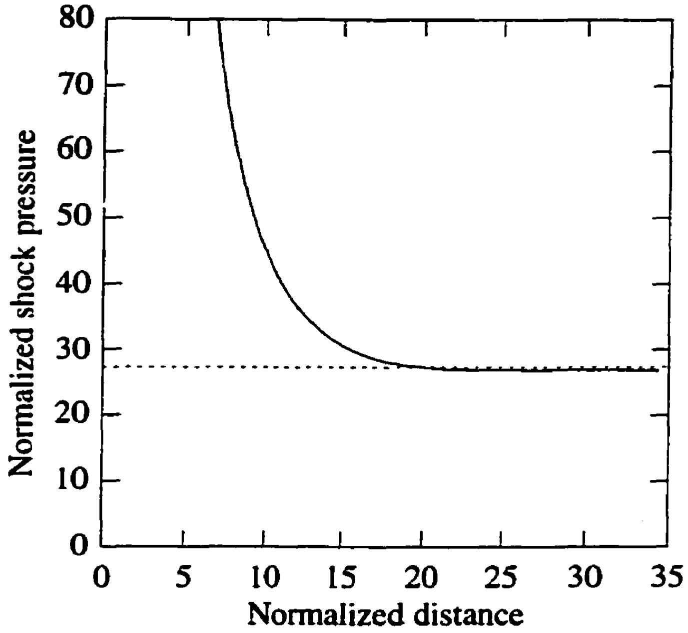

Figure 4.11: The shock pressure vs. distance for a detonation initiated with a strong blast wave ($E_a = 10$, $Q = 41.667$, $\gamma = 1.2$, $k_f = 0.9299$, $M > M_{cr}$) The dotted line represents the shock pressure predicted by the steady-state analysis

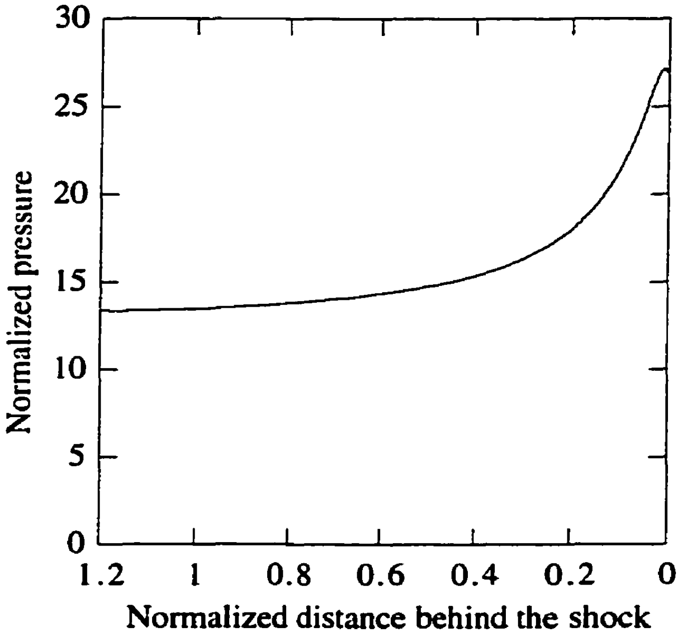

Figure 4.12: The pressure profile around the reaction zone for a detonation initiated with a strong blast wave ($E_a = 10$, $Q = 41.667$, $\gamma = 1.2$, $k_f = 0.9299$, $M > M_{cr}$)

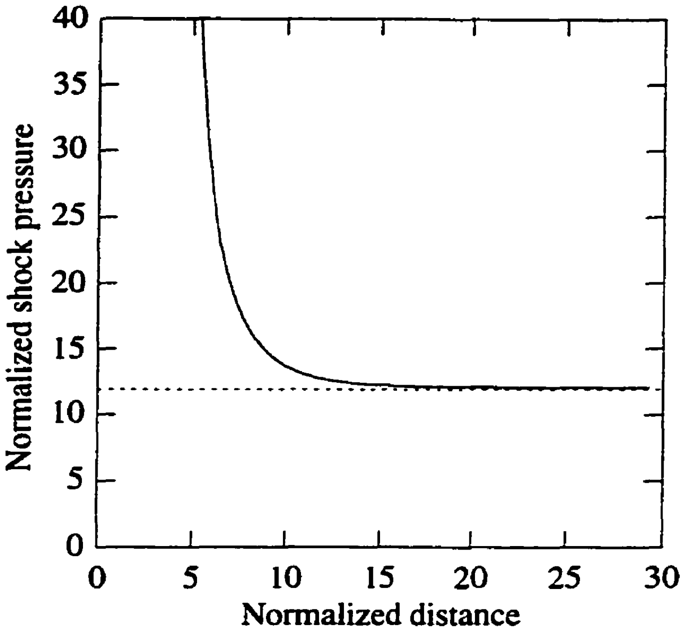

Figure 4.13: The shock pressure vs. distance for a detonation initiated with a strong blast wave ($E_a = 10$, $Q = 41.667$, $\gamma = 1.2$, $k_f = 4.578$, $M = M_{cr}$) The dotted line represents the shock pressure predicted by the steady-state analysis

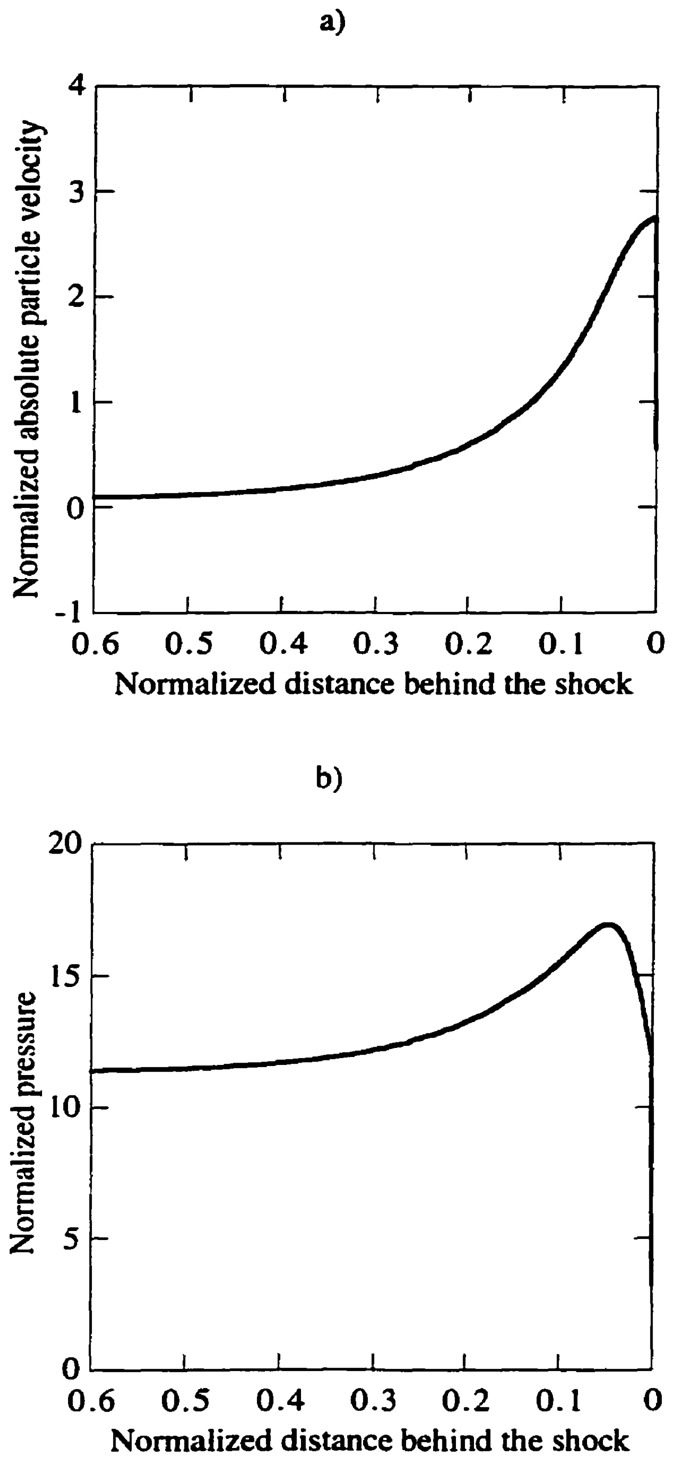

Figure 4.14: The particle velocity (a) and pressure (b) profiles around the reaction zone for a detonation initiated with a strong blast wave ($E_a = 10$, $Q = 41.667$, $\gamma = 1.2$, $k_f = 4.578$, $M = M_{cr}$)

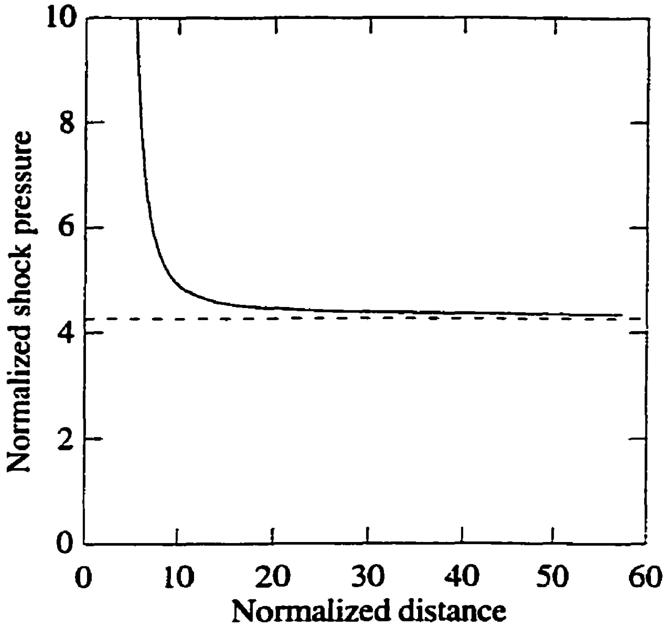

Figure 4.15: The shock pressure vs. distance for a low velocity detonation (LVD) initiated with a strong blast wave ($E_a = 10$, $Q = 41.667$, $\gamma = 1.2$, $k_f = 16.51$)

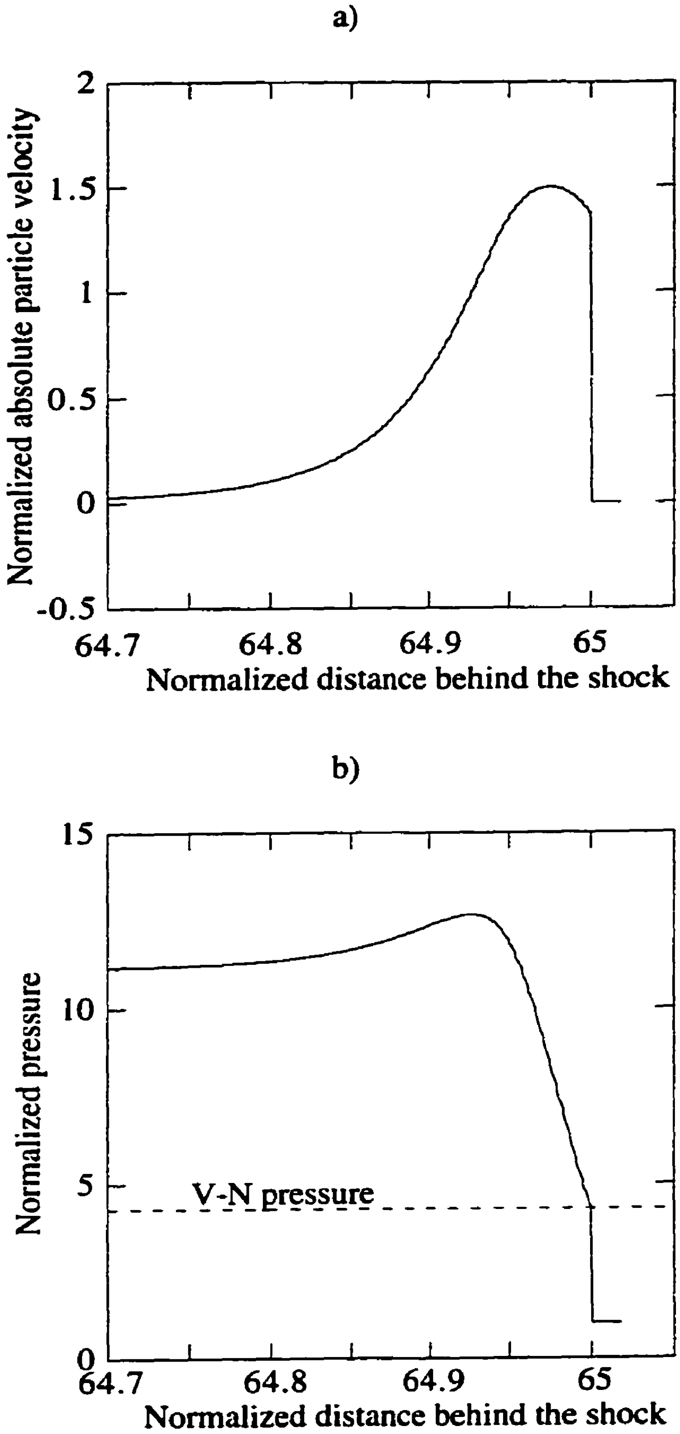

Figure 4.16: The particle velocity (a) and pressure (b) profiles around the reaction zone for a LVD initiated with a strong blast wave ($E_a = 10$, $Q = 41.667$, $\gamma = 1.2$, $k_f = 16.51$)

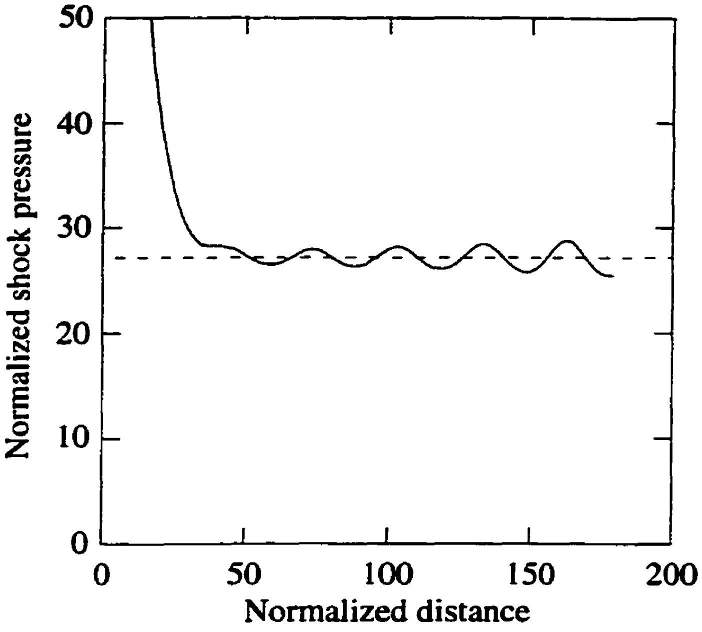

Figure 4.17: The shock pressure vs. distance for a detonation initiated with a strong blast wave ($E_a = 22$, $Q = 41.667$, $\gamma = 1.2$, $k_f = 0.1230$, $M > M_{cr}$) The dotted line represents the shock pressure predicted by the steady-state analysis

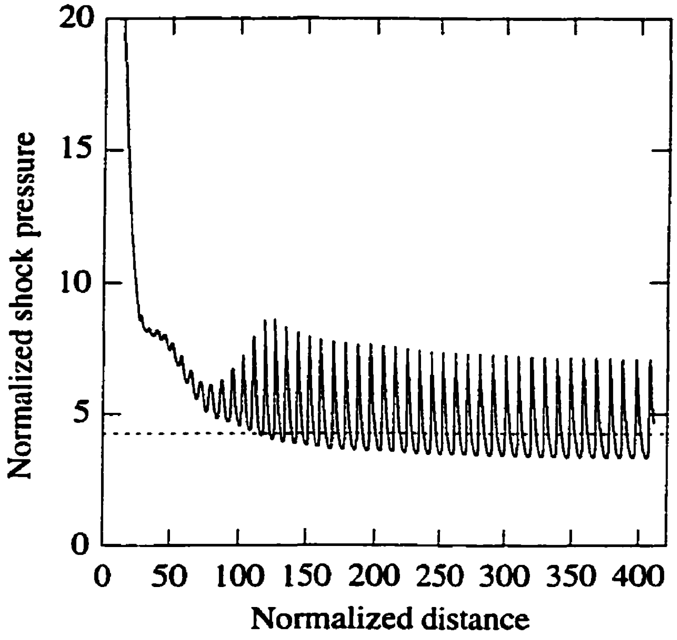

Figure 4.18: The shock pressure vs. distance for a low velocity detonation (LVD) initiated with a strong blast wave ($E_a = 22$, $Q = 41.667$, $\gamma = 1.2$, $k_f = 0.3973$)

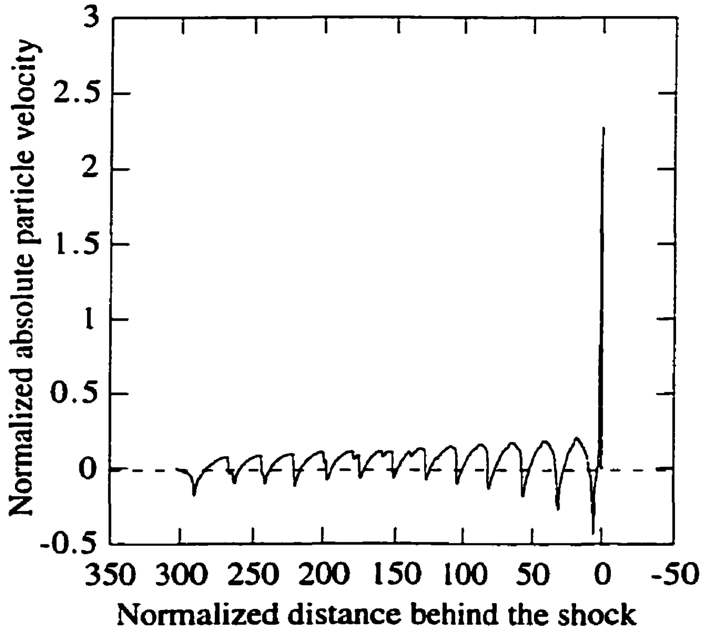

Figure 4.19: The absolute velocity profile for a low velocity detonation (LVD) initiated with a strong blast wave ($E_a = 22$, $Q = 41.667$, $\gamma = 1.2$, $k_f = 0.3973$)

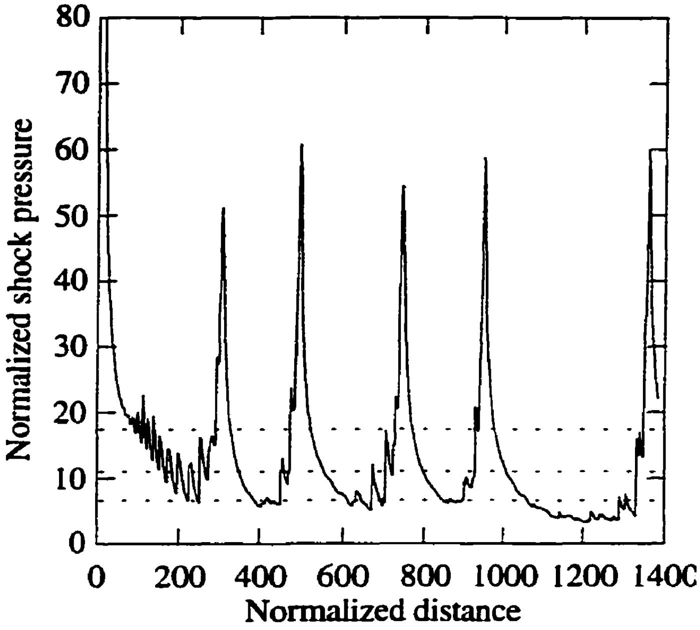

Figure 4.20: The shock pressure vs. distance for a detonation initiated with a strong blast wave ($E_a = 27$, $Q = 41.667$, $\gamma = 1.2$, $k_f = 0.07065$) The dotted lines indicate the three possible steady-state solutions

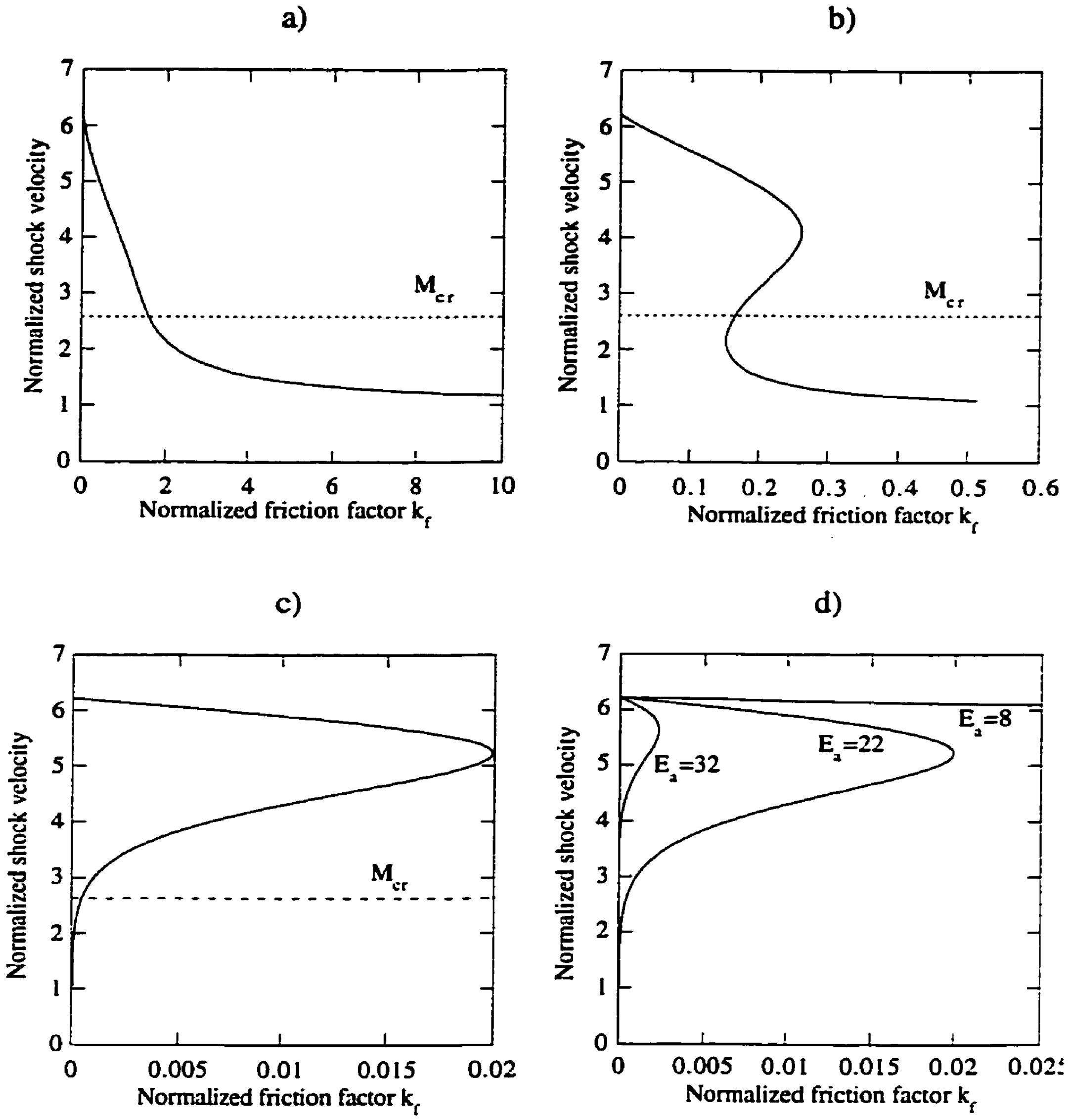

Figure 4.21: The M *vs* k_f curves (with heat transfer) for the cases (a) $E_a = 8$, (b) $E_a = 12$, (c) $E_a = 22$ and (d) various activation energies ($Q = 41.667$, $\gamma = 1.2$) M_{cr} is shown in dotted line in a) to c)

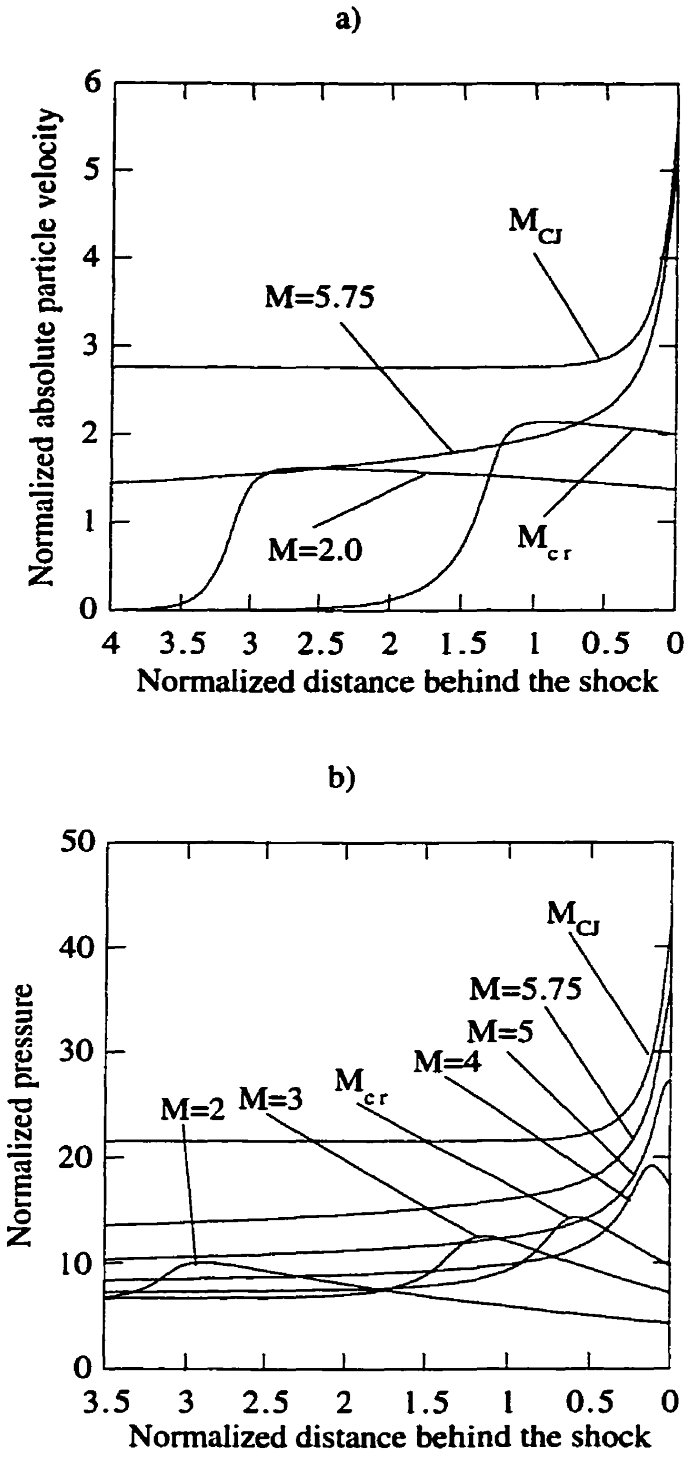

Figure 4.22: The absolute velocity (a) and pressure (b) profiles for different values of $1 < M < M_{cr}$ ($E_a = 12$, $Q = 41.667$, $\gamma = 1.2$)

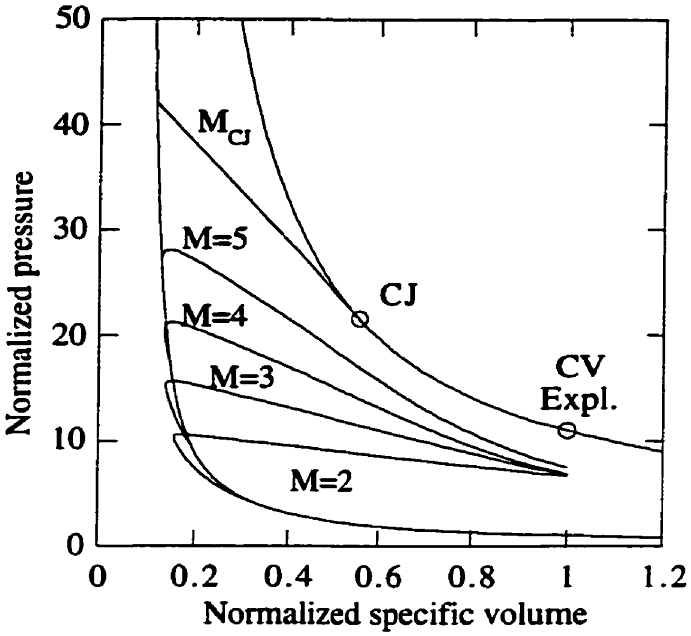

Figure 4.23: Pressure-volume ($p-v$) diagram for different values of $1 < M < M_{cr}$ ($E_a = 12$, $Q = 41.667$, $\gamma = 1.2$) The hollow circles indicate the C-J and the constant volume explosion states

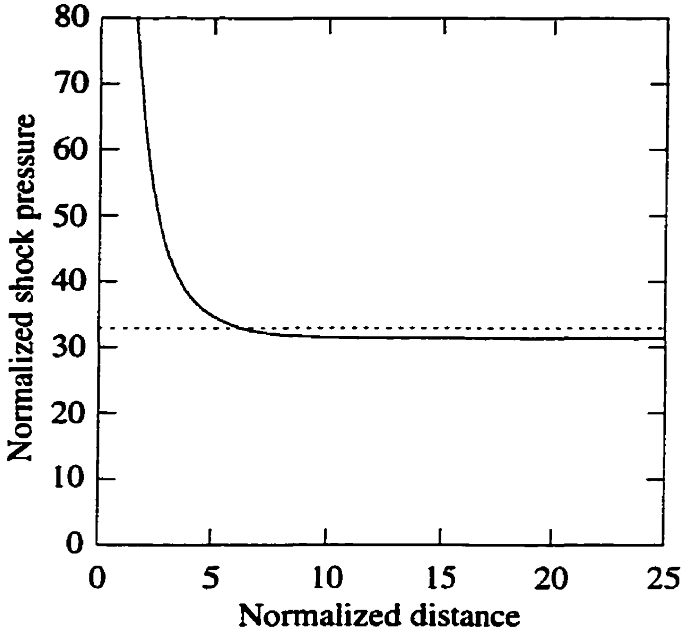

Figure 4.24: The shock pressure vs. distance for a detonation initiated with a strong blast wave ($E_a = 8$, $Q = 41.667$, $\gamma = 1.2$, $k_f = 0.2017$) The dotted line indicates the predicted steady-state solution

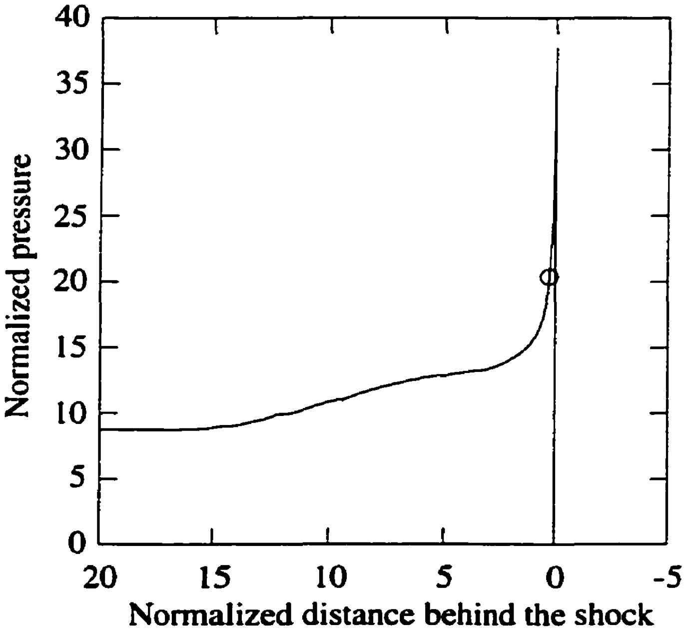

Figure 4.25: The pressure profile around the reaction zone for a detonation initiated with a strong blast wave ($E_a = 8$, $Q = 41.667$, $\gamma = 1.2$, $k_f = 0.2017$) The hollow circle indicates the plane where the effective heat release rate vanishes

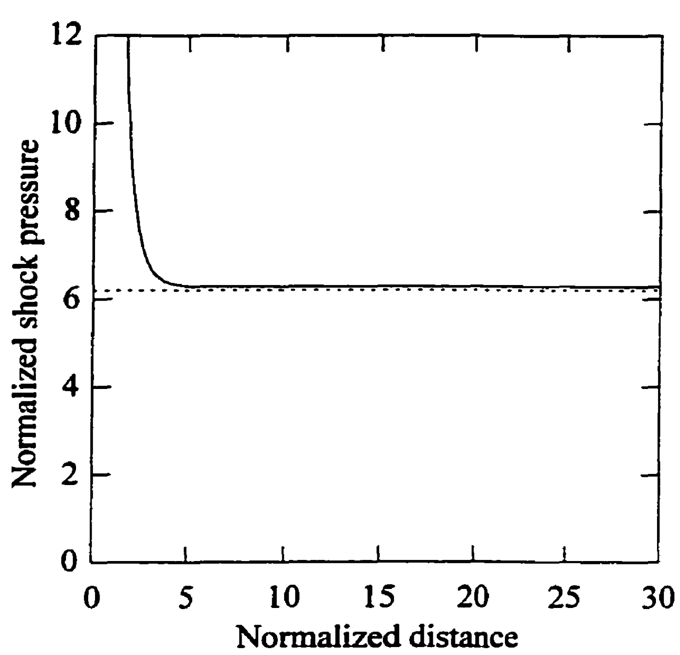

Figure 4.26: The shock pressure vs. distance for a LVD initiated with a strong blast wave ($E_a = 8$, $Q = 41.667$, $\gamma = 1.2$, $k_f = 1.762$) The dotted line indicates the predicted steady-state solution

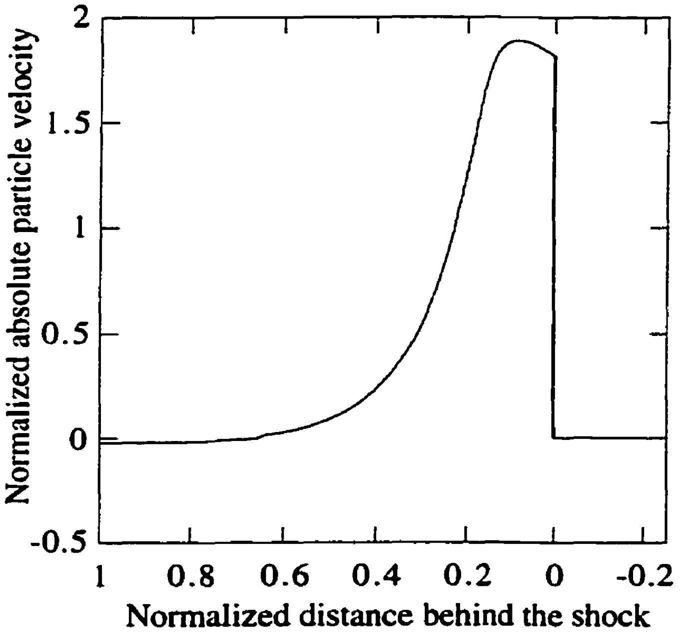

Figure 4.27: The absolute particle velocity profile around the reaction zone for a LVD initiated with a strong blast wave ($E_a = 8$, $Q = 41.667$, $\gamma = 1.2$, $k_f = 1.762$)

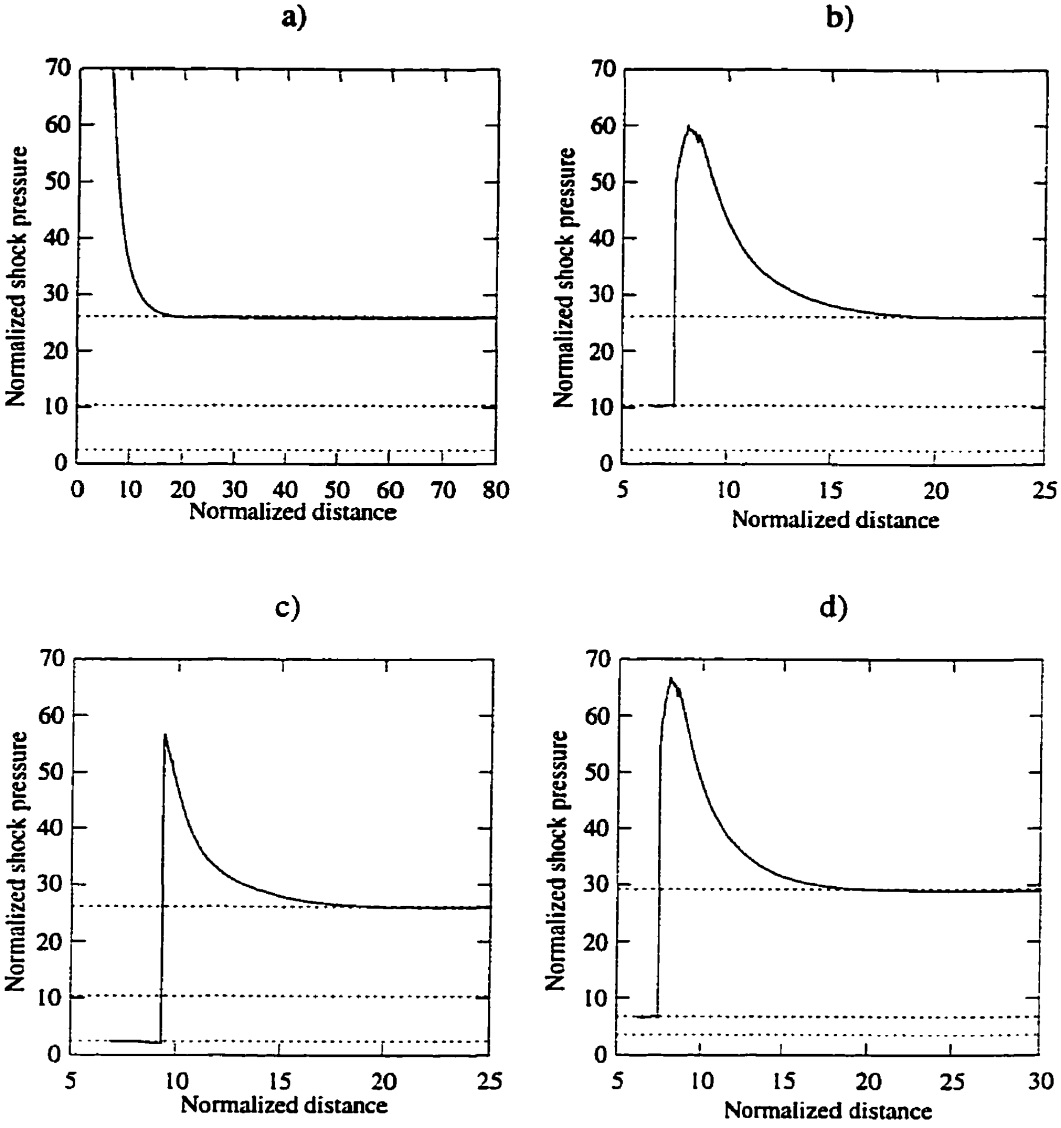

Figure 4.28: The shock pressure vs. distance for a detonation initiated (a) by a blast wave, (b) by a steady ZND profile for regime II, (c) by a steady ZND profile for regime IV, and (d) by a steady ZND profile for regime III ($E_a = 12$, $Q = 41.667$, $\gamma = 1.2$, $k_f = 0.2$ for a) to c) and $k_f = 0.16$ for d)). The dotted lines indicate the three possible steady-state solutions

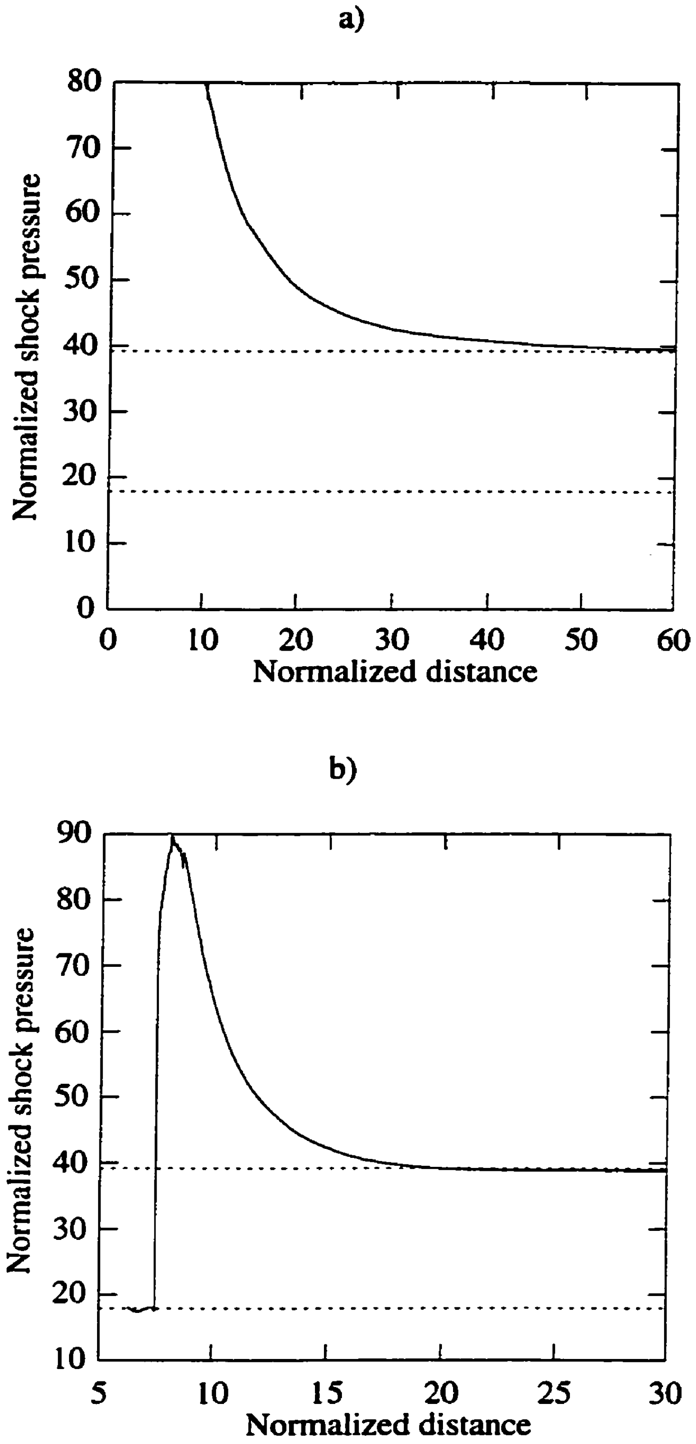

Figure 4.29: The shock pressure vs. distance for a detonation initiated (a) by a strong blast wave and (b) by a steady-state ZND profile for regime II ($E_a = 22$, $Q = 41.667$, $\gamma = 1.2$, $k_f = 0.007071$). The dotted lines indicate the two possible steady-state solutions

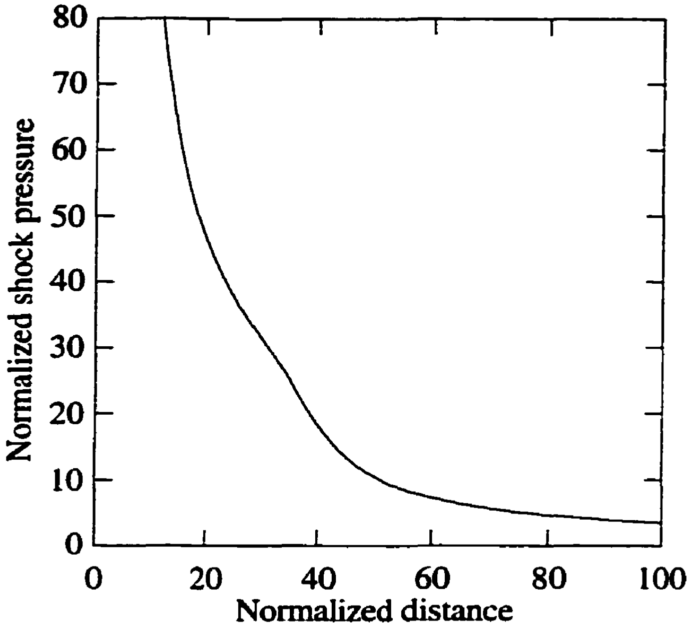

Figure 4.30: The shock pressure vs. distance for a detonation initiated with a strong blast wave ($E_a = 22$, $Q = 41.667$, $\gamma = 1.2$, $k_f = 0.025$)

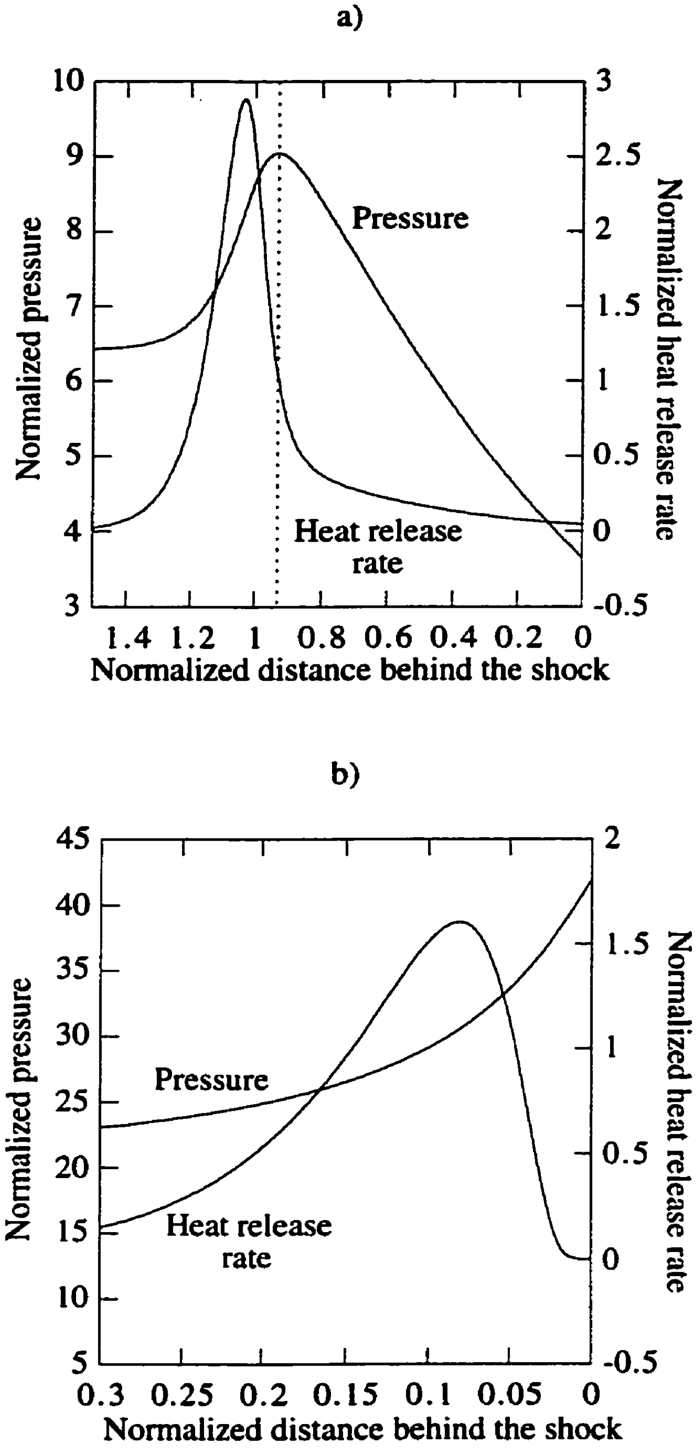

Figure 4.31: The pressure and chemical heat release rate profiles (a) for a LVD $k_f = 0.6543$, and (b) for an ideal detonation $k_f = 0$ ($E_a = 10$, $Q = 41.667$, $\gamma = 1.2$)

Tables

Table 3.1: Chemical kinetics scheme for $H_2 - Cl_2$ used by Guénoche et al. [33]
$k = AT^n exp(-E_a/RT)$ $(cm^3 mol^{-1} s^{-1})$ References given in [33]

Chemical reaction	A	n	$E_a(cal/mol)$	M
$2H + M \leftrightarrow H_2 + M$	10^{18}	-1	0	HCl, Cl_2, Cl
	$2 X 10^{19}$	-1	0	H
	$9 X 10^{16}$	-0.6	0	H_2
$Cl_2 + M \leftrightarrow 2Cl + M$	$6.15 X 10^{21}$	-2.07	57 040	H_2, Cl_2, HCl, H
	$6.15 X 10^{22}$	-2.07	57 050	Cl
$HCl + M \leftrightarrow H + Cl + M$	$6.76 X 10^{21}$	-2	102 170	H_2, Cl_2, HCl, H, Cl
$Cl + H_2 \leftrightarrow HCl + H$	$4.80 X 10^{13}$	0	5260	-
$H + Cl_2 \leftrightarrow HCl + Cl$	$6.61 X 10^{11}$	0.68	1090	-

Table 3.2: The theoretical and experimental results in the $H_2 - Cl_2$ mixture

		Detonation velocities				
ϕ	p_o kPa	ZND m/s	C-J m/s	Experimental m/s	Corrected m/s	% Correction
1.0	6.00	1804	1632	1672	1684	0.70
1.0	6.00	1804	1632	1667	1679	0.70
1.0	7.33	1804	1638	1668	1676	0.54
1.0	7.33	1804	1638	1666	1675	0.54
1.0	8.67	1804	1644	1679	1686	0.43
1.0	8.67	1804	1644	1677	1684	0.43
1.0	10.0	1804	1648	1675	1681	0.35
1.0	10.0	1804	1648	1676	1682	0.35
1.0	11.3	1804	1652	1674	1679	0.30
1.0	11.3	1804	1652	1666	1671	0.30
1.0	12.7	1804	1655	1672	1676	0.26
1.0	12.7	1804	1655	1675	1679	0.26
1.0	23.3	1804	1674	1691	1692	0.12
1.0	23.3	1804	1674	1688	1690	0.12
1.5	4.67	1911	1756	1797	1827	1.7
1.5	4.67	1911	1756	1790	1820	1.7
1.5	6.00	1910	1763	1789	1811	1.2
1.5	6.00	1910	1763	1785	1806	1.2
1.5	7.33	1909	1770	1799	1815	0.94
1.5	7.33	1909	1770	1785	1802	0.94
1.5	8.67	1909	1775	1797	1810	0.72
1.5	8.67	1909	1775	1788	1801	0.72
1.5	10.0	1910	1779	1792	1803	0.62
1.5	10.0	1910	1779	1786	1797	0.62
1.5	11.3	1910	1783	1799	1808	0.53
1.5	11.3	1910	1783	1781	1790	0.54
1.5	23.3	1910	1805	1823	1827	0.20
1.5	23.3	1910	1805	1817	1821	0.20
0.67	3.33	1529	1321	1387	1420	2.4
0.67	3.33	1529	1321	1416	1449	2.4
0.67	3.33	1529	1321	1372	1405	2.4
0.67	4.67	1529	1330	1384	1406	1.6
0.67	4.67	1529	1330	1371	1392	1.6
0.67	4.67	1529	1330	1379	1401	1.6
0.67	6.00	1529	1337	1365	1380	1.1
0.67	6.00	1529	1337	1366	1381	1.1
0.67	6.00	1529	1337	1367	1382	1.1
0.67	7.33	1529	1343	1333	1345	0.90
0.67	7.33	1529	1343	1349	1361	0.90
0.67	7.33	1529	1343	1338	1350	0.90
0.67	8.67	1529	1348	1339	1349	0.69
0.67	8.67	1529	1348	1348	1357	0.69
0.67	8.67	1529	1348	1343	1352	0.69
0.67	10.0	1529	1352	1337	1345	0.59
0.67	10.0	1529	1352	1355	1363	0.59
0.67	10.0	1529	1352	1344	1352	0.59
0.67	22.0	1529	1375	1376	1379	0.22
0.67	22.0	1529	1375	1387	1390	0.22
0.67	22.0	1529	1375	1394	1397	0.22

Table 3.3: Average shock pressures measured over a few cycles for oscillatory pathological detonations ($Q_1 = 50$, $Q_2 = -10$, $\gamma = 1.2$, $E_{a_2} = 32$, and $k_1 = k_2$) with various values of the exothermic activation energy E_{a_1} The ideal C-J shock pressure value is 40.46.

Activation Energy E_{a_1}	Average Shock Pressure	Steady-State Pressure Prediction	Deviation
24	42.39	42.07	+ 0.76 %
25	41.80	41.82	- 0.033 %
26	40.99	41.57	- 1.39 %
27	41.21	41.34	- 0.31 %